Cdt1 is limiting for pre-RC formation after UVC irradiation in early G1 phase in fission yeast

Dingli Dai

Thesis for Master's degree in Molecular Biosciences
60 study points

Department of Biosciences
Faculty of Mathematics and Natural Sciences

UNIVERSITY OF OSLO
06/2014

Cdt1 is limiting for pre-RC formation after UVC irradiation in early G1 phase in fission yeast

Dingli Dai

Thesis for Master's degree in Molecular Biosciences
60 study points

Department of Biosciences
Faculty of Mathematics and Natural Sciences

UNIVERSITY OF OSLO
06/2014

2014

Cdt1 is limiting for pre-RC formation after UVC irradiation in early G1 phase in fission yeast

Supervisors: Erik Boye, Beata Grallert

http://www.duo.uio.no/

Trykk: Reprosentralen, Universitetet i Oslo

ACKNOWLEDGMENTS

This work was carried out at the Department of Cell Biology, Institute for Cancer Research, The Norwegian Radium Hospital from February 2013 to May 2014. During this period I got to know a lot of people and had fantastic time doing scientific research. Therefore, I would first like to say thanks to one of my supervisors, Erik Boye, for including me in his group as well as being willing to discuss my data with me during this study.

I would also like to give my sincere thanks to another of my supervisors, Beata Grallert, for sharing her profound knowledge about fission yeast with me and helping me with my experiments.

And to both Erik and Beata, thanks for giving me advice during the writing process.

To the people who offered me their generous help, both from the group and outside the group, thank you so much.

To my friends who are always supporting me and comforting me when I was upset, every word you have said to me during these two years is precious to me.

To my families, thank you for believing in me.

Lastly, to my beloved parents, Qiuhua Ding and Shijun Dai, I will not say ‘‘thanks’’ to you since this word is so pale to express my feeling in front of your love. I owe my deepest and endless gratitude to you for everything you have done for me ever since the day I came to this world. All the love you give me is the best power driving me being optimistic. You are the greatest parents in the world!

Oslo, May 2014

Dingli Dai

ABSTRACT

The formation of the pre-RC is an important event during DNA replication initiation. It occurs from late M phase until early G1 phase and is required to license the replication origin before the binding of other initiation factors. Cdt1, one of the pre-RC components, has been shown to be a target of regulation after DNA damage in different model organisms.

Previous work from our group identified a novel G1/S checkpoint in fission yeast, and this checkpoint is dependent on the Gcn2 kinase which has a known role of leading to downregulation of global translation under amino acid starvation. The activation of this checkpoint after UVC irradiation in early G1 phase results in delayed pre-RC formation and consequently, a delayed G1/S transition. However, the underlying connection between the delayed pre-RC formation and the regulation of Cdt1 in response to UVC irradiation in early G1 phase is not yet clear.

The work carried out in this study is aimed to investigate the impact of changes in Cdt1 level on the kinetics of pre-RC formation in fission yeast, especially when the G1/S checkpoint is activated by UVC irradiation. We explored the expression of Cdt1 after UVC irradiation in early G1 phase and show that Cdt1 level is reduced. We also show that *gcn2*Δ cells with defective G1/S checkpoint have more Cdt1 than that in cells with intact G1/S checkpoint after UVC irradiation in early G1 phase. These observations lead us to speculate that the reduced Cdt1 level is limiting for pre-RC formation when the G1/S checkpoint is activated.

We show that consistently, in cells overexpressing Cdt1 the increase in pre-RC formation correlates with the increase in Cdt1 level after UVC irradiation in early G1 phase. This result suggests that the mechanism of the G1/S checkpoint involves reducing the Cdt1 level, which in turn is limiting for pre-RC formation and thus leads to a delayed G1/S transition.

ABBREVIATIONS

6-4 PP	6-4 photoproduct
Ade	Adenine
ATM	Ataxia telangiectasia mutated
ATR	Ataxia telangiectasia and Rad3-related
BCA	Bicinchoninic acid
bp	Base pair
BSA	Bovine serum albumin
C (1C, 2C, 4C)	Copy (DNA content)
Cdc	Cell division cycle
Cdk	Cyclin-dependent kinase
CDKC	Cyclin-dependent kinase complex
Cdt	Cdc10-dependent-transcription
Chk	Checkpoint kinase
CKI	Cyclin-dependent kinase inhibitor
CPD	Cyclobutane pyrimidine dimer
clonNAT	Trade name for nourseothricin
DAPI	4',6-diamidino-2-phenylindole
DMSO	Dimethyl sulfoxide
DNA	Deoxyribonucleic acid
DSB	Double strand break
DTT	Dithiotreitol
ECL	Enhanced chemiluminescent
EDTA	Ethylenediaminetetraacetic acid
eIF2α	Eukaryotic initiation factor 2α
EMM	Edinburg minimal medium
EtOH	Ethanol
FSC	Forward scatter

g	Gram
G0 (phase)	Gap 0 (quiescent state)
G1 (phase)	Gap 1
G2 (phase)	Gap2
Gcn2	General control non-derepressible 2
GFP	Green fluorescent protein
GINS	From the Japanese go-ichi-ni-san meaning 5-1-2-3, after the four related subunits of the complex Sld5, Psf1, Psf2 and Psf3
h	Hour
HRP	Horseradish peroxidase
IgG	Immunoglobulin G
J	Joule
kb	Kilo base
kDa	Kilo dalton
Leu	Leucine
Log	Logarithmic
M	mol/l
M (phase)	Mitosis
m^2	Square meter
MCM	Mini-chromosome maintenance
ME	Malt extract
MetOH	Methanol
min	Minutes
MMS	Methyl methane sulfonate
MQ-H_2O	Milli-Q -H_2O
NER	Nucleotide excision repair
ng	Nanogram
nm	Nanometer
nmt	No message in thiamine
nt	Nucleotide

NTS	Non-transcribed strand
OD	Optical density
ORC	Origin recognition complex
PABP	Poly(A)-binding protein
PAGE	Polyacrylamide gel electrophoresis
PB	Processing body
PBS	Phosphate buffer saline
PCNA	Proliferating cell nuclear antigen
PCR	Polymerase chain reaction
PEG	Polyethylene glycol
PIP	PCNA-interacting protein
pre-IC	Pre-initiation complex
pre-mRNA	Precursor mRNA
pre-RC	Pre-replication complex
PVDF	Polyvinylidine fluoride
RNA	Ribonucleic acid
Rnase A	Ribonuclease A
RNR	Ribonucleotide reductase
RT	Room temperature
RT-PCR	Reverse transcription polymerase chain reaction
S (phase)	DNA synthesis
sec	Second
SDS	Sodium dodecyl suplhate
SG	Stress granule
S. pombe	*Schizosaccaromyces pombe*
SSC	Side scatter
TAE	Tris-acetate-EDTA
TAP	Tandem affinity purification
TBS-T	Tris-buffered saline Tween-20

TC	Ternary complex
TCA	Trichloroacetic acid
TE	Tris-EDTA
Tris	2-amino-2-(hydroxymethyl)-1,3-propanediol
TS	Transcribed strand
U	Units
Ura	Uracil
UVC	Ultraviolet C
V	Volt
W	Watt
wt	Wild type
YES	Yeast extract with supplements
x g	Times gravity
µL	Microliter
°C	The degree Celsius
Δ	Gene deletion

TABLE OF CONTENTS

1 INTRODUCTION

The main interest of this study is to investigate the relationship between a pre-RC (pre-replication complex) component Cdt1 and the pre-RC formation after the Gcn2-dependent G1/S checkpoint is activated by UVC-induced DNA damage in fission yeast. Therefore in this introduction chapter I will start with introducing fission yeast as a model organism. I will also give general description about the eukaryotic cell cycle and its regulation mechanisms before continuing to G1/S transition. The emphasis will be in DNA replication initiation. Particularly, the pre-RC formation, an important event during DNA replication initiation and two components of the pre-RC, Cdt1 and MCM2-7 will be focused on. Then I will give a general view of DNA damage induced by UVC irradiation. At the end, I will introduce the background of this study in light of previous work.

1.1 *Schizosaccharomyces pombe* as a model organism

The complexity of higher eukaryotic organisms makes the study on them difficult. Especially when using higher eukaryotes to start an investigation with little known background, their complicated regulation system may even disorient the study at the very beginning. In order to understand biological principles in an easier way, model organisms were introduced given the fact that basic biological processes are shared between organisms to a great extent. So far, many significant discoveries have been made by using model organisms, and these discoveries shed light on the establishment of biological theories which have led to profound studies.

Schizosaccharomyces pombe is one of the four fungal model organisms that have been used extensively for genetic research, the other three members are *Saccharomyces cerevisiae, Neurospora crassa and Aspergillus nidulans* (Hedges, 2002). *S. pombe* is a free-living unicellular eukaryote, it grows by elongation and undergoes cell division by medial fission, and therefore has been conferred on the common name ‘‘fission yeast’’.

First isolated from East African millet beer and originally used for brewing, fission yeast is a non-pathogenic organism thus can be handled easily with little precautions. Cells of fission yeast have a rod-shape covered by cell wall. Their sizes normally range from 7 to 14 μm in length and 3 to 4 μm in diameter making them easy to be visualized under the microscope (Figure 1.1). Furthermore, the growth of fission yeast is quite rapid under a normal laboratory condition, and is also simple and

inexpensive to be maintained. Counting these features together, fission yeast exhibits a lot of advantages for cell biology study.

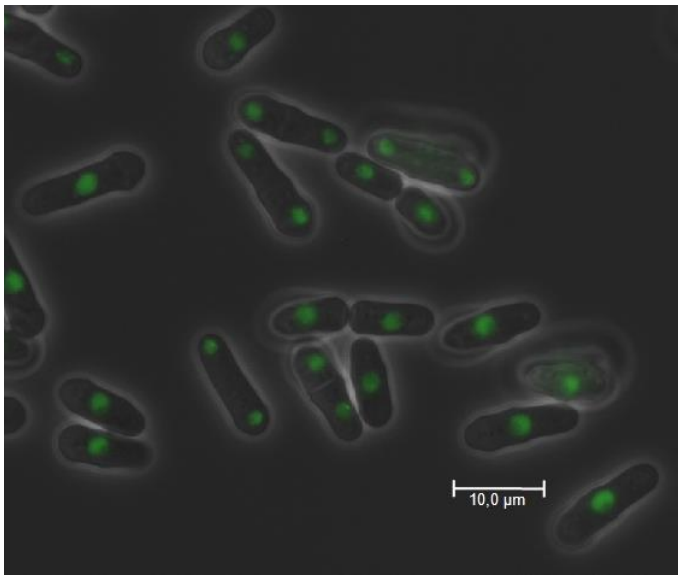

Figure 1.1. Merged phase contrast and fluorescence microscopy picture of *Schizosaccharomyces pombe.* Fission yeast cells expressing GFP-fused nuclear protein. Scale bar indicates 10.0 µm.

Generally fission yeast remains in a haploid cell (1n); however, a transient diploid state (2n) can also be observed in sexual differentiation and maintained under specific conditions. The haploid state of fission yeast makes it easy to isolate recessive mutations as well as to perform genetic manipulation (PombeNet at Forsburgs Lab).

The genome of fission yeast consists of three different chromosomes of a rather small total size (13.8 Mb). 4824 protein-coding genes are distributed on the chromosomes. Analysis of fission yeast genome which was sequenced in 2002 has revealed that 50 genes share significant similarity with human disease genes, and half of these 50 genes are cancer related (Wood et al., 2002). Compared to another popular model organism *S. cerevisiae,* the budding yeast*,* fission yeast holds not only a large number of conserved genes with humans, but also shares similarity in chromosome structure and RNAi machinery with humans (Kniola et al., 2001; Martienssen et al., 2005). With the aid from well-established molecular genetics tools, the physiological characteristics make fission yeast an ideal model organism for molecular cell biology study with respect to its relevance to higher eukaryotes. Substantial work has been carried out in recent decades on fission yeast, and Sir Paul M. Nurse was awarded the Nobel Prize in Physiology or Medicine in 2001 jointly with Leland H. Hartwell and Tim Hunt for his discoveries of key regulators of the cell cycle by studies in fission yeast (Nobelprize.org - Nobel Prize in Physiology or Medicine 2001).

1.2 The eukaryotic cell cycle

A range of highly ordered events take place during the proliferation of an eukaryotic cell leading to an increase in mass and duplicated chromosomes, then separating into new individuals, and this process is termed cell cycle. Eukaryotic cells have two distinguishable cell cycles namely mitosis and meiosis. Meiosis is a special nuclear division and happens only when gametes or spores need to be generated. The cells undergoing meiotic cell division have an important feature which is the genetic recombination between homologous chromosomes. In contrast, mitosis is the regular cell cycle. For fission yeast cells, they will keep undergoing mitotic cell cycle as long as a proper growing condition is given, and only under nutrient starvation will they entry a transient meiotic cell cycle in which they mate and sporulate (PombeNet at Forsburg's Lab).

A cell after one round of mitosis will generate two daughter cells containing identical chromosomes of the same number as those in the parent cell. For the maintenance of the homeostasis in an organism, the regulation of mitotic cell cycle is playing a significant role.

1.2.1 The mitotic cell cycle

In the mitotic cell cycle, a set of events take place in a defined sequence resulting in two daughter cells containing identical genetic content. A rigid control over the cell cycle is vital for the development from a fertilized egg into an organism as well as to maintain the growth of an organism. According to the central events, a cell cycle is divided into four stages namely G1 phase, S phase, G2 phase and M phase (Figure 1.2).

G1 phase is the start of a new cell cycle; it is the gap between the previous chromosome segregation and the next round of chromosome duplication. G1 phase is also the time for a cell making the decision of its fate: it can choose to grow in mass by undergoing the biosynthesis of proteins in preparation for S phase, or it may enter a quiescent state termed G0 phase. In addition, there is an important transition point in the G1-phase termed 'R-point' (restriction point), at which cells are committed to complete the cell cycle without growth factors (Pardee, 1974). A ''Start'' point approaching the R-point in function also exists in G1 phase in yeast (Nurse, 1975). S phase marks its onset when DNA synthesis commences, and ends when all chromosomes have been replicated (or multiplicated in the case of ploidy). After the completion of S phase, another gap termed G2 phase allows the cells continuing the growth in mass before the onset of M phase. M phase is a relatively short period in

which the chromatin becomes into condensed chromosomes in preparation for the karyokinesis (division of a nucleus). The karyokinesis is commonly but not necessarily accompanied by cytokinesis (division of cytoplasm). During M phase biosynthesis events are slowed down and sister chromatids become separated from each other into two identical subgroups. M phase is further divided into five distinguishable stages: prophase, prometaphase, metaphase, anaphase, and telophase.

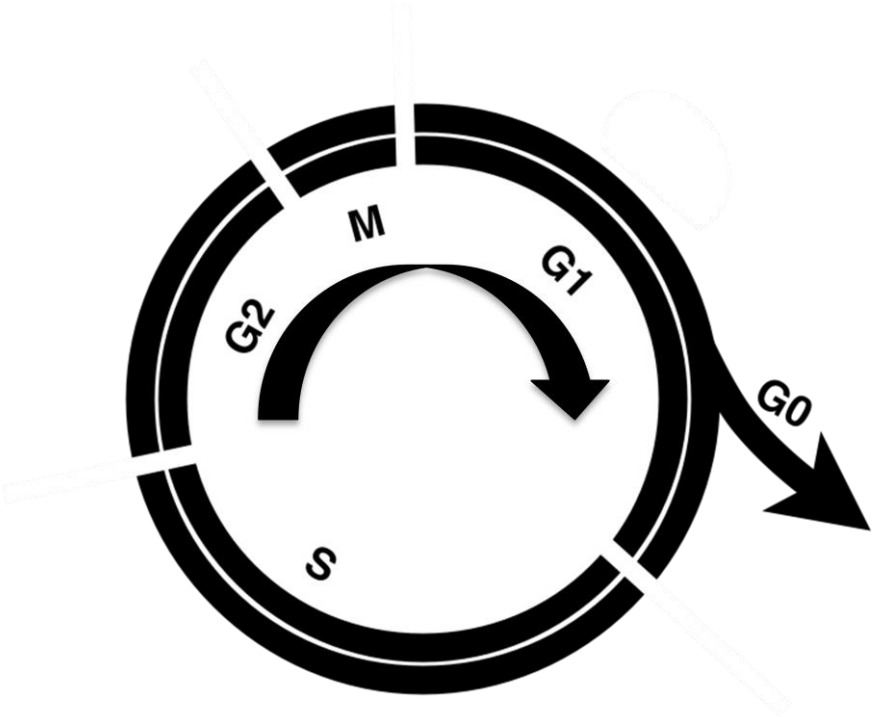

Figure 1.2. Schematic of a cell cycle. G0 = Gap 0, G1 = Gap 1, S = Synthesis, G2 = Gap 2, M = Mitosis. The arrow inside indicates the direction of the cell cycle. The arrow outside indicates the entry into a quiescent state.

1.2.2 The mitotic cell cycle of fission yeast

The mitotic cell cycle of fission yeast resembles that of higher eukaryotes; however, it differs in the length of each phase. During vegetative growth, almost 70% of the time in the cell cycle is distributed to G2 phase while the remaining time is shared by G1, S and M phase (reviewed in (MacNeill and Fantes, 1997; Nurse, 1997)). A diagram of fission yeast mitotic cell cycle is depicted in Figure 1.3. As diagrammed, the fission yeast cell cycle has another peculiar feature in which the timing for karyokinesis and cytokinesis is different. The nuclear division is finished by the end of mitosis, while the formation of septum occurs in G1 phase and followed by cytoplasmic segregation in S phase. This special phenomenon in fission yeast implies that under a natural vegetative growth condition, a new round of DNA synthesis has already occurred

prior to that two daughter cells come into being. Therefore when subjecting a log-phase fission yeast population, in which the majority of cells are in G2 phase, to flow cytometry for DNA content analysis (Figure 1.4), a main peak representing cells containing 2C DNA content (doubled genome) is shown in the histogram, and a bump representing a small fraction of S phase cells undergoing DNA synthesis and cytokinesis simultaneously.

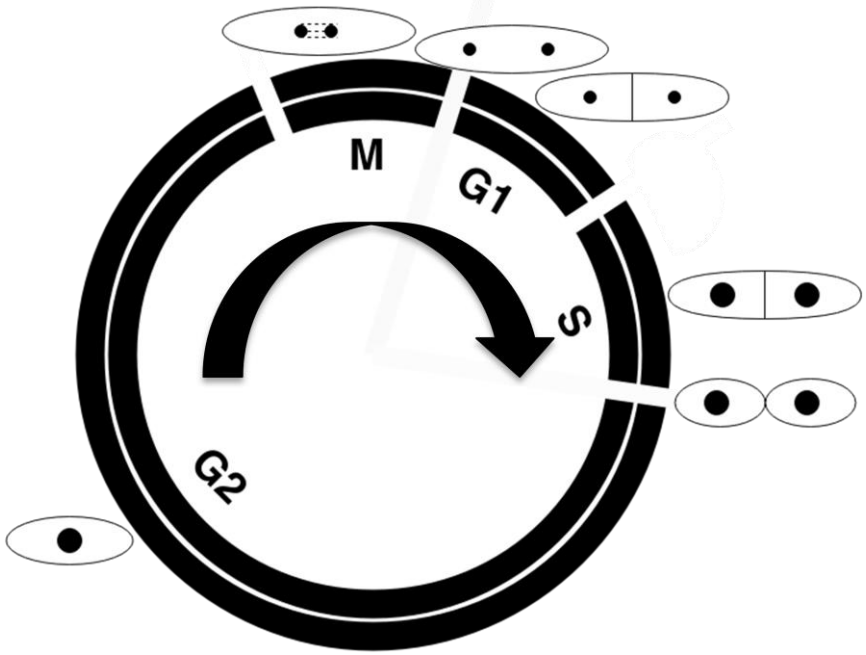

Figure 1.3. Schematic of the cell cycle of fission yeast. The G2 phase is very long and takes 70% of the time of a cell cycle, the remaining three phases are short and each takes almost 10% of the time. The arrow inside indicates the direction of the cell cycle. The oval shapes represent fission yeast cells in different phases and the sizes of dots represent different DNA contents. The cell at the M/G1 transition has finished the karyokinesis and contains 2C DNA content (doubled genome), while the cytokinesis happens later. The G1-phase cell has two nuclei and each contains 1C DNA content, the septum is still formed in G1. The S-phase cell is undergoing DNA synthesis and contains 2C-4C DNA content. The cell at the S/G2 transition has finished the cytokinesis and DNA synthesis, therefore each daughter cell contains 2C DNA content. The G2-phase cell is growing in size. The M-phase cell is undergoing karyokinesis, and the dotted lines indicate microtubules.

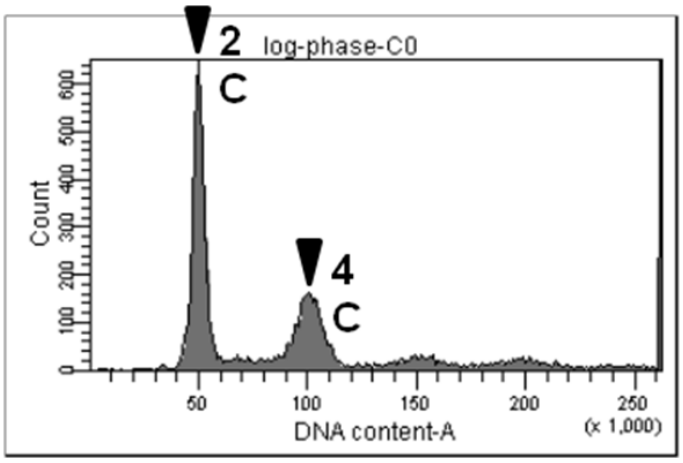

Figure 1.4. Flow cytometry histogram of log-phase fission yeast cells. The horizontal axis represents DNA content and the vertical axis represents the number of cells. The majority of log-phase cells are in G2 phase, and accordingly, the main peak represents cells containing 2C DNA content. A small fraction of S phase cells undergoing DNA synthesis and cytokinesis simultaneously are represented in the 4C bump. No cells containing 1C DNA content can be observed in the log-phase culture.

1.3 Regulation of the cell cycle

In a cell cycle, the main task is to replicate chromosomes faithfully, and then segregate them equally into two daughter cells. This task is brought out with the help from the periodic expression of a high proportion of proteins that play discrete roles at different phases (Breeden, 2003). In fission yeast, 407 periodically expressed genes have been identified, among which 136 genes show high-amplitude changes of expression (Rustici et al., 2004).

The timing for all the cell-cycle events must be regulated precisely. Lost control of the cell cycle brings dire consequences to a cell such as genetic mutations, morphological transformation and unrestrained proliferation.

Cdks (cyclin-dependent-kinases) and checkpoints are playing crucial roles in regulating the progression of the cell cycle. Different Cdks pairing with their cyclin partners drive the transition of different cell-cycle phases to the next when the condition is fulfilled (Morgan, 1995). Checkpoints monitor the completion of cell-cycle events and convey their message when activated through signaling pathways (Hartwell and Weinert, 1989).

1.3.1 Cdks and cyclins

A Cdk takes action by forming a cyclin-dependent kinase complex (CDKC) together with its corresponding regulatory subunit cyclin. Cyclins help increase the enzymatic

activity of the Cdks dramatically and guide the CDKCs to the appropriate substrates. In mammalian cells four Cdks and four types of cyclins have been identified to be involved in cell cycle regulation, whereas in fission yeast there is only one Cdk, namely Cdc2, which is the homology of mammalian Cdk1 and budding yeast Cdc28 (Lee and Nurse, 1987). Cdc2 regulates the cell cycle by associating with four distinct cyclins: Puc1 and three B-type cyclins (Cdc13, Cig1and Cig2) (Martin-Castellanos et al., 1996). One important feature of most cyclins is that their expression is fluctuating during the cell cycle to oscillate the activity of CDKCs, while the expression of Cdks is relatively stable.

As depicted in Figure 1.5, four cyclins carry out their distinct duties throughout the cell cycle upon binding to Cdc2 in fission yeast. Cdc2/Puc1 is known to play an important role in regulating the duration of G1 phase in response to cell size (Martin-Castellanos et al., 2000). Cdc2/Cig1 functions in promoting the cell cycle progression from G1 to S (Bueno et al., 1991). Cdc2/Cig2 has been shown to introduce the onset of S phase (Mondesert et al., 1996). Cdc2/Cdc13 initiates mitosis, and it is also important for DNA replication when Cig2 loses its function (Booher and Beach, 1987; Mondesert et al., 1996). In addition, it has been shown that Cdc2/Cdc13 is essential for determining the temporal order of S phase and M phase by blocking DNA re-replication (Hayles et al., 1994).

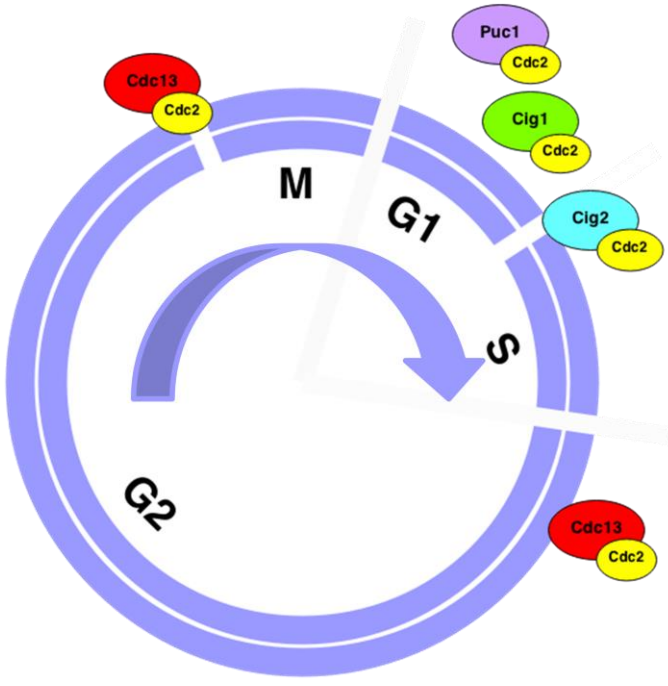

Figure 1.5. Regulation of fission yeast cell cycle by Cdc2 and cyclins. Cdc2/Puc1 and Cdc2/Cig1 regulate G1 phase, Cdc2/Cig2 promotes the onset of S phase, Cdc2/Cdc13 promotes the initiation of M phase and blocks DNA re-replication. The arrow inside indicates the direction of the cell cycle.

In addition to the regulation by cyclins, there are two negative regulation mechanisms of Cdk activity, one is the inhibition by Cdk inhibitors (CKIs) and another one is the inhibitory phosphorylation of Cdks by kinases. These two mechanisms cooperate with the regulation by cyclins to fine-tune Cdk activity throughout a cell cycle. In fission yeast, there is a single CKI, Rum1, which acts on mitotic Cdc2/Cdc13 to ensure the correct timing of S phase and M phase (Benito et al., 1998; Correa-Bordes and Nurse, 1995); and two inhibitory kinases, Mik1 and Wee1, which continue to keep the low activity of Cdc2/Cdc13 during S phase and G2 phase through phosphorylating on Tyr15 of Cdc2 (Lundgren et al., 1991; Russell and Nurse, 1987).

1.3.2 Checkpoints

To monitor the completion of cell-cycle events, surveillance mechanisms termed checkpoints are distributed at different stages throughout a cell cycle. According to their distinct duties, checkpoints are classified into four subgroups which are in response to DNA damage, DNA replication perturbation, improper spindle assembly and abnormality in cytoskeleton respectively (http://eishinoguchi.com/checkpoint).

DNA damage is one of the most common cellular events, and DNA damage activated checkpoint usually result in a temporary arrest of the cell cycle allowing time for DNA-repair. Protein factors involved in checkpoints triggered by DNA damage can be classified into four categories, namely sensors, mediators, transducers and effectors (reviewed in (Niida and Nakanishi, 2006)). In fission yeast, there are three checkpoints in response to DNA damage: G1/S checkpoint, intra-S checkpoint and G2/M checkpoint.

Activated checkpoints trigger a cascade of signaling events halting the cell cycle so that the cell has the time for undergoing rescue events; mostly the cell cycle is stalled via the regulation of Cdk activity, but there also exist Cdk-independent checkpoint mechanisms. Previous work from our group has identified a novel DNA damage-responding G1/S checkpoint involving Gcn2 kinase in fission yeast, and this checkpoint blocks G1/S transition by delaying pre-RC formation (Nilssen et al., 2003; Tvegard et al., 2007). However, the molecular mechanism of how Gcn2 is activated and how this checkpoint carries out its downstream events requires elucidation.

1.3.2.1 Gcn2 kinase

Gcn2 (general control non-derepressible 2) was originally described in budding yeast, it is a serine/threonine kinase which senses amino acid starvation. Under amino acid starvation, Gcn2 is activated and phosphorylates eIF2α, a component of the ternary complex which is essential for translation initiation, and thereby inhibits the formation of the ternary complex (Ramirez et al., 1991). Activated Gcn2 leads to a downregulation of global protein translation except for some selected candidates such as Gcn4 (Hinnebusch, 1993). Recent work has revealed that Gcn2 also has a central role in the UVC irradiation-induced G1/S checkpoint mechanism in fission yeast (Tvegard et al., 2007). And this checkpoint does not only respond to UVC irradiation which causes DNA lesion, it also can be activated by other cellular stresses caused by MMS (methyl methane sulfonate) and H_2O_2 (Krohn et al., 2008). This evidence implies that including the role in sensing amino acid starvation and G1/S checkpoint, Gcn2 may also be an essential module in regulating multiple pathways.

1.4 G1/S transition

Maintaining the integrity of the genome is one of the most important events within a cell cycle. During mitosis the chromatin is condensed into chromosomes and biosynthesis events are slowed down, therefore in G1 phase, cells need not only to lose the tight structure of chromosomes to make them become accessible to the replication machinery, and they also need to start biosynthesis in preparation for DNA synthesis. In S phase, once DNA synthesis has started, cells have to guarantee that DNA is replicated with high fidelity and the replication occurs only once within the cell cycle. Therefore choosing the correct timing for S phase entry is vital to a cycling cell.

The main task addressed here is how a cell determines the timing for G1/S transition. To start S phase at the right timing, cells undergo highly ordered actions step by step, and all factors involved in these steps have to show up in an available form and sufficient amount when they are required. The incoordination of a single factor can affect a sequence of events after it, and thereby changes the timing for G1/S transition. In response to extracellular environment, cells are balancing the inter-cooperation among these factors in real time at different levels such as transcriptional level, translational level and post-translational level et al.

1.4.1 Cdc10 transcription factor

Most events in G1 phase start with protein synthesis, and in fission yeast Cdc10 is a core transcription factor required by the transcription of several G1 and S phase-

specific genes that are important for DNA replication initiation. *Cdc10* shares region of homology with *SWI4* and *SWI6* in budding yeast, the products of the later two genes are also transcription factors regulating periodic expression of G1-specific genes (Andrews and Herskowitz, 1989; Breeden and Nasmyth, 1987; Johnston and Lowndes, 1992; Nasmyth and Dirick, 1991). Target genes of Cdc10 are *cdt1*, *cdc18* (homolog of *cdc6* in budding yeast and mammalian cells), *cdt2*, *cdc22*, *mik1* and *cig2*, and protein products of all these genes are playing important roles for G1/S transition (Hofmann and Beach, 1994; Johnston and Lowndes, 1992; Nasmyth and Nurse, 1981; Nguyen et al., 2001). A temperature sensitive mutation of *cdc10* termed *cdc10-M17* was discovered by Kim Nasmyth and Paul Nurse in 1981. This mutant becomes inactivated at restrictive temperature (36°C) and functions normally again when being placed back at permissive temperature (25°C). The *cdc10-M17* mutation has been widely employed in many cell cycle studies carried out on fission yeast.

1.4.2 DNA replication initiation

DNA replication initiation is the first front before DNA replication. This process involves the cooperation and coordination of multiple initiation protein factors, they start the assembly of replication machinery from late mitosis and throughout G1 phase at specific DNA sequences termed replication origins (Takeda et al., 2005). The stepwise mechanisms of DNA replication initiation in bacteria, archaea and eukaryotes are conserved, but the complexity of them differs. Furthermore, archaea and eukaryotes share homologous system for DNA replication initiation, while bacteria share no homology but analogy (Aves, 2009; Bell and Dutta, 2002). So far our knowledge of eukaryotic DNA replication initiation is still lacking many details (Kelly and Brown, 2000; Moser and Russell, 2000; Tabancay and Forsburg, 2006). To have a better understanding of the whole process of DNA replication, it is highly demanded to have deeper perspectives into the distinct roles of each initiation factor, as well as the cross-linked regulation network among these factors over DNA replication initiation.

A detailed figure depicting the process of DNA replication initiation in fission yeast is shown here (Figure 1.6). DNA replication initiation starts from late mitosis when the origin recognition complexes (ORCs) bind to replication origins in an ATP-dependent manner. The binding of ORCs is essential for the subsequent joining of Cdc18 and Cdt1 from late M phase and the recruitment of these two factors are required for the loading of MCM2-7 (mini chromosome maintenance complex 2-7). At this point, a key intervening process termed replication origin licensing is completed upon the loading of ORC and the three licensing factors: Cdc18, Cdt1 and MCM2-7. Replication origin licensing makes origins competent for replication. The complex resulted from the

licensing process is termed pre-replication complex (pre-RC) which is a key intermediate in DNA replication initiation. The licensed origins will recruit additional factors which then become phosphorylated by different regulatory factors. Lastly, Cdc45 and GINS (GINS functions to activated MCM2-7 was described after this figure was published, therefore it is not shown in Figure 1.6), two cofactors which activate the MCM2-7 complex, are loaded marking the completion of the formation of pre-initiation complex (pre-IC). The pre-IC is accessible for primase, DNA polymerase, enzymes that are essential for the elongation step of DNA synthesis (Boye and Grallert, 2009; Ilves et al., 2010).

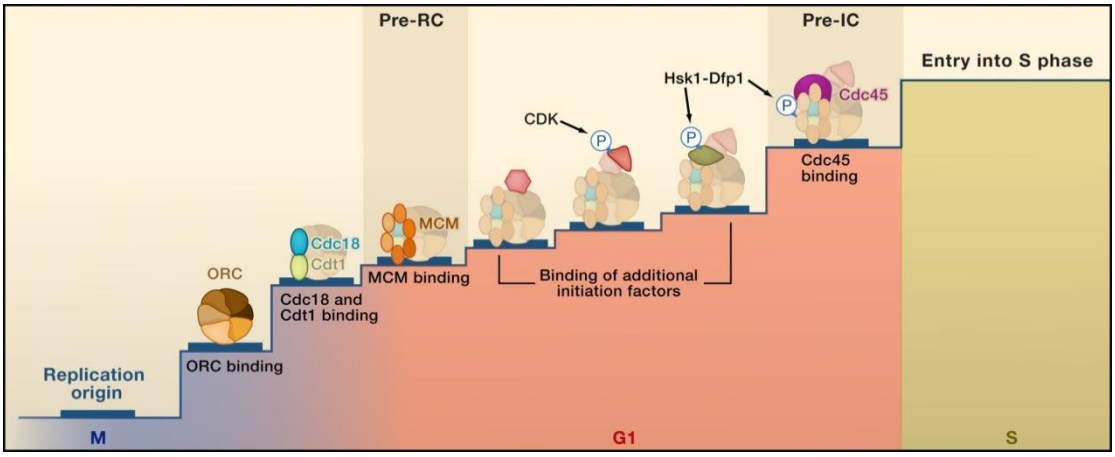

Figure 1.6. The process of DNA replication initiation in fission yeast. The origin recognition complex ORC first binds to the replication origin in late mitosis allowing the binding of Cdc18 and Cdt1. Then MCM2-7 is recruited completing the pre-RC formation and marking the replication origin is licensed. Several additional initiation factors bind to the pre-RC and some of them get phosphorylated by CDK or Hsk1-Dfp1. After the loading of Cdc45 and GINS (GINS is not shown in this figure) which activate MCM2-7, the formation of pre-IC is completed. The replication origin is then ready for the loading of primase, DNA polymerase and enzymes that are essential for DNA replication in S phase. (Boye and Grallert, 2009)

1.4.3 The pre-RC

The formation of the pre-RC by ORC, Cdc18/Cdc6, Cdt1 and MCM2-7 in G1 phase licenses replication origins, it is an essential mechanism for regulating DNA synthesis to only once per cell cycle as well as preventing re-replication of DNA (Diffley, 1996; Tada and Blow, 1998). First the pre-RCs are formed on many replication origins with the loading of inactivated MCM2-7 complexes, the MCM2-7 complexes are then activated on some but not all origins; activated MCM2-7 complexes inhibit further loading to excess MCM2-7 complexes, and therefore re-replication at the same origin is prevented.

ORC, a six-subunit complex, is the very first protein associating with the DNA and essential for the recruitment of other factors onto the chromatin. It is conserved among all studied eukaryotic model organisms (Gilbert, 2001), but the association

between ORCs and replication origins differs (Bell and Dutta, 2002). In fission and budding yeast, ORC stays with the origin throughout the cell cycle with specific subunit(s) which are modified differentially during different phases (Aparicio et al., 1997; Diffley et al., 1994; Lygerou and Nurse, 1999; Nguyen et al., 2001; Remus et al., 2005). One study on fission yeast has shown that ORC controls DNA replication initiation through the interaction between one of its subunits Orc1 with Cdc18 and Cdc21 (*cdc21* is the fission yeast homolog of *mcm4*) *in vivo* (Grallert and Nurse, 1996). In mammalian cells and *Xenopus* egg extracts, Orc1/ORC only binds to the chromatin from late mitosis and dissociates from the chromatin when the cell is finishing DNA synthesis (Li and DePamphilis, 2002; Romanowski et al., 1996; Sun et al., 2002). It is suggested that ORC functions not only to recruit other factors onto the chromatin, it is also important for selecting origins. Another study carried out in fission yeast has found that the origins which recruit ORCs with higher affinity with early timing outcompete other origins, thus become more frequently fired during S phase (Wu and Nurse, 2009).

After ORC is loaded, two licensing factors Cdc18/Cdc6 and Cdt1 are recruited to the origin. They are characterized as accessory proteins that are accumulated from late mitosis and throughout G1 in the nucleus. It is known that Cdc18/Cdc6 and Cdt1 are essential for the assembly of MCM2-7 complexes, however the mechanisms underlying how Cdc18/Cdc6 and Cdt1 function require more profound studies. MCM2-7 is important for unwinding double-stranded DNA and is the lastly loaded licensing factor before the completion of pre-RC formation. This study will particularly focus on Cdt1 and MCM2-7.

1.4.3.1 Cdt1

Cdt1 is a protein lacking enzymatic activity, its encoding gene *cdt1* is under the control of the transcription factor Cdc10 (Hofmann and Beach, 1994). In normal cycling fission yeast cells the protein level of Cdt1 peaks from G1 phase until the onset of S phase (Gopalakrishnan et al., 2001; Nishitani et al., 2000). Given the pre-condition that ORC has bound to the replication origin, Cdt1 cooperates with Cdc18/Cdc6 to load MCM2-7 onto the chromatin, and this cooperation is suggested to be conserved in all eukaryotes. In mammalian cells, Cdt1 has been shown to associate with DNA directly (Yanagi et al., 2002).

The cruciality of Cdt1 is reflected on its essential role in forming pre-RC, and the relationship between the regulation of its expression and DNA re-replication. In fission yeast, overexpression of Cdc18 alone (Nishitani and Nurse, 1995), or both Cdc18 and Cdt1 induces re-replication at the same origins (Nishitani et al., 2000). Expression of both Cdc18 and Cdt1 in G2 fission yeast cells induces uncontrolled re-

firing of replication origins, presumably because Cdt1 stabilizes Cdc18 on the chromatin (Yanow et al., 2001). In contrast, overexpression of Cdc6 alone in cancer cells induces very subtle re-replication, however when Cdt1 is overexpressed with or without Cdc6, robust re-replication was observed (Vaziri et al., 2003). These discoveries imply that Cdt1 is a vital regulatory factor in DNA replication, thus a precise control of the protein level and the timing for expression of Cdt1 is required to maintain the normal proliferation of cells.

In order to restrict DNA replication to only once per cell cycle, higher eukaryotes modulate Cdt1 activity by utilizing Cdt1 inhibitor geminin (Cook et al., 2004; McGarry and Kirschner, 1998; Wohlschlegel et al., 2000) and proteolysing Cdt1 in parallel with DNA replication by $CDL4^{Cdt2}$-mediated ubiquitylation in a PCNA-dependent manner (Arias and Walter, 2006; Li et al., 2003; Nishitani et al., 2004; Senga et al., 2006); in S and G2 phase Cul4-Skp2 is predominantly mediating the degradation of Cdt1 (Nishitani et al., 2006). While in fission yeast, it has been shown that DNA damage induces the proteolysis of Cdt1 depending on $Cul4\text{-}Ddb1^{Cdt2}$ -mediated ubiquitylation, and this ubiquitylation occurs via the modulation of dual PIP degrons in Cdt1 by PCNA (Guarino et al., 2011; Ralph et al., 2006). It seems to be a conserved mechanism in eukaryotes that Cdt1 is proteolysed in response to DNA damage (Hall et al., 2008; Higa et al., 2003; Kearsey and Cotterill, 2003).

1.4.3.2 Loading of MCM2-7

MCM2-7 has been characterized as a putative DNA helicase or the core of DNA helicase (Ishimi, 1997; Remus and Diffley, 2009). The six-subunited ring structure of MCM2-7 complex is highly conserved in all eukaryotes, and each subunit is thought to have its unique function given the fact that deletion of any single MCM gene leads to lethality in both budding and fission yeast (reviewed in (Bell and Dutta, 2002; Dutta and Bell, 1997; Kelly and Brown, 2000)). For instance, a study on budding yeast has shown that one MCM2-7 subunit, MCM3, has a conserved C-terminus domain which is essential for interacting with ORC-Cdc6 and stimulating the ATPase activity of ORC-Cdc6, and is also required for the recruitment of Cdt1–MCM2–7 to ORC–Cdc6 (Frigola et al., 2013).

With the help from the two licensing factors Cdc18/Cdc6 and Cdt1, MCM2-7 is loaded onto replication origin to form pre-RC. A study on budding yeast has found that at each ORC-bound origin, two Cdt1 molecules are required for loading two MCM2-7 complexes (Takara and Bell, 2011). Unlike the cell-cycle phase-specific expression of Cdc18/Cdc6 and Cdt1, MCM2-7 is constantly expressed throughout the cell cycle. By the end of DNA replication initiation, MCM2-7 is activated by Cdc45

and GINS which culminate the end of this process, and thereby the transition from G1 to S phase is committed.

1.5 DNA damage and UVC irradiation

Both endogenous and exogenous DNA damage occurs in cells all the time. Endogenous DNA damage can be the consequence of the side-effect from metabolic activities (McCulloch and Kunkel, 2008), whilst exogenous DNA damage may happen when a cell is exposed to agents such as UV irradiation, certain chemicals and ionizing radiation.

The most potent DNA-damaging agent UV light (100-400 nm) is classified into three classes according to the wavelength. UVA (315-400 nm) and UVB (280-315 nm) have longer wavelength and they can cause oxidative stress and protein denaturation in cells; UVC (100-280 nm) has shorter wavelength and higher energy, thus is more harmful to cells. A predominant damage induced by UVC is the formation of cyclobutane pyrimidine dimers (CPDs) (Figure 1.7) and helix-distorting 6-4 photoproducts (6-4 PPs) (Ravanat et al., 2001).

Unrepaired DNA damage risks the fate of a cell with many possibilities among which the carcinogenic transformation is the most notorious one. In order to maintain genome integrity, cells are equipped with multiple DNA-damage responding mechanisms such as checkpoints and DNA repair pathways.

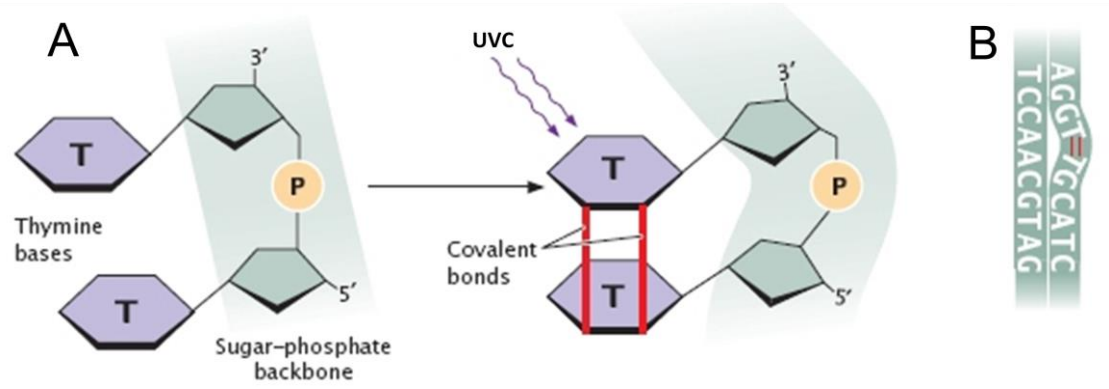

Figure 1.7. UVC irradiation induces the formation of a cyclobutane pyrimidine dimer (CPD). (A) Formation of cyclobutane thymine dimer by two adjacent thymine bases in DNA after UVC irradiation. (B)A bulge is made by the formation of the CPD and results in distorted DNA molecule which cannot function properly. (Freeman, 2005)

1.6 Background

Previous work in our lab has identified the Gcn2-dependent G1/S checkpoint in fission yeast, and the activation of this checkpoint by UVC irradiation leads to delayed pre-RC formation, which consequently delays G1/S transition (Nilssen et al., 2003; Tvegard et al., 2007); however, the molecular mechanisms of upstream and downstream events of the delayed pre-RC formation are not yet clear (Figure 1.8).

Using different model organisms, a number of studies on the pre-RC components have provided evidence showing that perturbed regulation of these factors can lead to genome instability. Therefore it is vital for a cell to carry out tight control over pre-RC components in response to different cellular stresses.

Cdt1, one of the pre-RC components, has been shown to be downregulated, modified, inhibited or degraded in response to DNA damage in different model organisms (Costanzo et al., 2003; Hu et al., 2004; Hu and Xiong, 2006; Tada, 2007). The negative regulation of Cdt1 after DNA damage seems to be conserved among eukaryotes. However, the connection between the regulation of Cdt1 in response to DNA damage and pre-RC formation is poorly studied.

In this study, by employing fission yeast as our model organism, we shall explore the downstream events after the activation of the Gcn2-dependent G1/S checkpoint by UVC irradiation. We shall particularly focus on the regulation of Cdt1 and the impact of changes in Cdt1 level on the kinetics of pre-RC formation.

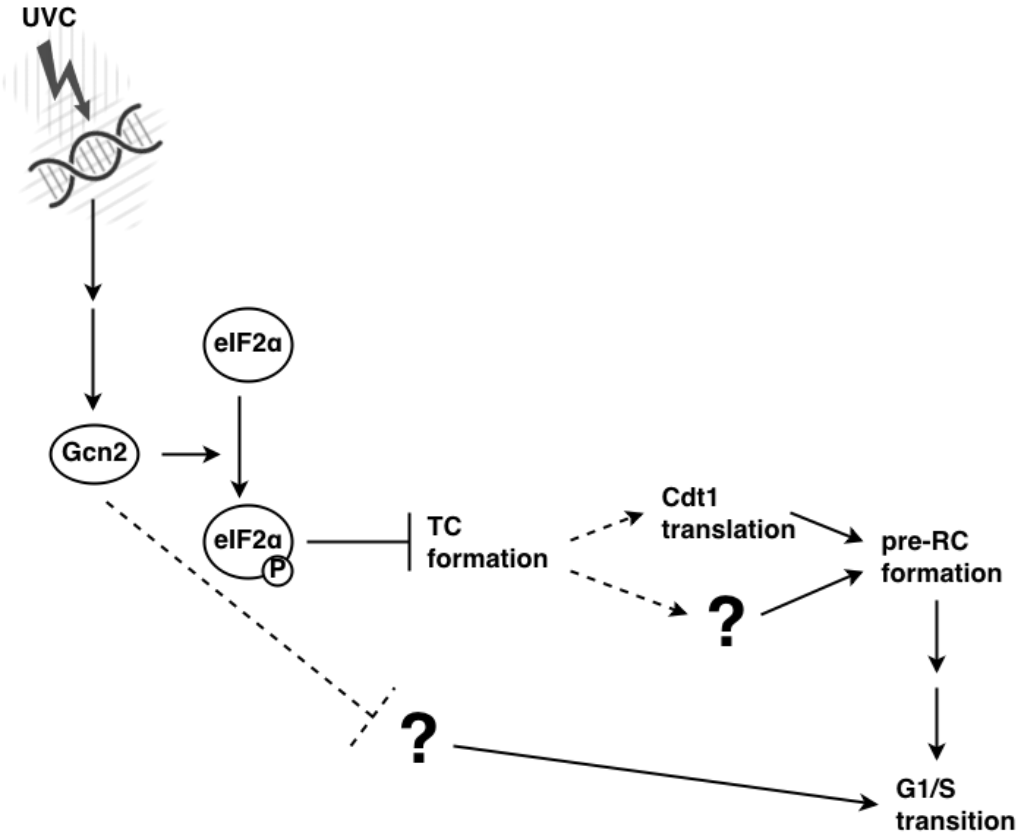

Figure 1.8. A current model for the Gcn2-dependent G1/S checkpoint in fission yeast. The checkpoint is activated by UVC irradiation and consequently delays G1/S transition. The delayed G1/S transition has shown to be a consequence of delayed pre-RC formation, which is presumably due to the Gcn2-dependent downregulation of global protein translation which includes the translation of Cdt1. However, Gcn2 may also function through other pathways to regulate G1/S transition.

2 AIM OF STUDY

The main goal of this work is to investigate the relationship between Cdt1 level and pre-RC formation after the activation of G1/S checkpoint by UVC irradiation in fission yeast. Our hypothesis is that Cdt1 level is limiting for pre-RC formation after UVC irradiation in early G1 phase. To test this hypothesis, the strategy described below was followed:

1. Investigate Cdt1 level in cells after UVC irradiation in early G1 phase in the presence and absence of Gcn2.

2. Generate a strain in which the Cdt1 level can be elevated after UVC irradiation.

3. Measure the pre-RC formation after UVC irradiation of Cdt1-overexpressing cells, and compare the result with the pre-RC formation in non-irradiated cells.

4. Investigate whether further elevated Cdt1 level could increase pre-RC formation after UVC irradiation.

3 MATERIALS

3.1 Fission yeast strains

Fission yeast strains listed below (Table 3.1) were used in this study.

Table 3.1. Fission yeast strains. Strain 19 and 20 were used for identifying the mating type of strains made by genetic cross. Strain 983 carrying *GFP*-tagged *cdc21*, and *cdc21* is the fission yeast homolog of *mcm4.*

Strain	Referred to as	Genotype	Source
19		*L972 h-*	Lab collection
20		*h+ SA21*	Lab collection
489		*cdc10-M17 h-*	Lab collection
983	*cdt2+*	*cdc10-M17 cdc21-GFP h-*	Lab collection
1187		*cdc10-M17 cdt1-18myc ura4-D18 leu1-32 h-*	B. Grallert
1237	*wt*	*cdc10-M17 cdt1-TAP:kanR leu1-32 h+*	Lab collection
1238	*gcn2Δ*	*cdc10-M17 gcn2::ura4+ cdt1-TAP:kanR ade6-M210 ura4-D18h-*	Lab collection
1253	*wt*	*cdt1:cdt1-TAP:kanR cdc10-M17 ade6-M210 ura4-D18 leu1-32 h-*	T. Tvegård
1830	*cdt2+*	*cd10-M17 mcm7:GFP:natMX6 h-*	B. Grallert
1906		*cdt1:cdt1-TAP:kanR cdc10-M17 hpz1::natMX6 ura4-D18? leu1-32?*	C. A. Bøe
1920		*leu1:nmt41.cdt2 cdt2::ura4+ ura4-D18 h-*	O. Nielsen
1942	*nmt41.cdt2*	*leu1:nmt41.cdt2 cdt2::ura4+ ura4-D18 cdc10-M17 cdt1:TAP:kanR h-*	This study
1943	*nmt41.cdt2*	*leu1:nmt41.cdt2 cdt2::ura4+ cdc10-M17 cdt1:TAP:kanR h-*	This study
2015	*nmt41.cdt2 mcm2:GFP*	*mcm2:GFP:natMX6 leu1:nmt41.cdt2 cdt2::ura4+ cdc10-M17 cdt1:TAP:kanR h-*	This study
2016	*nmt41.cdt2 mcm6:GFP*	*mcm6:GFP:natMX6 leu1:nmt41.cdt2 cdt2::ura4+ cdc10-M17 cdt1:TAP:kanR h-*	This study

3.2 Plasmid and primers

3.2.1 Plasmid

The plasmid shown below was used in this study for amplifying transforming DNA by general PCR (Figure 3.1).

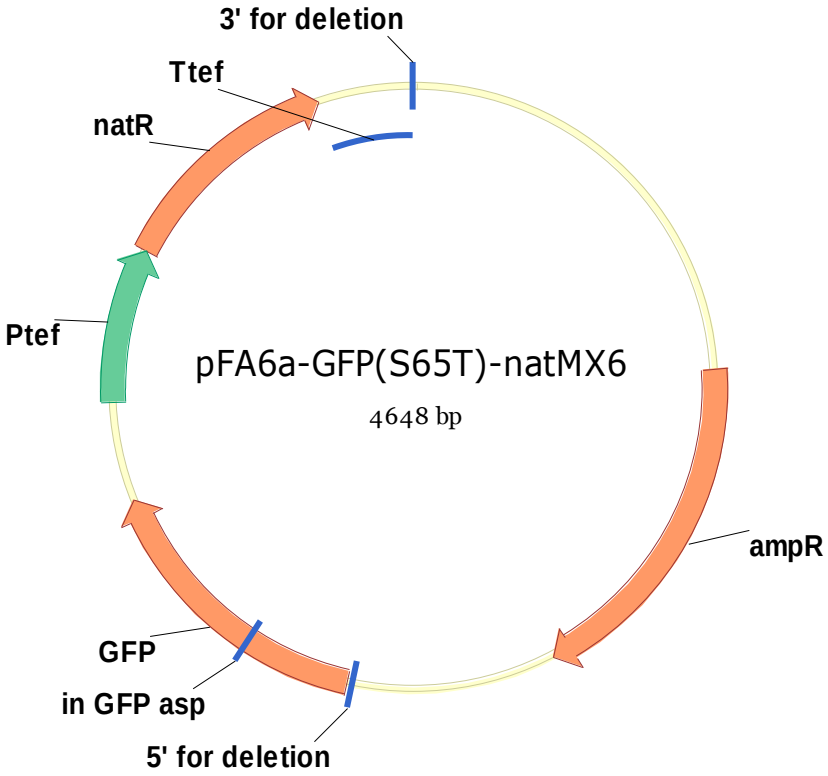

Figure 3.1. Map of plasmid # 309: pFA6-Gfp(S65T)-natMX6.

3.2.2 Primers

Primers listed below were used in this study. Primers listed in Table 3.2 were used for amplifying different transforming DNA from the plasmid (Figure 3.1) by general PCR. Primers listed in Table 3.3 were used for screening for successful transformants by colony PCR.

Table 3.2. Hybrid tagging primers for amplifying different transforming DNA from the plasmid. The sequence written in lowercase (20 nt) is complementary to the sequence in the plasmid, the sequence written in uppercase (80 nt) is the homologous sequence for targeting the transforming DNA at the right locus of the genome.

Primer name	Direction	Sequence 5' - 3'	Supplier
Mcm2 tagging primer	**Forward**	TGATTATTGATTCCTTTGTGAATGCC CAAAAAATGAGTGTTAAACGAAGTTT GTCAAGAACATTTGCTAAATATCTTAT T - cggatccccgggttaattaa	DNA technology A/S
Mcm2 tagging primer	**Reverse**	ACAGATGCAGTAACAAAAGGAGGGT CAAAGAACGGGGAAATCAAAATCACT GGACTCCATAAACTGATTGTGTCAAA AAA - gaattcgagctcgtttaaac	DNA technology A/S
Mcm6 tagging primer	**Forward**	TTCCTTTTGAAGAACGCGTATTTTCA ATACACCCTAACTGTGACATTGATGC TCTACTGAGCAATGGCGATGTTCCG AAC - cggatccccgggttaattaa	DNA technology A/S
Mcm6 tagging primer	**Reverse**	AACAATTAATGTCAGGTCTGTTTCAA AAATACGCCTCACTGATAAAACTTAT AAGAGATCGTTACGAATCTTTTATAA CC - gaattcgagctcgtttaaac	DNA technology A/S
Mcm7 tagging primer	**Forward**	ATACAGACCTTGGTGTTCTTTTAACT ACAAACAATGGTCAAACAATAATGTT CCTCGATCCGGATTTACATATGGAGA AT - cggatccccgggttaattaa	DNA technology A/S
Mcm7 tagging primer	**Reverse**	ATTTCTATAGGTTGTAAATTAGCTTAA AGCAATTAATTGGCAGAAAAATTAAA TGATAGGAGTTATCTATTAGTAAATT G - gaattcgagctcgtttaaac	DNA technology A/S

Table 3.3. Primer used in colony PCR for screening for Hybrid tagging primers for successful transformants.

Primer name	Direction	Sequence 5' - 3'	Supplier
Mcm2 checking primer	**Forward**	TACTGTGCGTCATCTGGAGTCT	DNA technology A/S
Mcm2 checking primers	**Reverse**	CCCTTTAAATTTGGAAATGGAC	DNA technology A/S
Mcm6 checking primer	**Forward**	TGGCAATGATAATGTTTCTTCG	DNA technology A/S
Mcm6 checking primer	**Reverse**	GAACAGTCTCACCCTTCCTTTG	DNA technology A/S
Mcm7 checking primer	**Forward**	ATAGAGTGGAGATTGGCGATT	DNA technology A/S
Mcm7 checking primer	**Reverse**	ATGGTCCTTCCAAATCTAACGA	DNA technology A/S

3.3 Enzymes

Enzymes listed in Table 3.4 were used for PCR (DreamTaq PCR Master Mix (2X) and AccuPrime Pfx DNA Polymerase), genetic cross (S.H.P/H.PJ. Helix Pomatia Juice (helicase)), flow cytometry (Ribonuclease A) and MCM-chromatin binding assay (Zymolase) in this study.

Table 3.4. Enzymes used in this study.

Enzyme	Supplier
S.H.P/H.PJ. Helix Pomatia Juice (helicase)	Biosepra
Zymolase	Nakalai Tesque
Ribonuclease A	Sigma-Aldrich
DreamTaq PCR Master Mix (2X)	Thermo Scientific
AccuPrime Pfx DNA Polymerase	Invitrogen

3.4 Antibodies

Table 3.5. Antibodies used in Western blot for detecting proteins in this study.

Antibody	Antigen	Origin	Dilution	Supplier
Primary	α-tubulin	Mouse	1:30000	Sigma-Aldrich
	TAP	Rabbit	1:1000	Sigma-Aldrich
	Cig2	Mouse	1:1000	Abcam
Secondary	Anti-mouse IgG, HRP-linked Antibody	Horse	1:1000	Cell Signaling

3.5 Molecular weight standards

Molecular weight standards listed in Table 3.6 were loaded to the gel for estimating the size of protein or DNA in the sample. Pictures of the standards are provided in Appendix 2.

Table 3.6. Molecular weight standards used in this study.

Molecular weight standard	Range	Supplier
Precision Plus Protein Dual Color Standards	10 - 250 kDa	Bio-Rad
GeneRuler 1 kb DNA Ladder	250 - 10000 bp	Thermo Scientific

3.6 Chemicals and reagents

Table 3.7. Chemicals and reagents used in this study.

Chemical/reagent	Supplier
6X Orange loading dye	Fermentas
Acetone, Methanol	Merke
Acetic acid, Adenin, Agarose type 1, Bromphenol blue, DAPI, DMSO, DTT, EDTA, Glucose, Glycerol, HCl, KAc, KCl, Lithium acetate, NaF, NaCl, NaN_3, Peg 4000, SDS, Sorbitol, TCA, Thiamine, Tris, Triton X-100, Tween-20, Uracil	Sigma-Aldrich
10% Mini-PROTEAN TGX Gel, Any kD Criterio TGX Gel, Bio-safe Coomassie Brilliant Blue Stain, ECL substrate, ECL enhancer reagent, Ponceau S	Bio-Rad
ClonNAT	WERNER BioAgents
Ethanol	Kemetyl Norge AS
GelRed, Sytox green	Life Technologies
Membrane blocking agent	GE Healthcare
Protease Inhibitor Cocktail Tablets	Roche Applied Science
Sheared herring testes	Intergen

3.7 Kits

Table 3.8. Kits used in this study.

Kit	Supplier
AccuPrime Pfx DNA Polymerase	Invitrogen
DreamTaq PCR Master Mix (2X)	Invitrogen
Pierce BCA Protein Assay Kit	Thermo Scientific

3.8 Solutions

3.8.1 Fission yeast growth media and agarose plates

Growth media	Ingredients
YES medium	0.5 % yeast extract

	30 g/L glucose 250 mg/L histidine 250 mg/L leucine 250 mg/L adenine 250 mg/L uracil 250 mg/L lysine
EMM medium	32.3 g/L EMM Supplemented with: 80 µg/mL amino acids when needed
YES agar	YES medium supplemented with 20 g/L agarose
EMM agar	48.8 g/L EMM agarose
ME agar	30 % malt extract 20 g/L agarose
EMM agar with Phloxine B	EMM agar supplemented with 20 µg/mL Phloxine B
EMM agar with clonNAT	EMM agar supplemented with 100 µg/mL clonNAT
YES agar with Phloxine B	YES agar supplemented with 20 µg/mL Phloxine B

3.8.2. Buffers and other solutions

Solution	Ingredients
Agarose gel solution, 1%	1% agarose 1 x TAE buffer
DAPI/PBS mountant	50% glycerol 50% PBS 0.4 µg/mL DAPI
Denaturing sample buffer (1x) **(Laemmli sample buffer)** **For 8 mL**	0.5 mL 1 M tris-HCl pH 6.8 0.8 mL 100% Glycerol 1.6 mL 10% SDS 0.8 mL 1 M DTT 2 mL 0.1% Bromphenol blue Add MQ-H_2O to 8 mL

Denaturing sample buffer (2x)	1 mL 1 M tris-HCl pH 6.8
(Laemmli sample buffer)	1.6 mL 100% Glycerol
For 8 mL	1.6 mL 20% SDS
	1.6 mL 1M DTT
	0.2 mL 2% Bromphenol blue
	Add MQ-H_2O to 8 mL
EDTA pH 8.0 (0.5 M)	146.12 g/L EDTA
	NaOH to pH 8.0
EMM sorbitol pH 7.0	15 mM KH phthalate
	15 mM Na_2HPO_4
	90 mM NH_4Cl
	1.2 mM Sorbitol
	NaOH to pH 7.0
Extraction buffer	20 mM Pipes-KOH pH 6.8
	0.4 M sorbitol
	1 mM EDTA
	150 mM KAc
	To 50 mL extraction buffer:
	1.0 M spermidine HCl
	1.0 M spermin HCl
LiAC/TE (10x)	1 M lithium acetate
	1X TE
	Acetic acid to pH 7.5
PBS (1x)	137 mM NaCl
	2.7 mM KCl
	4,3 mM Na_2PO4
	1.47 mM KH_2PO_4
PEG/LiAc/TE	40% PEG 4000
	1x LiAc/TE
Running buffer (10x)	30.2 g/L Tris
	144 g/L glycine
	1% (w/v) SDS

Sodium Acetate pH 5.2 (3M)	40.8 g NaAc*3 H_2O to 100 mL H_2O Adjust to pH 5.2 with glacial acetic acid
STOP buffer (2x)	20 mM Tris-HCl pH 8.0 150 mM NaCl 50 mM NaF 10 mM EDTA 1 med mer NaN_3
TAE buffer (10x)	48.8 g Tris base 11.4 mL glacial acetic acid (17.4 M) 3.7 g EDTA Dilute buffer to 1x by adding MQ-H_2O
TBS-T	20 mM Tris-HCl pH 7.5 8 g/L NaCl 0.05% (v/v) Tween-20
TE pH 7.5 (10X)	0.1 M Tris-HCl pH 8.0 0.01 M EDTA pH 8.0 0.02 HCl to pH 7.5
Transfer buffer	50 mM Tris 380 mM glycine 0.1% (w/v) SDS 20% (v/v) methanol

4 METHODS

4.1 General cell biology methods

4.1.1 Growth and maintenance of fission yeast

4.1.1.1 Choosing the medium

YES (Yeast Extract with Supplements) medium, EMM (Edinburgh Minimal Medium) medium and ME (Malt Extract) medium are commonly used for culturing fission yeast. It is important to choose the right medium with respect to the purpose of the experiment and the special needs of strains.

YES medium and EMM medium were both used for maintaining vegetative growth of fission yeast cells in this study. YES medium provides a nutritionally rich growing condition, therefore it was used to harvest large amount of cells within a relatively short time; while EMM medium provides a standard growing condition with the minimal essential ingredients required to maintain the growth. When culturing auxotrophic strains in EMM medium, supplements were added to the medium to the concentration of 80 μg/mL. In addition, since YES medium contain macromolecules that can absorb UV light, UVC irradiation was performed on the cell culture in EMM medium.

ME medium contains poor nutrients and is used for switching fission yeast cells from mitotic cell cycle to meiotic cell cycle. Cells growing on an ME agar plate will reach an oligotrophic status after several rounds of vegetative growth. Under such a nutrient-stressed condition, the cells having the opposite mating types (h+/h-) will conjugate with each other and then sporulate (there also exists another mating type h90, the cell having this mating type is homothallic and can mate with itself). In this study ME medium was used for harvesting spores after crossing two strains and testing the unknown mating type of cells.

Generation time

The growth rate of fission yeast cells differs depending on the medium and temperature. Table 4.1 below gives the generation time of fission yeast growing under several common conditions.

Table 4.1. Generation time of fission yeast in different media at different temperatures.

Medium	Temperature	Generation time
YES	25°C	3h
	36°C	2h
EMM	25°C	4h
	36°C	3h

The generation time can be slightly different depending on the genotype of strains. To calculate the accurate generation time, the optical absorbance at 595 nm wavelength ($OD_{595\ nm}$) at two known time points of a log-phase liquid culture needs to be measured (Hitachi U-1900 Spectrophotometer was used). The $OD_{595\ nm}$ values are used in the following equation.

$$T = \frac{\log(2^{t2-t1})}{\log(y/x)}$$

In the equation, T is the generation time (hours), x is the $OD_{595\ nm}$ at time point t1 and y is the $OD_{595\ nm}$ at time point t2.

Cell density

$OD_{595\ nm}$ of the culture reflects the cell density. For fission yeast, a linear relationship between $OD_{595\ nm}$ and the cell density is kept up to $OD_{595\ nm}$ = 1.0 where the cell density is approximately 2×10^7 cells/mL.

4.1.1.2 Growth on agar plates

To grow cells on an agar plate, cells from the frozen glycerol stock stored at -80°C should first be patched onto an EMM/YE agar plate before they are cultured in liquid medium or used for crossing. The agar plate are sealed with parafilm and kept in the 25°C incubator for at least 2 days until cells have grown into visible colonies. The agar plate can then be kept at 4°C for short-term (30 days) storage.

4.1.1.3 Storage of strains and re-isolation cells from the frozen stock

As mentioned above, for short-term storage cells growing on an agar plate could be stored at 4°C. While for long-term (several years) storage, strains should be maintained in a cryotube containing a mixture consisting of 0.5 mL YES medium and the equal volume of 50% glycerol, then frozen at -80°C.

To re-isolate cells from the frozen stock, use a sterile spatula to scrap out a small amount of cells from the cryotube (the cryotube should be maintained inside a cryotube cooler in the mean time), then patch the cells onto a fresh agar plate and incubate the cells at 25°C for 2-3 days until colonies are visible.

4.1.1.4 Liquid cultures

Liquid cultures were used to harvest large amounts of exponentially growing (log-phase) cells. To make a liquid culture, start with inoculating 15 mL YE/EMM medium in a 50 mL Falcon Tube with a loop of cells taken out from the agar plate. This culture is then kept in the 25°C incubator overnight allowing the cells undergoing vegetative growth for several generations. Cells are then spun down at 1700 x g for 3 min and the cell pellet is transferred to a flask containing 50 mL YE/EMM medium as the pre-culture. The pre-culture is grown in 25°C water bath with shaking until its $OD_{595\ nm}$ reaches 0.1-1.0, and then it can be used for preparing the main culture.

To harvest a main culture of a certain cell density, the following equation is used to calculate how much pre-culture is needed.

$$Vpre = \frac{ODmain \times Vmain}{ODpre \times 2^n}$$

In the equation, V_{pre} stands for the needed amount of the pre-culture, V_{main} stands for the volume of the main culture, OD_{pre} is the $OD_{595\ nm}$ of the pre-culture and OD_{main} is the desired $OD_{595\ nm}$ of the main culture when it is harvested. The letter ‘‘n’’ stands for the number of generations, it is determined by the growing time and the growth rate (see Table 4.1) of the main culture. The strains used in this study are all temperature sensitive, therefore before synchronizing the cells the main cultures were grown at the permissive temperature 25°C.

Note that since the fission yeast grows very slowly at low cell density, a main culture should not start with too few cells ($OD_{595\ nm} < 0.1$).

4.1.1.5 Culturing cells carrying the *nmt41* promoter

Fission yeast cells carrying the *nmt* promoter need to be cultured with caution.

To perform gene knockdown in fission yeast, one strategy is to construct the target gene to be under the control of an *nmt* (no message in thiamine) promoter. The protein product of *nmt1* takes part in the biosynthesis of thiamine. It can be fully and rapidly repressed by the addition of thiamine (Maundrell, 1990). When the target

gene is constructed to be controlled by the *nmt1* promoter, the expression of this protein can be easily manipulated by adding thiamine to the medium. Due to mutations of the TATA box, the *nmt1* gene has two variations *nmt41* and *nmt81*. These two variants have lower transcription efficiency but their transcription initiation site and sensitivity to thiamine are not affected (Basi et al., 1993). In this study, strains carrying *nmt41.cdt2* were constructed and used.

Since the *nmt41* promoter is sensitive to thiamine, before the expression of the target gene needed to be knocked down, the cells were cultured in supplemented EMM medium which does not contain thiamine in order to maintain normal cell growth. Thiamine was added into EMM medium to a concentration of 5 μg/mL when the *nmt41* promoter needed to be fully repressed.

4.1.2 Genetic techniques of fission yeast

4.1.2.1 Genetic crossing, random spore analysis and identification of the mating type

Genetic crossing and random spore analysis

Genetic crossing is useful to construct a new strain. The principle of this method is homologous recombination which is the random exchange of nucleotide sequences between two homologous DNA segments (Figure 4.1). To carry out genetic crossing, two strains of opposite mating types are crossed onto an ME agar plate to allow the conjugation and sporulation. The progenies (spores) generated after the crossing are contained inside asci and need to be let out before being streaked onto another plate.

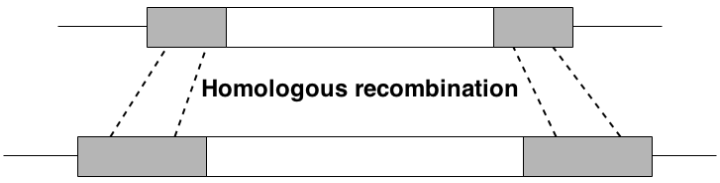

Figure 4.1. Principle of homologous recombination. Homologous sequences (gray) flanking the ingoing sequence (white) allow for the exchange of two defined stretches of DNA sequence between two homologous DNA segments.

Protocol for genetic crossing and random spore analysis:

1. Inoculate 500 µL MQ-H_2O inside an Eppendorf tube with a toothpickful of both parental strains that are to be crossed. Vortex the tube to make sure the cells are mixed well.
2. Pipette 15 µL of the inoculated H_2O to make a spot onto an ME agar plate. One can carry out several crosses on one plate.
3. Incubate the crosses at 25°C for 2 days.
4. Check for asci by taking some cells from the middle of one cell-spot and place them on a microscope slide with some water.
5. If many asci can be observed under the microscope, inoculate 500 µL MQ-H_2O with a toothpick of cells taken by streaking across the whole cell-spot.
6. Add 5 µL Helix Pomatia Juice to this asci-suspension and incubate at 36°C for 4h.
7. After the incubation, check if the asci wall is fully digested under a microscope. If yes, spin down the suspension at the full speed (ca. 17000 x g) of a table centrifuge for 2min.
8. Discard the supernatant and resuspend the spore-pellet in 50 µL MQ-H_2O.
9. Streak out 10 µL of the spore-water onto a fresh YES plate for single colonies. Use at least 3 plates for one cross.
10. Incubate the cells at 25°C until single colonies can be visualized.
11. Replica-plate the colonies to secondary selective plates for further analysis.

Identification of the mating type

When the mating type of a strain is unknown, a quick way to identify it could be done by crossing this strain with another two strains of known mating type h+/h-. Iodine staining is then used to check if spores (asci) are generated after crossing.

Protocol for identification of the mating type:

1. Cross the strain of unknown mating type with h+ and h- strains respectively by following step1, 2, 3 from the protocol for genetic crossing and random spore analysis described above.
2. Dust some iodine crystals on the lid of the plate and incubate for 3min.

When the iodine crystals vaporize, the iodine gas will reach the cells and form an iodine complex with helicoid carbohydrate macromolecules which are the components of asci wall. If there are asci generated from the cross, the asci will be stained and turn into dark purple. According to whether spores are made after the cross, the mating type of the strain can be identified.

4.1.2.2 Replica-plating

Replica-plating is used for large-scale screening for colonies carrying different genetic markers such as auxotrophic markers *ura4-D18*, *ade6-M210* and *leu1-32*. In this study replica-plating was used to select desired colonies after genetic cross. To perform replica-plating, use replica-plating tools to copy the pattern of fission yeast colonies from the master plate to different selective plates according to the markers the cells carry.

4.1.2.3 Transformation

To incorporate genes of interest into fission yeast genome, transformation is a method with high efficiency. Transformation uses homologous recombination to achieve the insertion of the exogenous transforming DNA sequence into the genome at the right locus. In this study, transformation was used for tagging several MCM2-7 subunit genes with GFP-tags (Figure 4.2). The method used in our lab is derived from "Bählers method" (Bahler et al., 1998). The transformation frequency is expected to be 10^4 to 10^5 per microgram of DNA.

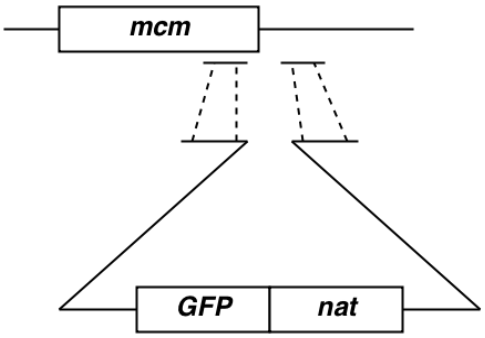

Figure 4.2. Incorporation of the transforming DNA after a MCM2-7 subunit gene. The transforming DNA contains homologous sequences at each end allowing for its incorporation after *mcm*. Resulting strains will carry the *GFP* tagged *mcm*, followed by *nat* which serves as a marker by conferring resulting strains clonNAT resistance.

Protocol for lithium acetate transformation of fission yeast:

1. Spin down 50 mL cell culture of $OD_{595\ nm}$ =0.3 at 1200 x g for 4 min.
2. Wash once with equal volume of water. Spin down at 1200 x g for 4 min.
3. Resuspend the cell pellet in 1 mL of water. Transfer to an Eppendorf tube. Spin down at 17000 x g for 1 min.
4. Wash once with 1 mL of LiAc/TE. Spin down at 17000 x g for 1 min.
5. Resuspend the cell pellet in 100 µL of LiAc/TE for per transformation.

6. Mix 100 µL of the concentrated cells with 2 µL of sheared herring testes DNA and 10 µL of transforming DNA (100–300 ng/µL). Incubate at room temperature for 10 min.
7. Mix gently with 260 µL of 40% PEG/LiAc/TE and incubate for 30-60 min at 25°C. This step may be increased for at least up to 2 h for better transformation efficiency.
8. Add 43 µL of DMSO and heat shock the cell suspension for 5 min at 42°C in water bath. Spin down at 17000 x g for 1 min.
9. Resuspend the cells in 50% EMM with essential supplements (15 mL H_2O + 15 mL EMM). Incubate the cells on the roller at room temperature overnight.
10. Plate out 200 µL culture to each selective plate. Use 5 plates for one transformation.
11. Incubate at 25°C for 5-6 days until the colonies are visible.
12. Streak out the colonies that are growing on the selective plate onto another fresh selective plate as for double-check.

4.1.3 Synchronization of fission yeast

Synchronous cells are useful for cell cycle study. There are different ways to synchronize cells such as elutriation, arresting cells by drug or nitrogen starvation and using cell cycle mutants. In this study, cell cycle mutants carrying *cdc10-M17* were used for arresting cells in early G1 phase. As described in 1.4.1, *cdc10* encodes a transcription factor which controls the transcription of genes essential for G1 phase events. Cell cycle mutants carrying *cdc10-M17* are temperature-sensitive. The mutants gene functions normally when cells are growing at permissive temperature 25°C, but becomes inactive when the temperature is shifted up to 36°C (restrictive temperature), leading to the block of two pre-RC components gene *cdc18* and cdt1, and thereby the cell cycle is arrested in early G1 phase in which pre-RC formation takes place.

To synchronize strains carrying *cdc10-M17*, log-phase cultures ($OD_{595\ nm}$ is around 0.15) are shifted up from 25°C to 36°C for 4 h (Figure 4.3). During the 4 h shift-up at 36°C, most of the cells will finish the cytokinesis and halt their cell cycle progression in early G1.

4.1.4 UVC irradiation of fission yeast in liquid culture

UVC irradiation of fission yeast is used to induce DNA damage to the cells. In this study cells were irradiated in liquid culture. UVC light of 254 nm wavelength (Sylvania Fluorescence Lamp, UVC light) was used.

To carry out UVC irradiation of cells in liquid culture, a certain volume of the cell culture is first poured into a Petri dish of the corresponding volume, and then placed in the safe hood with the fluorescence lamp (the culture also needs to be stirred when being UVC irradiated). The duration of UVC irradiation is determined by the following formula.

$$T(sec) = \frac{UVC\ dose\ (J/m^2)}{UVC\ intensity\ (W/m^2)}$$

The dose of UVC for liquid culture used in this study was 1100 J/m^2, which gave an incident dose rate of approximately 250 J/m^2 per min in the liquid culture (Nilssen et al., 2003). For synchronized cells, UVC irradiation was carried out immediately after the 4 h shift-up (Figure 4.3).The intensity of UVC was measured by a UVX radiometer (AH Diagnostic). This UVC treatment induces 0.2-0.3 CPDs per kb in both the transcribed strand (TS) and non-transcribed strand (NTS) of DNA, and gives cells a survival rate around 15% (Boe et al., 2012; Nilssen et al., 2003).

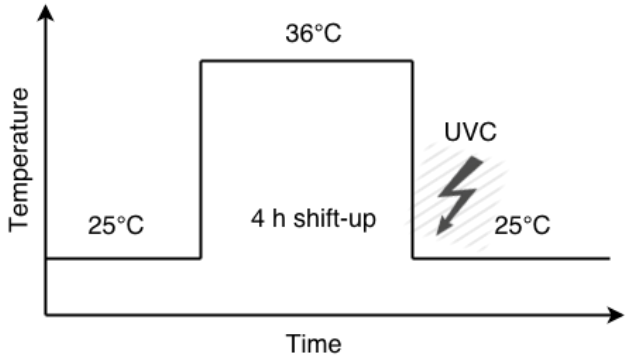

Figure 4.3. Synchronization and UVC irradiation of fission yeast. Temperature is shifted up from the permissive temperature 25°C to the restrictive temperature 36 °C for 4 h in order to synchronize cells in early G1 phase. UVC irradiation is carried out immediately after the 4 h shift-up. After UVC irradiation, temperature is shifted down to the permissive temperature 25°C and cells are released from the cell-cycle block.

4.1.5 Flow cytometry

Flow cytometer is an efficient instrument widely used in cell biology study. It can detect the signals emitted from thousands of cells within minutes. The primary structure of a flow cytometer (Figure 4.4) consists of a fluidics system, a laser, several detectors and dichroic mirrors. The fluidics system compresses the sample into cell stream of approximately one cell in diameter through a procedure termed hydrodynamic focusing, and then presents them to the laser interrogation. The laser beam is used to excite the fluorescence from the stained-sample, and it is also

scattered by the cell at the same time. The excited fluorescence is then filtered and forwarded in a wavelength-dependent manner by dichroic mirrors to the corresponding detectors. Detectors convert light signal into voltage pulse, they are separated into two subgroups depending on the signals they detect: forward scatter of low angle and side scatter of large angle. Once signals are collected, detectors convert them into voltage pulse immediately which is then analyzed by the software. The magnitude of FSC forward scatter is proportional to the size of the cell, while SSC side scatter reflects the granularity and structural complexity inside the cell. A flow cytometer can also sort cells into several subgroups in the mean time when collecting signals.

In this study, flow cytometry was used to detect signals given by stained-nuclei in order to monitor cell cycle progression.

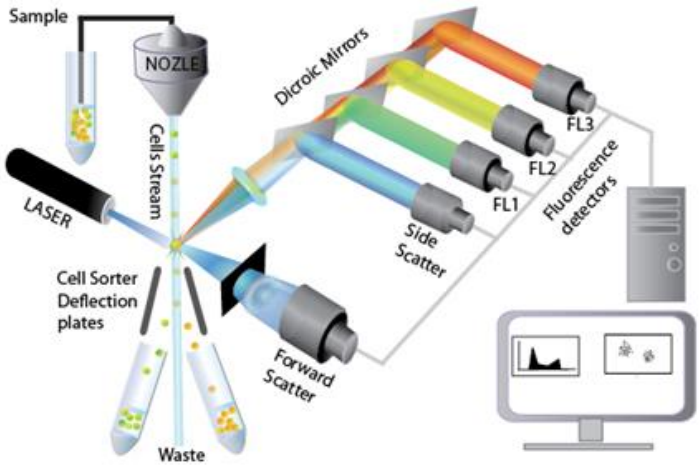

Figure 4.4. Schematic of the primary structure of a flow cytometer.

(http://utbiorad.casaccia.enea.it/facs-flow-cytometry.html)

4.1.5.1 Taking cell samples for flow cytometry

Protocol for taking cell samples for flow cytometry:

1. Pipette 1 mL of cell culture into an Eppendorf tube and spin down the cells at 17000 x g for 2 min.
2. Remove the supernatant and try to keep the cell pellet intact.
3. Add 1 mL of ice cold 70% ethanol to the cells on a vortexer drop by drop.
4. The samples now can be stored at 4°C for several months.

In this study cell samples for flow cytometry were fixed with ethanol before they were stained. Ethanol fixation enables a long-term storage of the cells, and also compromises plasma membrane making it accessible for the nucleic acid stain.

4.1.5.2 Preparing cell samples for flow cytometry

Before applying the cell samples to the flow cytometer, some pre-work was done in order to wash off the ethanol and stain the nucleic acid.

Protocol for preparing cell samples for flow cytometry:

1. Spin down 500 µL of ethanol-fixed sample for 2 min at 17000 x g.
2. Discard supernatant and resuspend the pellet in 1 mL 20 mM EDTA. Spin down for 2 min at 17000 x g.
3. Discard supernatant and resuspend pellet in 1 mL 20 mM EDTA. Spin down for 2 min at 17000 x g.
4. Discard supernatant and resuspend pellet in 500 µL 20 mM EDTA containing RNase A (> 70 U/mL, 3.5 µL RNase A in 1 mL 20 mM EDTA).
5. Incubate at 36 °C overnight.
6. Sonicate the sample in a water bath for 5 min.
7. Add 0,5 mL 20 mM EDTA containing 2 µM 5 mM Sytox Green, so that final concentration of Sytox Green in the sample is 1 µM
8. Run the sample using the flow cytometer (LSR II Flow Cytometer, BD Bioscience) as described in the manual provided from the core facility.

In this study Sytox Green was used to stain cells. Sytox Green is a high-affinity nucleic acid stain and is excitable at 450-490 nm. Since Sytox Green can stain both DNA and RNA. In order to eliminate the disturbance from RNA staining, RNase A was added to digest RNA.

4.1.5.3 Interpreting flow cytometry data

As described in 1.2.2, the timing of cytokinesis and karyokinesis of fission yeast is diffrent. Therefore the traditional flow cytometry method for monitoring cell cycle progression cannot be applied to fission yeast. Our lab has developed a flow cytometric method specially for analyzing the cell cycle progression of fission yeast. This method is based on the measurement of the width and total area of fluorescence signals emitted from the stained-nuclei (Knutsen et al., 2011). When running the cell samples by flow cytometer, their FSC (forward scatter) is plotted vs. SSC (side scatter) in a two dimensional graph (Figure 4.5A), cells in the gate at the corner represent single cells. The DNA content of these gated cells is plotted in a

histogram vs. the number of the cells. The histogram of early G1-synchronized cells by blocking *cdc10-M17* will have a main peak representing 1C-containing cells (Figure 4.5B), while the histogram of log-phase cells will have a main peak representing 2C-containing cells (see Figure 1.4). In this study 10000 cells were counted from each sample.

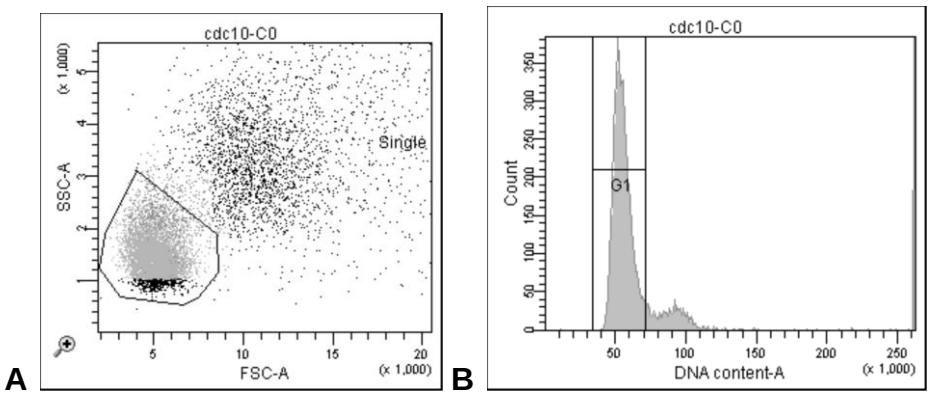

Figure 4.5. Flow cytometry data of early G1-synchronized cells. (A) A two dimensional light scatter graph. Cells in the gate are singlets, whiles cells outside the gate are doublets. (B) A histogram is generated showing cells in the gate from the two dimensional light scatter graph. The horizontal axis represents DNA content and the vertical axis represents the number of cells. Cells in the G1-gate contain 1C DNA content, while a small fraction of cells outside the G1-gate contain more than 1C DNA content. This histogram shows that most of the cells are in G1 phase indicating that cells are properly synchronized.

4.2 Protein methods

4.2.1 TCA extraction of total protein

TCA is widely used for the extraction of macromolecules including proteins, DNA and RNA. It has been tested that the optimal mass to volume ratio for the most efficient performance of TCA is 15%. The trichloroacetate moiety of TCA is essential for its capability to precipitate proteins in a folded state (Sivaraman et al., 1997).

Before TCA extraction, samples were taken from the cell culture at different time points of a time course, and then all samples were processed together for TCA extraction of total protein.

Protocol for taking protein samples:

1. Spin down 1 × 10^8 cells at 1200 x g for 4 min.
2. Resuspend the cell pellet in 1 mL of ice cold stop buffer and transfer to an Eppendorf tube.
3. Spin down at 17000 x g for 3 min.

4. Discard the supernatant while trying to keep the pellet intact.
5. Snap-freeze the pellet in liquid nitrogen.
6. When all samples are taken, store them at -80°C.

Protocol for TCA extraction of total protein:

1. Allow the frozen samples to thaw on ice for a couple of minutes.
2. Resuspend the pellet in 1 mL of 20% TCA.
3. Spin down the cells at 17000 x g for 3 min and remove the supernatant. At this point you will observe that the pellet has become white.
4. Resuspend the cells with 1 mL of Tris pH=8.0 in order to neutralize the TCA.
5. Spin down at 17000 x g for 3 min and remove the supernatant. The pellet will recover its original color.
6. Resuspend the pellets in 1× Laemmli sample buffer. (The volume of Laemmli sample buffer depends on the the purpose of the experiment, usually 120 µL is added).
7. Boil for 2 min at 95°C.
8. Add acid-washed glass beads and boil for 2 more minutes at 95°C.
9. Break the cells by using Fast-Prep (FastPrep FP120 ribolyzer, Thermo Scientific) for 4 × 40 sec. Cool down the samples for 2min between each two runs.
10. Check whether most of the cells are broken under a light microscope, if there are still many unbroken cells, lyse the cells for several more runs.
11. Use a hot 25G needle, pierce the bottom of the tube and place the tube on another micro tube, place them together inside a 15 mL falcon tube (Figure 4.6).
12. Spin down at 1200 x g for 5min. Now the sample is in the lower tube, keep it and throw away the tube with glass beads.
13. Spin down the sample at 17000 x g for 5 min.
14. Store the samples at -20°C.

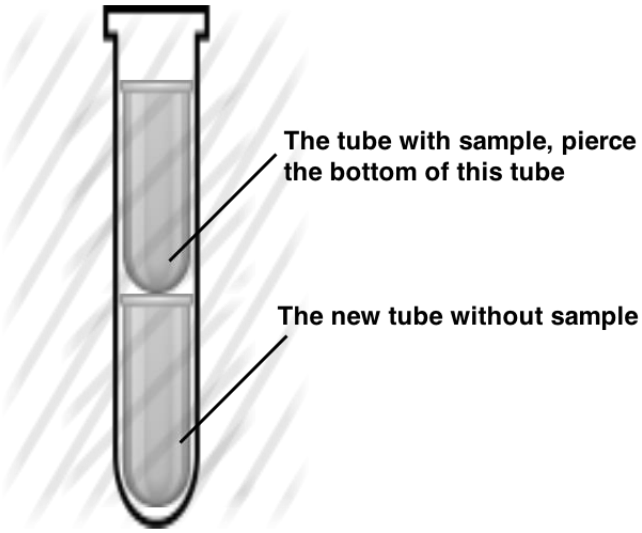

Figure 4.6. The assembly of tubes in step 11. The upper tube contains the sample and glass beads inside, and is pierced with the hot 25G needle at the bottom. The lower tube is a clean one. After centrifugation, the sample will be spun down to the lower tube through the hole while the glass beads will stay in the upper tube.

4.2.2 BCA protein assay for determining the concentration of proteins

BCA protein assay is a widely used method for quantifying protein concentration. BCA protein assay determines the protein concentration through reflecting it as the color exhibited by the sample after a series of chemical reactions. The principle of this method utilizes the biuret reaction which is the reduction from Cu^{2+} to Cu^{+} by the peptide bonds of the protein in an alkaline solution. One cuprous cation can then chelate with two BCA molecules to form a coordination complex that emits a violet color. This color can absorb light with a wavelength of 562 nm (Smith et al., 1985). The reaction is shown below (Figure 4.7).

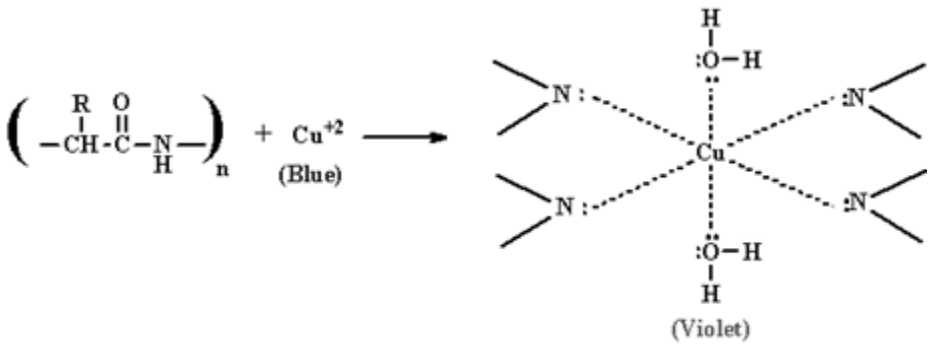

Figure 4.7. Diagram of the biuret reaction. After the copper ion is reduced from cupric to cuprous form in the alkaline environment, the cuprous cation then chelates with two BCA molecules forming a coordination complex emitting a violet color. (http://www.uwplatt.edu/~sundin/351/351h-pro.htm)

The violet color from different samples differs proportionally to the concentration of the total protein. The colorimetric detection can be done by a microplate photometer (Thermo Scientific).

In this study BCA Protein Assay Kit from Thermo Scientific was used, and the assay was carried out by following the protocol provided by the manufacturer.

4.2.3 Protein staining

4.2.3.1 Coomassie brilliant blue staning of SDS-polyacrylamide gels

There are two structurally similar triphenylmethane dyes: G-250 and R-250 which both can be called Coomassie brilliant blue. The only difference between them is that G-250 has two more methyl groups. Molecules of these dyes can stabilize their negatively charged anionic form after binding to proteins and emit a blue color.

Coomassie brilliant blue staining was used to check the remaining protein in an SDS-polyacrylamide gel after transfer. To perform Coomassie brilliant blue staining of an SDS-polyacrylamide gel, G-250 dye is added until the gel is covered, the gel is then incubated at room temperature for 30 min-1 h with slight shaking. The dye is then discarded and the gel is soaked in water for 30 min-1 h in order to remove background staining.

4.2.3.2 Ponceau S staining of PVDF membranes

Ponceau S is a negative stain with a light red color and can bind to positively charged amino groups. It can form non-covalent bonds in the non-polar regions of a peptide without causing deleterious effects to the primary structure. In this study a rapid staining of PVDF membranes by Ponceau S dye was performed to detect the proteins on the membrane. Since Ponceau S staining is reversible, the membrane can be recovered after proteins have been visualized. The following protocol was used for Ponceau S staining of proteins on a PVDF membrane.

Protocol for total protein detection by Ponceau S:

1. After transferring proteins from SDS-polyacrylamide gel onto the membrane, immerse the membrane in sufficient Ponceau S staining solution and stain for 1 min with slight shaking.
2. Rinse membrane with distilled water until the background is clear.
3. Dry the membrane under at room temperature.

If the membrane needs to be recovered after visualizing the proteins, wash the stained membrane with 0.1 M NaOH aqueous solution by following protocol below.

Protocol for stripping off Ponceau S staining:

1. Rinse the membrane with distilled water and rapidly immerse it in an aqueous solution of 0.1 M NaOH. Protein bands will start to disappear after 10-30 seconds.
2. Rinse membrane with running distilled water for 2-3 minutes.
3. Continue with other procedure being followed (e.g. immunodetection).

4.2.4 Western blot

Western blot, the synonym for immunoblot, is widely used for protein analysis. The principle of Western blot exploits immunostaining of specific proteins with corresponding antibodies. It consists of several steps as described below.

1) Sample preparation

This step was performed by using SDS-PAGE (sodium dodecyl sulfate-polyacrylamide gel electrophoresis) to separate the proteins in TCA-extracted samples.

SDS-PAGE

Proteins are not like DNA molecules which have a constant charge-to-mass ratio. Under a certain pH, the charge of proteins varies depending on the amino acid sequence. Moreover, native-stated protein molecules have numerous tertiary structures, and they make it difficult to separate different proteins based exclusively on their molecular weight. To solve this problem, an anionic detergent SDS is utilized to denature the proteins, and make the highly folded conformation of proteins into a linear shape through disrupting non-covalent bonds. SDS binds the proteins at a consistent rate of about one SDS molecule per two amino acids, and this stoichiometry masks the intrinsic charge of a protein molecule by replacing it with an average negative charge. This average negative charge is significantly great and can create electrostatic repulsion to keep the linear shape of a protein molecule (Figure 4.8). In addition, DTT (dithiothreitol) should also be added to the protein sample in order to further disrupt the disulfide bond formed between two cystein residues. In a sample treated with these chemicals, all protein molecules become linear-shaped and obtain a uniform charge-to-mass ratio.

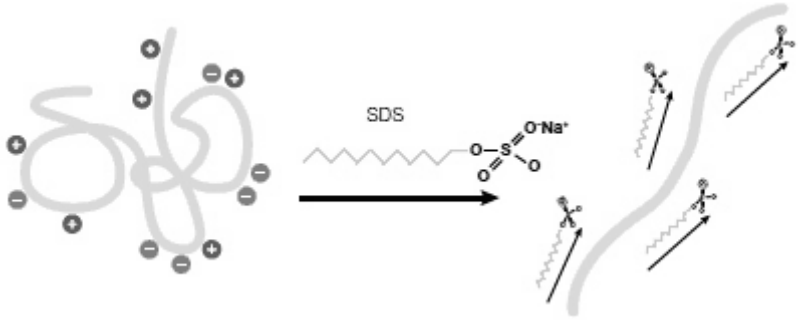

Figure 4.8. Effect of SDS on the conformation and charge of a protein molecule. SDS brings a protein molecule average negative charge and makes it into a linear shape. (http://www.bio-rad.com/ja-jp/applications-technologies/protein-electrophoresis-methods)

Polyacrylamide as gel matrix for electrophoresis works in a similar way as agarose (see 4.3.2). The combination of SDS and PAGE generates a system to sort proteins of different molecular weight efficiently.

TCA-extracted samples taken out from the freezer were pretreated before they were loaded to the SDS-polyacrylamide gel.

Protocol for pretreatment of the protein samples:

1. Put the samples on ice and let them thaw for several minutes.
2. Boil the samples at 95°C for 3 min to make sure that all proteins are denatured.
3. Spin down the samples at 17000 x g for 2 min to get the cell debris down.

Regarding to the size of the proteins of interest in this study (ranging from 35 kDa to 70 kDa), 10% and AnykD pre-cast gels from Bio-Rad were used.

Protocol for SDS-PAGE:

1. Assemble the gel chamber (BioRad) and fill it with 1× running buffer between the gels and leave it for a couple of minutes to make sure the buffer is not leaking.
2. Remove the comb from the gel and remove air bubbles from the wells with a syringe.
3. Load one well with 10 µL of the molecular weight ladder.
4. Load the samples (normally 8-15 µL in each well).
5. Fill the chamber with 1× running buffer until the anode.
6. Run the gel at 150V for 40 min (BioRad Power Pac 200) or until the color front has ran out of the gel.

7. Disassemble the gel chamber. Remove the stacking gel and the gel front and soak the gel in transfer buffer for 15 min before continuing to the transfer step.

2) Transfer

Which transfer method (dry, semi-dry and wet) to use is dependent on the size of proteins of interest. In this study semi-dry transfer was used. Membranes used here were made of PVDF which has non-specific affinity to amino acid residues, therefore proteins can be immobilized to the surface of the membrane.

Protocol for semi-dry transfer:

1. Rinse the membrane in MetOH for 15 seconds and then leave it in MQ-H_2O for 10 min.
2. Incubate the gel, membrane and two thick filter papers in transfer buffer for 15 min.
3. Assemble the blotting sandwich (Figure 4.9).
4. Run the transfer for the gels at 15V for 40 min (BioRad Trans-Blot, Semi-Dry transfer Cell).

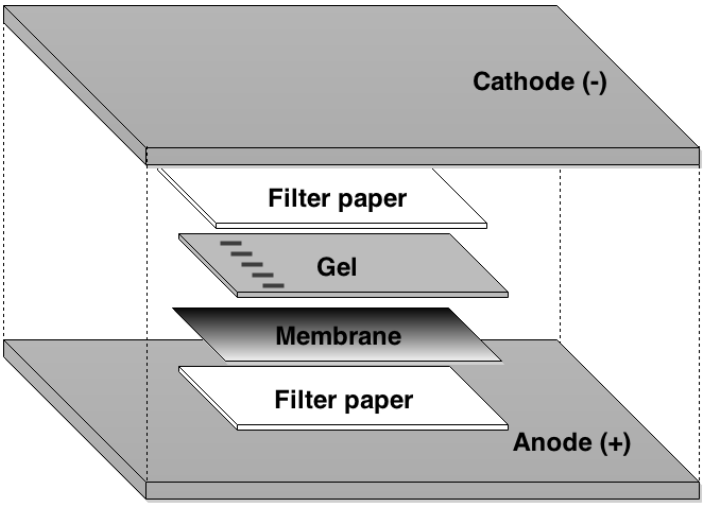

Figure 4.9. The assembly of the blotting sandwich.

After the transfer, the SDS-polyacrylamide gel was subjected to Coomassie brilliant blue staining to monitor the quality of the transfer.

3) Blocking

Since antibodies are also proteins, they can bind to the blank regions on a PVDF membrane and cause background signals when visualizing proteins. To avoid the unwanted bindings between antibodies and the membrane, a blocking solution

containing non-specific proteins should be added for masking all the blank regions on the membrane. The incubation of the membrane with blocking solution was done for 1 h at room temperature or at 4°C overnight.

4) Immunodetection

The detection of the protein of interest can be either one-step or two-step depending on the protein to be detected and the tags conjugated to the protein. One-step detection only needs one incubation with a primary antibody which has already been conjugated with the reporter enzyme; while two-step detection includes a first incubation with the primary antibody that recognizes the protein of interest, and a second incubation with the secondary antibody which is conjugated with reporter enzymes. The secondary antibody can recognize primary antibodies that are produced from the same animal species. The reporter enzyme can excite chemiluminescence or fluorescence from its substrate. After incubating with antibodies, the membrane is then washed with TBS-T in order to remove excess antibodies.

Protocol for immunodetection:

1. Incubate the membrane with primary antibody diluted to the appropriate concentration in TBS-T, 1h at room temperature or overnight at 4˚C.
2. Wash the membrane 3 x 10 min with 5 mL TBS-T. (In the case of one-step detection, the membrane can be forwarded to visualization after this step). Incubate the membrane with secondary antibody diluted to the appropriate concentration in TBS-T, for 1 hour at RT.
3. Wash the membrane 3 x 10 min with 5 mL TBS-T.

5) Visualization

After the last wash with TBS-T, the membrane can be forwarded to visualization. The protein of interest on the membrane is visualized via the reaction between the enzymes conjugated to the antibody and the substrates of the enzymes in the ECL/ECF solution. In this study ECL was used.

Protocol for visualization of the membrane:

1. Put the membrane on a glass plate and remove the excess liquid with filter paper. Distribute 1-2 mL of mixed ECL solution onto the membrane evenly. No incubation is needed.
2. Remove excess ECL solution with filter paper.

3. Take pictures of the membrane by using Syngene Chemigenius Chemi Genius 2 Bio Imaging System.
4. Cover the membrane with aluminum foil and store in the fridge.

6) Stripping and re-probing

Analysis of different proteins on the same membrane can be performed either by cutting the membrane after transfer into different parts containing distinct proteins, or by stripping off the antibodies from the membrane after the previous round of detection, so that the membrane can be re-probed with antibodies against other proteins. In this study, due to the similar size of α-tubulin and our protein of interest, membranes were stripped and re-probed for analyzing different proteins on the same membrane.

Protocol for stripping the membrane:

1. Soak the membrane in stripping buffer for 15-20 min.
2. Rinse the membrane with TBS-T.
3. Block the membrane with blocking solution for 1h at room temperature.
4. The re-probing is essentially the same as described in the protocol for immunodetection.

4.3 DNA methods

4.3.1 Polymerase chain reaction

Polymerase chain reaction (PCR) is used to amplify DNA fragments of interest. It consists of 20-40 repeated thermal cycles in order to get sufficient DNA products. Each thermal cycle consists of three discrete steps: 1) DNA denaturation, 2) primer annealing and 3) elongation.

In this study general PCR was used to clone transforming DNA from plasmids, and colony PCR was used to analyze transformants. BioRad C100 Thermal Cycler was used in this study.

4.3.1.1 General PCR

AccuPrime™ Pfx DNA Polymerase kit was used in general PCR in this study for amplifying transforming DNA from plasmids. In order to obtain PCR products for tagging different genes, hybrid primers were used for making different transforming

DNA from the same plasmid (Figure 4.10). The reaction mixture set-up and the PCR program are shown below (Table4.2-4.5).

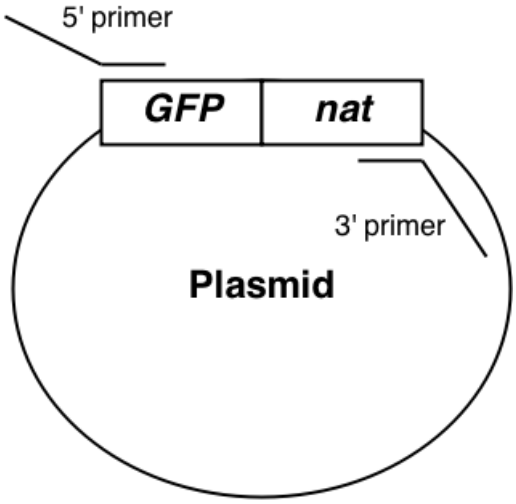

Figure 4.10. Schematic of using hybrid primer strategy for making different transforming DNA from the same plasmid in this study. The 5' hybrid primer consists of a long homologous sequence (80 nt) for targeting the transforming DNA at the right locus of the genome, and a relatively short sequence (20 nt) which is complementary to the 5' end of the *GFP* gene. The 3' hybrid primer also consists of a long homologous sequence (80 nt) for targeting the transforming DNA, and a relatively short sequence (20 nt) which is complementary to the 3' end of the selective marker *nat*. Depending on which hybrid primers are used in the PCR, specific transforming DNA can be amplified for tagging a specific gene.

Table 4.2. PCR reaction mixture set-up for amplifying transforming DNA for tagging *mcm2*.

	For 50 µL
10X AccuPrime™ PCR Buffer	5.0 µL
10 µM tagging primer mix	1.0 µL
Template 100X plasmid 309	1.0 µL
DMSO	1.25 µL
H_2O	41.55 µL
AccuPrime™ Pfx DNA Polymerase	0.2 µL

Table 4.3. PCR reaction mixture set-up for amplifying transforming DNA for tagging *mcm6.*

	For 50 µL
10X AccuPrime™ PCR Buffer	5.0 µL
5M NaCl	0.5 µL

$MgSO_4$ 15mM	5.0 µL
DMSO	1,25 µL
10 µM tagging primer mix	1.5 µL
Template 100X plasmid 309	1.0 µL
H_2O	35.35 µL
AccuPrime™ Pfx DNA Polymerase	0.4 µL

Table 4.4. PCR reaction mixture set-up for amplifying transforming DNA for tagging *mcm7.*

	For 50 µL
10X AccuPrime™ PCR Buffer	5.0 µL
5M NaCl	0.5 µL
$MgSO_4$ 10mM	5.0 µL
DMSO	1.25 µL
10 µM tagging primer mix	1.5 µL
Template 100X plasmid 309	1.0 µL
H_2O	35.35 µL
AccuPrime™ Pfx DNA Polymerase	0.4 µL

Table 4.5. PCR program for amplifying transforming DNA.

	Cycles	**Time**	**Temperature**
Initial denaturation	1	2 min	95 °C
Denaturation	30	45 sec	95°C
Annealing		45 sec	48°C
Elongation		140 sec	68°C
Final elongation	1	15 min	68°C
Hold	--	--	12°C

4.3.1.2 Colony PCR

To analyze the transformants, colony PCR was used in this study. DNA extracted from fresh colonies after transformation was applied to colony PCR in order to verify whether the transforming DNA had been indeed integrated into the genome at the right locus. However, the colony PCR cannot amplify long fragments (larger than

3000 bp) efficiently, and therefore such long fragments amplified from the genomic DNA of the transformants could not be visualized after gel electrophoresis. The reaction mixture set up and the PCR program are shown below (Table 4.6 and 4.7). DNA was prepared according to the following protocol.

Table 4.6. PCR reaction mixture set-up for colony PCR.

Solution	For 20 µL
Template	1.0 µL
dH_2O	4.0 µL
Triton X-100 (10% stock)	4.0 µL
Checking primer mix (10 µM stock)	1.0 µL
DreamTaq PCR Master Mix (2X)	10.0 µL

Table 4.7. PCR program for colony PCR.

	Cycles	Time	Temperature
Initial denaturation	1	2 min	94 °C
Denaturation	35	15 sec	94 °C
Annealing		30 sec	40-45 °C
Elongation		5 min	68 °C
Final elongation	1	10 min	68 °C
Hold	--	--	12°C

Protocol for preparing DNA template for colony PCR:

1. Label Eppendorf tubes on the lid and poke a hole in the lid with 25G needle.
2. Dispense 50 µL 0.25% SDS in TE to the tubes.
3. Pick up cells from a fresh colony (no more than 1-2 days old) with a yellow pipette tip (about the size of a match-head). Put the tip in the tube and put a finger-tip over the pipette tip to mix the cells into the solution by vortexing.
4. Boil in a heating block for 5 min.
5. Spin down in microcentrifuge for 1 min at 17000 x g.
6. Recover 80% of supernatant (avoid the pellet) into a labeled Eppendorf tube. Recover the supernatants quickly after spinning.
7. The template DNA can be kept at 4°C for later use.

4.3.2 Agarose gel electrophoresis

DNA molecules have an even negative charge (1 unit negative charge for each phosphate group) due to the sugar-phosphate backbone. This property allows the separation of DNA molecules based on their size.

Agarose gel matrix contains supercoiled bundles of helical agarose molecules. These molecules can form micro pores with each other allowing the pass of macro biomolecules ranging from 0.5 kb to 25 kb. The resolution of a gel depends on the size of the pores which are determined by the amount of agarose contained in the gel. The gel is placed in an electric field with direct current which directs the negatively charged DNA molecules moving from cathode to anode. The speed of the migration through the gel of a DNA molecule and its size are reversely correlated, therefore the small DNA fragments will be aggregated at the lower part of the gel while the large ones will be aggregated at the upper part.

Before dispensing DNA samples into the wells of the agarose gel, they have to be mixed with loading dye. The loading dye visualizes the front line of the migrating DNA molecules and contains chelating agent EDTA which can protect DNA molecules from the metal-ion-dependent nucleases. To prepare the DNA samples for agarose gel electrophoresis, the 6× loading dye is diluted with DNA samples to 1×. The voltage applied can range from 100V to 120V. In this study 1% agarose gels and 1× TAE electrophoresis buffer were used.

4.3.3 Visualization of DNA fragments

To visualize the separated DNA fragments after electrophoresis, the agarose gel needs to be stained with a dye which can bind to DNA molecules. In this study GelRed was used to stain DNA molecules. To perform the staining, the gel is placed in diluted GelRed solution with slight shacking for 3 h before imaging (ChemiGenius 2 Bio Imaging System, Syngene).

4.3.4 Purification of DNA

PCR products usually contain a lot of contamination such as residual primers, proteins, RNA and salt. The contamination can be removed by DNA purification. Due to the negatively charged phosphate backbone, DNA is a highly polar macromolecule which is soluble in water while insoluble in 70% ethanol. In this study a method using 70% ethanol was used to purify PCR products.

Protocol for purification of DNA:

1. Add 1/10 x the volume of PCR product of 3M NaAc (pH=5,2) to the PCR product. (For example: if PCR product is 100 µL, add 10 µL 3M NaAc)

2. Add 2.5 x the volume of (PCR product+ NaAc) of 100% EtOH. (For example: if PCR product is 100 µL and 10 µL 3M NaAc is added after step 1, then 275 µL of 100% EtOH is needed)
3. Put the samples on ice for 15 min.
4. Spin down the samples at 21600 x g at 4°C for 30 min.
5. Wash the pellet with ca. 200 µL ice cold 70% EtOH.
6. Spin down the samples at 21600 x g at 4°C for 10 min.
7. Suck away the 70% EtOH and place the tubes on the bench with lid open until all the EtOH inside dries out.
8. Add H_2O to the pellet.(the volume of H_2O depends on the size of the pellet, usually 20 µL)
9. After measure the concentration of the precipitated DNA store the product at -20°C.

4.3.5 Measuring DNA purity and concentration

Nucleic acids consist of purines and pyrimidines which are heterocyclic rings and absorb light in UV region. The absorbance at 260 nm can be used to measure the concentration of nucleic acids, and the ratio of absorbance at 260 nm to the absorbance at 280 nm can be used to measure the purity of nucleic acids. For pure DNA this value should be around 1.8 and for pure RNA 2.0 is expected. In this study NanoDrop spectrophotometer was used to measure DNA purity and concentration.

To measure DNA purity and concentration by NanoDrop spectrophotometer, apply 1 µL of the DNA sample to the machine by following the protocol provided by the manufacturer.

4.4 Microscopy

Two microscopy techniques were used in this study. The bright-field microscope (Axioscope, Zeiss, Germany) with 40× objective was used to monitor the morphology and sporulation state of fission yeast cells, and the phase contrast and fluorescence microscope (Leica DM6000B, Wetzlar, Germany) with 63× objective was used when working with cells expressing GFP-fused proteins.

4.4.1 Bright-field microscopy

The nutritional status of fission yeast cells can be reflected through their morphology. When there was a need to evaluate o nutritional status of cells at certain stages of an experiment, bright-field microscopy was employed. Fission yeast cells can be

observed under the bright-field microscope at 40-fold magnification. To make the microscopy slide, 2μL of liquid culture is added to a glass slide and covered with a cover slip. If the cells are cultivated on an agar plate, pick a pipette tip of cells and mix them with 2 μL of water, and then load them onto the slide.

4.4.2 Phase contrast and fluorescence microscopy

Phase contrast microscopy exploits the property of light that the phase changes when light waves travel through a different medium. By converting the phase change into brightness change, this technique is able to visualize some cellular structures that are difficult to be observed by bright-field microscopy. Fluorescence microscopy utilizes an intensive light source such as light from xenon arc lamp or mercury-vapor lamp, in order to excite fluorescence from the specimen. The combination of phase contrast microscopy and fluorescence microscopy allows for the imaging of cells exhibiting fluorescence signals at high resolution. In this study, phase contrast and fluorescence microscopy was used for studying cells expressing GFP-fused proteins and localizing nuclei in the cells.

4.4.2.1 DAPI staining

DAPI (4',6-diamidino-2-phenylindole) is a fluorescent stain and is widely used as a counterstain in many experiments. DAPI specifically binds to AT rich regions of DNA, and can penetrate into a cell when it is of high concentration (0.2 μg/mL), therefore the cells do not need to be fixed before DAPI staining. In this study DAPI-staining was used to localize the nuclei in cells. To stain a specimen, 2 μL of 0.2 μg/mL DAPI is added to a cover slip, and then place the cover slip onto the cells on a glass slide. The staining of DAPI is expeditious, thus no incubation is required.

4.4.2.2 GFP-tag checking

In this study, colonies harvested after transformation were subjected to the fluorescence microscope to check whether cells from these colonies were indeed GFP-positive. Cells from these colonies were first cultivated in liquid medium until exponential growth ($OD_{595\ nm}$ = 0.3-0.5) before they were checked by fluorescence microscopy.

4.4.2.3 MCM-chromatin binding assay

Since MCM2-7 is the last component loaded onto the DNA replication origin and marks the accomplishment of pre-RC formation, MCM-chromatin binding assay was

used to quantify pre-RC-loaded cells in this study. Cells were cultured in liquid medium until exponential growth ($OD_{595\ nm}$ = 0.15-0.3) before samples were taken. Samples were taken at several time points of a time course and processed according to the following protocol.

Protocol for taking & processing MCM-chromatin binding assay samples:

1. Transfer around 15 mL cell culture to a falcon tube. Add 150 µL of 1M NaN_3 (and now this sample can be kept on ice for about 2h until all samples are taken).
2. Spin tubes (1200 x g, 4 min, 4^{o}C).
3. Resuspend in 1.8 mL EMM sorb buffer and transfer to 2 mL Eppendorf tubes.
4. Spin tubes (1540 x g, 1 min, 4^{o}C).
5. Resuspend in 450 µL EMM sorb buffer containing 10 mM DTT.
6. Add 100 µL of 40 mg/mL zymolyase 20T.
7. Digest at 36°C for 8-15 min.
8. Test for adequate digestion by adding 2 µL 10% SDS to a 2 µL sample (cells should go dark under phase contrast microscope, aim for >95% of the cells become dark).
9. Add 1.5 mL EMM sorb buffer.
10. Spin tubes (1540 x g, 1 min, 4^{o}C).
11. Resuspend in 2 mL EMM sorb buffer.
12. Spin tubes (1540 x g, 1 min, 4^{o}C).
13. Resuspend in 2 mL extraction buffer.
14. Spin tubes (1540 x g, 1 min, 4^{o}C).
15. Resuspend in 0.9 mL extraction buffer containing protease inhibitor.
16. Split into 2*450 µL
    a. To one 450 µL add 50 µL extraction buffer plus 10% Triton X-100 and incubate 5 min at 25°C inverting periodically (+Triton X-100, extracted sample).
    b. The other 450 µL is kept on ice in the meantime (-Triton X-100, control sample).
17. Spin tubes (1540 x g, 1 min, 4^{o}C).
18. Take off supernatant, flick tubes so cells come off tube wall and add 1.5 mL COLD (-20°C) methanol.
19. Leave on ice for at least 6 mins.
20. Spin tubes (1540 x g, 1 min, 4^{o}C).
21. Resuspend in 1 mL COLD (-20°C) acetone.
22. Store tubes at -20°C. Cells can stand for a few days.

Triton X-100 is a nonionic surfactant which can permeabilize both cytoplasmic and nuclear membrane. After adding 10% Triton X-100 to the cell suspension, cytoplasmic proteins and nuclear proteins that were not bound to the chromatin were leaked out from the cell. Thereby in the extracted samples only cells that contained chromatin-bound MCM2-7 could give out GFP signals, while cells in the control samples had their membrane intact and all could give out GFP signals. Representative pictures of the control sample and the extracted sample both taken right after cell synchronization are shown in Figure S5. Before counting positive cells from the extracted sample, the corresponding control sample was checked in order to make sure that all cells in the control sample gave out GFP signals.

The following protocol was followed to make microscope slides for MCM-chromatin binding assay by using the samples after processing.

Protocol for making microscope slides for MCM-chromatin binding assay:

1. Flip the tube slightly to separate cells, and then load 10 µL of cell suspension to a poly-L-lysine coated microscope slide.
2. Wait until the acetone dries out, apply 2 µL of 0.2 µg/mL DAPI to a cover slip and put it onto the microscope slide.
3. The samples can be stored in dark at 4^{o}C for several days.

In order to generate convincing result, at least 200 cells in total were counted from each sample. The poly-L-lysine coated microscope slides were used here because they permit electrostatic cell adhesion to the surface of the slide and can make cells form a monolayer, which makes it easy to visualize the GFP-signal and perform cell counting.

5 RESULTS

5.1 The protein level of Cdt1 in fission yeast cells released from the *cdc10*-block

Previous work on fission yeast from our group has shown that UVC irradiation in early G1 phase activates the Gcn2-dependent G1/S checkpoint which leads to delayed pre-RC formation, and consequently, the G1/S transition is delayed (Tvegard et al., 2007). However, the mechanism underlying the delayed pre-RC formation is not yet clear. Given the evidence from studies on different model organisms showing that one pre-RC component Cdt1 is regulated in different ways after DNA damage, we started with exploring the protein level of Cdt1 after the activation of the G1/S checkpoint by UVC irradiation.

Fission yeast strains used in this study carry the *cdc10-M17* mutation which allows cells to be synchronized in early G1 phase through the temperature shift-up (1.4.1 and 4.1.3), and the *cdt1-TAP* that encodes Cdt1 protein fused with a TAP-tag enabling the analysis of Cdt1 by Western blot. A flow cytometry experiment was performed before analyzing the Cdt1 level in order to check the synchrony of cells and monitor the cell cycle progression. Here we have designated the synchronization of cells by using the *cdc10-M17* mutation as *cdc10*-block. The *cdc10*-block resulted in a more than doubled population of cells, depleted Cdt1 protein, large ratio of 1C containing cells and cell synchrony in early G1 phase. UVC irradiation was added to the cells immediately when the *cdc10*-block is finished. From then on protein samples and flow cytometry samples were taken from both UVC-irradiated cells and non-irradiated cells in the same time course.

5.1.1 Cell synchrony of *wt* strains

Auxotrophic strains carrying *cdc10-M17* and *cdt1-TAP* behave normally when growing at 25°C in the EMM medium with supplements added, therefore we have designated them as *wt* strains in this study for simplicity. Cells from a *wt* strain (1253) released from the *cdc10*-block were first subjected to flow cytometry for checking the cell synchrony (Figure 5.1). We found that the flow cytometry data of this *wt* strain was quite different from what was previously observed from other *cdc10*-blocked cells. The histograms of the samples taken immediately after release from the *cdc10*-block (Figure 5.1A, B) of this *wt* strain displayed two peaks, indicating that there were two subgroups of cells containing 1C and 2C DNA content respectively; while what

should be expected is a single large peak representing that the majority of cells contain 1C DNA content (see Figure 4.5B and the legends). A main concern about the c*dc10*-block is whether it can indeed halt the cells in early G1 of the new cell cycle; otherwise if the c*dc10*-block is leaky, cells may proceed to further stages next to the early G1 of the new cell cycle after they have gone through the previous cell cycle during the 4 h c*dc10*-block. Wondering whether there was something particularly wrong with this *wt* strain or technical problems in the experiment, we tested another *wt* strain (1237) carrying different auxotrophic markers. We treated the cells in the same way and checked cell synchrony by flow cytometry (data not shown), and we have further performed several biological replicates on both two *wt* strains (data not shown); and all data showed similar results to what was observed in the first experiment.

These results implied that cells from these two *wt* strains might have delayed cytokinesis after the *cdc10*-block for some reason, which might result in some long-shaped cells containing two nuclei; and these cells would be represented in the 2C peak outside the 1C gate in the histograms of the samples taken right after release from the *cdc10*-block (Figure 5.1A, B). These cytokinesis-delayed cells were morphologically one single cell containing 2C DNA content; however, they had actually finished the mitosis of the previous cell cycle, and would divide into two individuals if the *cdc10*-block could be longer.

To verify this assumption, quantification of single-nucleated and two-nucleated cells was performed by phase contrast and fluorescence microscopy. Non-irradiated cells from a flow cytometry sample (the sample for Figure 5.1A) were stained with DAPI to visualize the nuclei, and 186 cells were counted in which 115 cells had one nucleus while 71 cells contained two nuclei (Figure 5.2). The ratio between single-nucleated cells and two-nucleated cells was in correspondence with what was observed from the histogram (Figure 5.1A) which showed a similar ratio between the cells containing 1C DNA content and the cells containing 2C DNA content. These data suggested that the fraction of cells represented in the peak outside the 1C gate (Figure 5.1A, B) were cells which had finished the mitosis of the previous cell cycle. In addition, we detected the Cdt1 abundance in the protein sample taken right after release from *cdc10*-block together with the flow cytometry sample by Western blot. Consistent with our expectation, there was no Cdt1 expressed in this protein sample (Figure 5.3), indicating that the expression of Cdt1 was indeed restrained as a consequence of the *cdc10*-block, thus the cells were not able to pass the early G1 of the new cell cycle. Putting all the evidence together, these *wt* cells synchronized by the *cdc10*-block could only be in a narrow gap between the mitosis of the previous cell cycle and the onset of a new G1 phase, which is to say they were indeed

synchronized in the early G1. We hereby concluded that the cytokinesis of these two *wt* strains (1237, 1253) was delayed after the *cdc10*-block somehow, but the cell synchrony is not affected.

The flow cytometry data also demonstrated that at 120 min after release from the *cdc10*-block, the majority of non-irradiated cells had doubled their DNA content while UVC-irradiated cells increased their DNA content very slowly, indicating that UVC irradiation delayed DNA synthesis (Figure 5.1C, D).

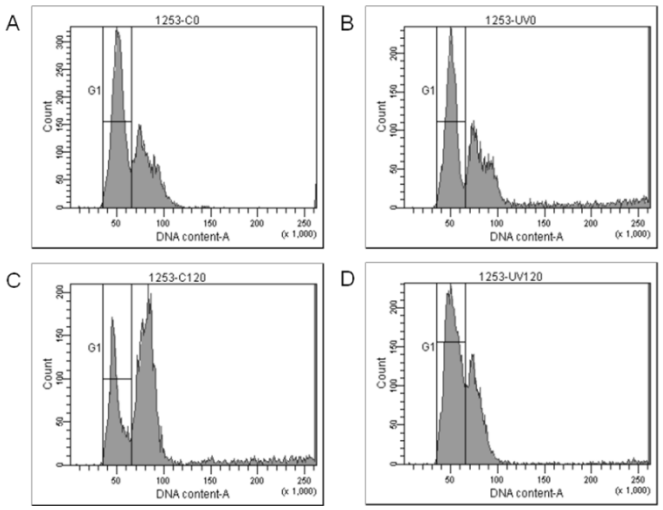

Figure 5.1. Monitoring cell cycle progression of *wt* cells (1253) released from the *cdc10*-block by flow cytometry. (A)(B) Histograms of samples +/- UVC taken right after release from the *cdc10*-block. (C)(D) Histograms of samples +/- UVC taken 120 min after release from the *cdc10*-block. ‘‘C’’ indicates control samples without UVC irradiation and ‘‘UV’’ indicates UVC-irradiated samples. Number of cells is shown on vertical axis and stained-DNA signal intensity is shown on horizontal axis. The peak in the G1 gate represents cells containing 1C DNA content.

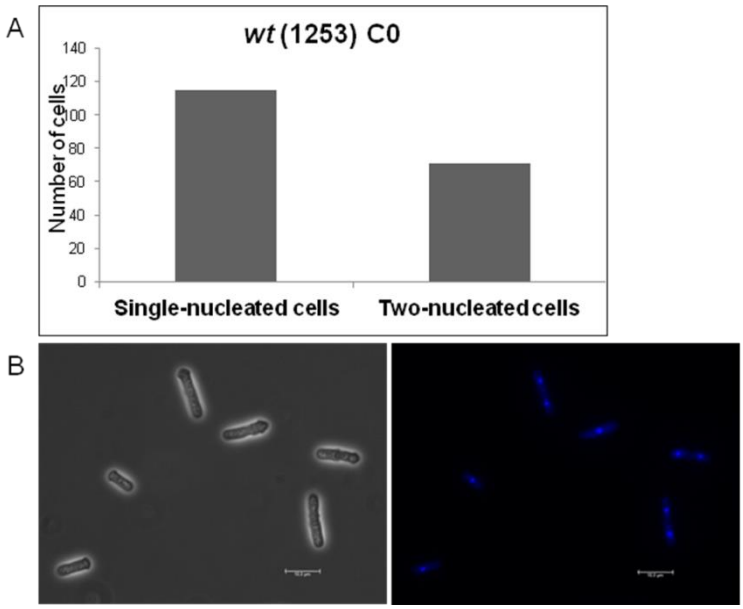

Figure 5.2. Quantification of single-nucleated and two-nucleated cells. (A) A column chart showing quantification result of single-nucleated and two-nucleated cells. Cells counted here were from the flow cytometry sample for Figure 5.1A. (B) Representative pictures from phase contrast and fluorescence microscopy showing the cells from the sample for quantification. From the left: a phase

contrast microscopy picture showing 6 fission yeast cells, a fluorescence microscopy picture showing cells with DAPI stained nuclei. Cells containing two nuclei had finished mitosis of the previous cell cycle and were undergoing cytokinesis of the new cell cycle. Scale bar indicates 10.0 μm.

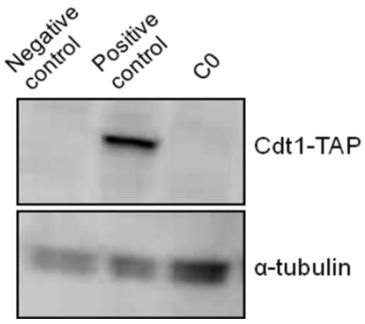

Figure 5.3. Western blot for detection of Cdt1. Cdt1 was detected by an antibody against TAP-tag which gave a band at 70 kDa. Cells carrying *cdt1* (489) were used as negative control, and log-phase cells carrying *cdt1-TAP* (1906) were used as positive control. ''C0'' indicates non-irradiated sample taken right after release from the *cdc10*-block together with the flow cytometry sample. The blot was re-probed with anti-α-tubulin antibody which gave a band at 50 kDa serving as loading control.

5.1.2 Analysis of the protein level of Cdt1 in *wt* cells

After confirming the *wt* cells were indeed synchronized in the early G1 phase, we continued to investigate the protein level of Cdt1 in these cells by Western blot (Figure 5.4). The result showed that UVC-irradiated cells exhibited a lower Cdt1 level than that in the non-irradiated cells; and Cdt1 appeared at 30 min after release from the *cdc10*-block in cells both with and without UVC irradiation. In non-irradiated cells the Cdt1 level peaked at 50 min, and was already slightly lower at 60 min than that at 50 min, indicating that Cdt1 was being degraded, most likely because cells had finished pre-RC loading and were undergoing DNA synthesis. This result was consistent with what was interpreted from flow cytometry data that the DNA content was increasing at 60 min after release from the *cdc10*-block (Figure S1). The Western blot also showed that in UVC-irradiated cells, Cdt1 level continued going up gradually until 90 min, however, at all time points the Cdt1 level in UVC-irradiated cells could never reach as high as that in their non-irradiated counterparts. We then hypothesized the possibility whether the low Cdt1 level in the UVC-irradiated cells was responsible for the delayed DNA synthesis observed from flow cytometry data by affecting the pre-RC formation.

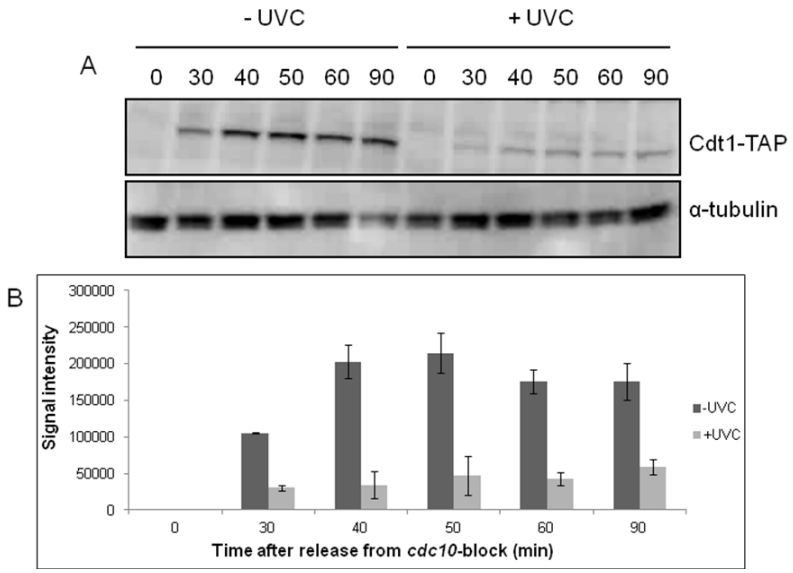

Figure 5.4. Western blot for detection of Cdt1 in *wt* cells released from the *cdc10*-block. (A) Cdt1 was detected by an antibody against TAP-tag which gave a band at 70 kDa . Samples +/- UVC were taken at 0 min, 30 min, 40 min, 50 min, 60 min, and 90 min after release from *cdc10*-block. UVC irradiation was added immediately after release from the *cdc10*-block. The blot was re-probed with anti-α-tubulin antibody which gave a band at 50 kDa serving as loading control. (B) Column chart showing quantified Cdt1 level by normalizing it to α-tubulin level. Data in this column chart are mean values of three experiments, error bars indicate standard deviation.

5.1.3 Analysis of the protein level of Cdt1 in *gcn2Δ* cells

Our group has shown previously that the pre-RC formation in *gcn2Δ* (1238) cells is not affected after UVC irradiation in early G1. If the reduced Cdt1 level is indeed responsible for the delayed pre-RC formation after UVC irradiation, one would expect that Cdt1 level is not reduced in *gcn2Δ* cells that lose the delay. To address this, we studied the protein level of Cdt1 in *gcn2Δ* cells. Flow cytometry experiment and Western blot on the *gcn2Δ* cells were performed in the same way as performed on the *wt* cells. The flow cytometry data showed the *gcn2Δ* cells were properly synchronized in the early G1 phase (Figure 5.5). Western blot result demonstrated that Cdt1 level was also lower in UVC-irradiated *gcn2Δ* cells than that in non-irradiated cells (Figure 5.6). We noticed that in non-irradiated cells Cdt1 still appeared at 30 min after release from the *cdc10*-block, and its level went down during 70 min and 90 min which corresponded to the increase of DNA content from 1C to 2C as observed in the flow cytometry histograms (Figure S2). This implied that cells had finished pre-RC loading and were undergoing DNA synthesis. The level of Cdt1 started to increase from 110 min indicating Cdt1 was being expressed again. In contrast, the UVC-irradiated *gcn2Δ* cells also expressed Cdt1 at 30 min after release from the *cdc10*-block, but the level of Cdt1 was always lower than that in the non-irradiated cells at all time points.

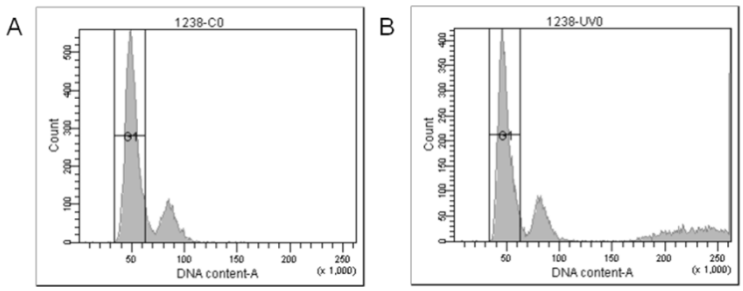

Figure 5.5. Monitoring cell cycle progression of *gcn2Δ* cells released from the *cdc10*-block by flow cytometry. Histograms of samples +/- UVC taken right after release from *cdc10*-block are shown here. Number of cells is shown on vertical axis and stained-DNA signal intensity is shown on horizontal axis. The peak in the G1 gate represents cells containing 1C DNA content. (A) Histogram of non-irradiated sample. (B) Histogram of UVC-irradiated sample.

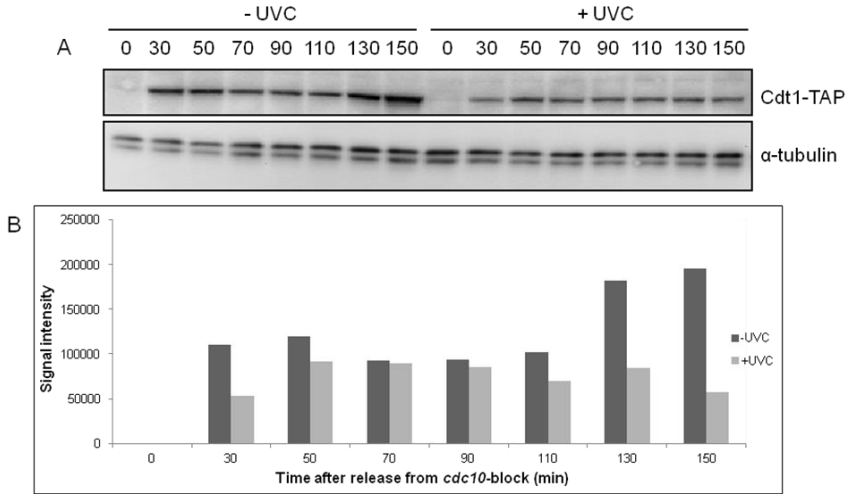

Figure 5.6. Western blot for detection of Cdt1 in *gcn2Δ* cells released from the *cdc10*-block. (A) Cdt1 was detected by an antibody against TAP-tag which gave a band at 70 kDa. Samples +/- UVC were taken at 0 min, 30 min, 50 min, 70 min, 90 min,110 min, 130 min, 150 min after release from *cdc10*-block. UVC irradiation was added immediately after release from the *cdc10*-block. The blot was re-probed with anti-α-tubulin antibody which gave a band at 50 kDa serving as loading control. (B) Column chart showing quantified Cdt1 level by normalizing it to α-tubulin level.

5.1.4 Comparison of the protein level of Cdt1 in *wt* cells and *gcn2Δ* cells

Even though Cdt1 level is lower in UVC-irradiated *gcn2Δ* cells than in the non-irradiated counterparts, pre-RC formation is not delayed suggesting that lower Cdt1 level after UVC is not responsible for pre-RC formation. However, overall Cdt1 levels, both with and without UVC irradiation, seem to be somewhat higher in the absence of Gcn2 than in the corresponding samples from *wt* cells, leaving open the possibility that Cdt1 levels correlate with pre-RC formation delay. In order to directly compare Cdt1 levels in the presence and absence of Gcn2, we explored the protein level of Cdt1 in *wt* and *gcn2Δ* cells on the same Western blot (Figure 5.7). From the column chart we could see that 1) the UVC-irradiated cells always had a lower Cdt1 level than that in the non-irradiated cells at the same time point regardless of the presence

of Gcn2, 2) the Cdt1 level was higher in *gcn2Δ* cells than that in *wt* cells (except the level at UV30) in both UVC-irradiated and non-irradiated cells.

These results led to a hypothesis that the Cdt1 level might be limiting for the pre-RC formation in *wt* cells after UVC irradiation, but in the absence of Gcn2 Cdt1 level was higher, and thus sufficient for pre-RC formation even when reduced in response to UVC irradiation.

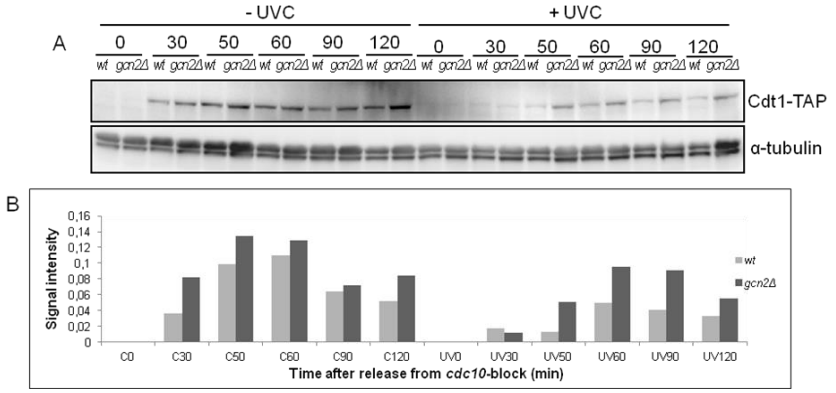

Figure 5.7. Comparing the protein level of Cdt1 in *wt* cells and *gcn2Δ* cells released from the *cdc10*-block by Western blot. (A) Cdt1 was detected by an antibody against TAP-tag which gave a band at 70 kDa. Samples +/- UVC were taken at 0 min, 30 min, 50 min, 60 min, 90 min and 110 min, and 120 min after release from *cdc10*-block. UVC irradiation was added immediately after release from the *cdc10*-block. The blot was re-probed with anti-α-tubulin antibody which gave a band at 50 kDa serving as loading control. (B) Column chart showing quantified Cdt1 level by normalizing it to α-tubulin level.

5.2 *nmt41.cdt2* strain making

To explore our hypothesis, we needed to construct a yeast strain in which the protein level of Cdt1 could be controlled independently from the cells' intrinsic regulatory system. A study has shown that Cdt2 is a component of a Cul4 E3 ubiquitin ligase which is essential for Cdt1 proteolysis induced by DNA damage as well as the maintenance of Cdt1 at a normal level in the absence of DNA damage in fission yeast (Ralph et al., 2006). The transcription of *cdt2* is under the control of the transcription factor Cdc10 (1.4.1). To be able to regulate the Cdt2 level independently of Cdc10, we obtained a strain carrying a *cdt2* gene driven by the thiamine-repressible *nmt41* promoter (4.1.1.5) and the endogenous *cdt2* is deleted (strain 1920, a kind gift of Olaf Nielsen). The strategy for constructing the strain was to modify the genotype of a *wt* strain by deleting its endogenous *cdt2* and inserting a thiamine-repressible promoter-controlled *cdt2* gene (*nmt41.cdt2*) into the genome, so that the level of Cdt1 could be manipulated via regulating the level of Cdt2. Such a strain is referred to as the *nmt41.cdt2* strain in this study. Figure 5.8 depicts the expected kinetics between the Cdt2 level and the Cdt1 level after addition of thiamine in *nmt41.cdt2* strain constructed by our strategy. A genetic cross between a *wt* strain (1237) and the stain

mentioned above (1920) was carried out to construct the strain. The genetic cross resulted in two *nmt41.cdt2* strains (1942 and 1943) which carry different auxotrophic markers (Table 5.9).

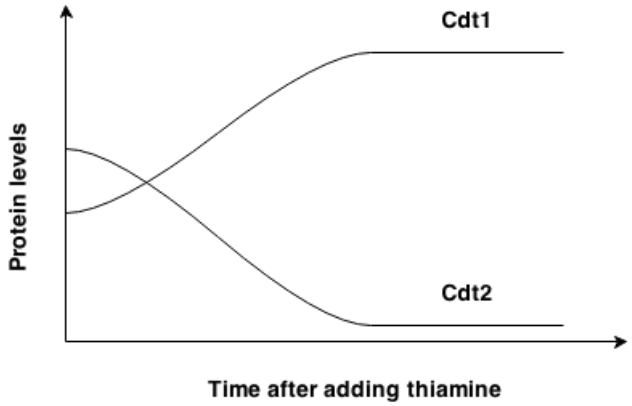

Figure 5.8. Expected kinetics between the Cdt2 level and the Cdt1 level after addition of thiamine in a *nmt41.cdt2* strain constructed by our strategy. The kinetics of Cdt2 level and Cdt1 level should have an inverse relationship after thiamine is added to the medium.

Table 5.9. The genotype of the *nmt41.cdt2* strains resulted from the genetic cross between 1237 and 1920.

Strain	Genotype
1942	*leu1:nmt41.cdt2 cdt2::ura4+ ura4-D18 cdc10-M17 cdt1:TAP:kanR h-*
1943	*leu1:nmt41.cdt2 cdt2::ura4+ cdc10-M17 cdt1:TAP:kanR h-*

5.2.1 Testing *nmt41.cdt2* strains

We next tested the phenotype of these newly constructed *nmt41.cdt2* strains. First we analyzed to what extent the expression of Cdt1 could be influenced by thiamine in these strains. Treating the *nmt41.cdt2* cells by adding thiamine in the medium to 5 μg/mL will repress the *nmt41* promoter and thereby the expression of Cdt2 is repressed, and the Cdt1 can be accumulated in the absence of Cdt2-dependent degradation. Protein samples of log-phase cells from strain 1943 were taken when they were cultivated in liquid EMM medium with and without thiamine, Western blot was performed for checking the Cdt1 level (Figure 5.10). Data demonstrated that without the addition of thiamine, the Cdt1 level in the *nmt41.cdt2* cells was obviously lower than that in log-phase *wt* cells, which probably was due to un-regulated expression of Cdt2. However, two hours after the thiamine treatment, the expression of Cdt1 had already achieved a level nearly as high as that in log-phase *wt* cells, and

the overexpression of Cdt1 went up all the way until seven hours of thiamine treatment, denoting the *nmt41.cdt2* strain was behaving as we expected.

We then tested the strength of the *nmt41* promoter. Since Cdt2 is mainly responsible for the DNA damage-induced Cdt1 degradation in fission yeast, if the repression of the *nmt41* promoter by thiamine treatment is not strong enough, there might still be Cdt2 in the cells and triggers the degradation of Cdt1 after UVC irradiation, which would be troublesome in the following study. Since an antibody against Cdt2 is not available, we tested the strength of the *nmt41* promoter through checking the Cdt1 level. A Western blot was carried out on log-phase *nmt41.cdt2* cells treated with thiamine for 2.5 h with and without UVC irradiation (Figure 5.11A), and another Western blot on log-phase *wt* cells with and without UVC irradiation was carried out as control (Figure 5.11B). The results showed that in log-phase *wt* cells which had normal Cdt2 expression, the degradation of Cdt1 was significant and drastic after UVC irradiation, while in thiamine-treated log-phase *nmt41.cdt2* cells which had repressed Cdt2 expression, there was no detectable degradation of Cdt1 after UVC irradiation, indicating that the repression of the *nmt41* promoter by 2.5 h of thiamine treatment was strong enough to block the expression of Cdt2.

We also investigated whether the *nmt41.cdt2* cells could still be synchronized in early G1 phase. A flow cytometry experiment was carried out on early G1-synchronized *nmt41.cdt2* cells treated with and without thiamine (Figure 5.12). Data showed that cells were synchronized properly no matter whether they were thiamine-treated or not. We hereby confirmed the *nmt41.cdt2* strains could be used in the following experiments, since it can both be synchronized and manipulated to express more Cdt1.

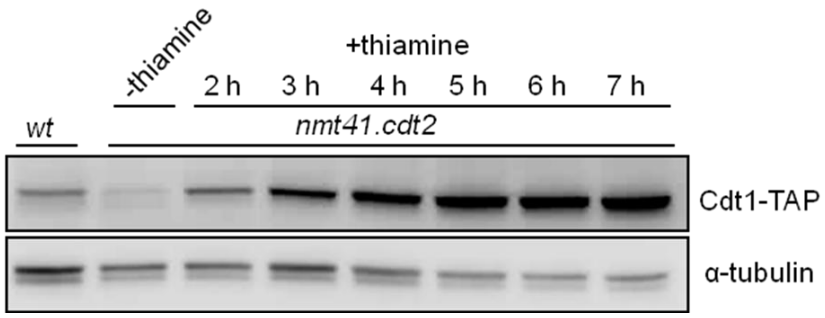

Figure 5.10. Testing the effect on Cdt1 level by thiamine in *nmt41.cdt2* cells by Western blot. Log-phase *nmt41.cdt2* cells were growing in the medium with thiamine added, and samples were taken at different time points after the addition of thiamine. One sample of log-phase *wt* cells were loaded here as a standard in order to show the normal Cdt1 level in log-phase cells. One sample of log-phase *nmt41.cdt2* cells without thiamine treatment was loaded as control. Cdt1 was detected by an antibody against TAP-tag which gave a band at 70 kDa. The blot was re-probed with anti-α-tubulin antibody which gave a band at 50 kDa serving as loading control.

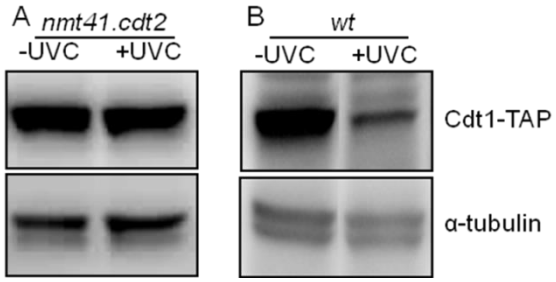

Figure 5.11. Testing the strength of the *nmt41* promoter by Western blot. (A) Log-phase *nmt41.cdt2* cells were treated with thiamine for 2.5 h, and the +UVC sample was taken immediately after UVC irradiation. (B) Log-phase *wt* cell samples served as a control, and the +UVC sample were taken immediately after UVC irradiation. Note that in order to have a clear comparison, the lane of the UVC-irradiated *wt* sample was cropped from the same picture and put next to the lane of non-irradiated *wt* sample. Cdt1 was detected by an antibody against TAP-tag which gave a band at 70 kDa. The blot was re-probed with anti-α-tubulin antibody which gave a band at 50 kDa serving as loading control.

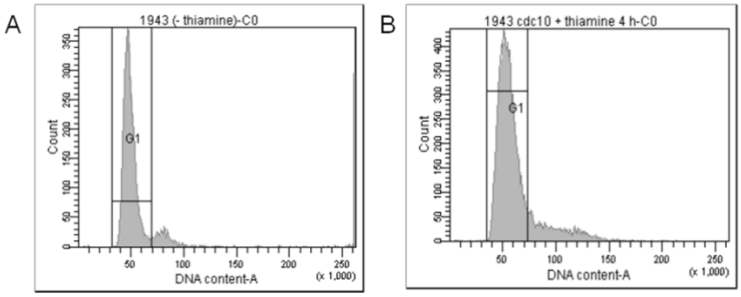

Figure 5.12. Monitoring cell cycle progression of early G1-synchronized *nmt41.cdt2* cells by flow cytometry. Histograms of samples +/- thiamine taken right after release from *cdc10*-block are shown here. Number of cells is shown on vertical axis and stained-DNA signal intensity is shown on horizontal axis. The peak in the G1 gate represents cells in early G1. (A) *nmt41.cdt2* cells growing in the medium without thiamine. (B) *nmt41.cdt2* cells growing in the medium with thiamine for 4 h. Note that the difference between the width of the peaks in these two histograms was due to different technical operations when using the flow cytometer. When low flow rate is applied, the peak is narrow, while under high flow rate the peak appears wider. But the width of peaks does not affect the interpretation of the data.

5.3 Tagging of MCM2-7 subunits in the *nmt41.cdt2* strain with GFP-tag

To quantify the pre-RC formation, the pre-RC needs to be visualized when it is formed. One approach to make the pre-RC visible is to fuse a GFP-tag to the C-terminus of one of the MCM2-7 subunits. The tagging of *mcm* genes in the *nmt41.cdt2* strain (1943) was performed by transformation based on homologous recombination with the PCR-amplified transforming DNA (4.1.2.3).

5.3.1 Amplification of transforming DNA by PCR

We wanted to tag three MCM2-7 subunits: MCM2, MCM6 and MCM7. The transforming DNA used here contains homologous regions to *mcm2/6/7* followed by *GFP* and a selective marker *nat* which confers the transformants clonNAT resistance (the schematic of transformation by using the transforming DNA is shown in Figure 4.2). The PCR reaction mixture set up and program were described in 4.3.1.1. PCR products were analyzed by agarose gel electrophoresis, the size of expected bands is 2350 bp (Figure 5.13). The results had confirmed that the desired DNA fragments were successfully amplified, thereafter the rest of the PCR products were purified to be made into concentrated ready-to-use transforming DNA (100 ng/µL-300 ng/µL). Quantification of DNA concentration was done by NanoDrop spectrophotometer (data not shown).

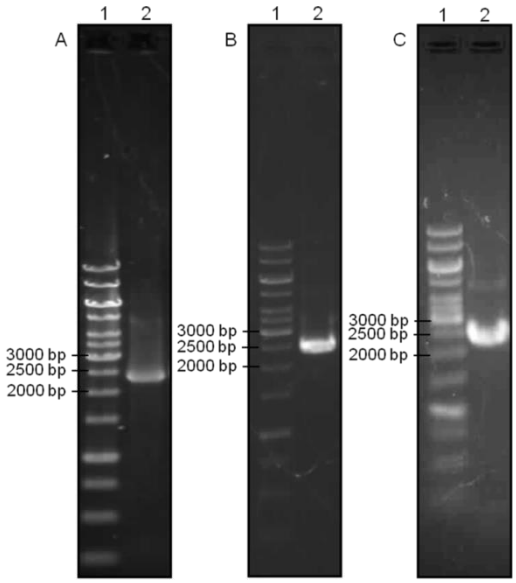

Figure 5.13. Confirming PCR products by agarose gel electrophoresis. Marker was loaded in lane 1 and PCR products were loaded in lane 2. The size of all fragments is 2350 bp. (A) Amplified transforming DNA for tagging *mcm2*. (B) Amplified transforming DNA for tagging *mcm6*. (C) Amplified transforming DNA for tagging *mcm7*.

5.3.2 Transformation of the *nmt41.cdt2* strain

Cells of the *nmt41.cdt2* strain (1943) were cultured in liquid EMM medium instead of YES medium before being transformed in order to avoid the repression of *nmt41* promoter by thiamine contained in YES medium. EMM agar plates containing 100 µg/mL clonNAT were made for selecting colonies. The transformation was performed as described in 4.1.2.3. Colonies were harvested from the primary selective plates and were then transferred onto a secondary selective plate for double-check. The candidates which were still growing on the secondary selective plate were forwarded to next step.

5.3.3 Checking of the transformants

Only the cells which had taken up the transforming DNA could grow on the selective plate; however it could not yet be distinguished whether the exogenous DNA existed as a stable episome or it had been indeed incorporated at the correct locus on the chromosome. To identify the true candidates, there are several approaches. Here, the colony PCR and phase contrast fluorescence microscopy were employed. We started with the colony PCR (4.3.1.2). The upstream primers (primer-in) used in this colony PCR were designed to anneal to a sequence inside the *mcm* gene, while the downstream primers (primer-ds) would anneal to a sequence downstream outside *mcm* gene (Figure 5.14). Therefore for the successful transformants a long sequence around 3000 bp would be amplified, while for the false positive transformants a shorter sequence which ranges 500-800 bp would be amplified. 10-12 colonies were randomly chosen from the secondary selective plate for each transformation and were then subjected to the colony PCR. Colony PCR products were separated by gel electrophoresis (Figure 5.15). Since the colony PCR used here cannot amplify long fragments efficiently, the long fragments (around 3000 bp) amplified from the successful transformants could not be visualized after gel electrophoresis; but short fragments (500bp-800bp) amplified from the false positive fragments could be visualized. The electrophoresis results showed that the colony PCR did not amplify short fragments from 8 colonies, indicating these colonies were successful transformants. According to the results, we harvested 6 colonies transformed with *mcm2:GFP:nat*, 2 colonies transformed with *mcm6:GFP:nat*, but no colony had been successfully transformed with *mcm7:GFP:nat*.

We next checked the expression of the green fluorescent protein in the successful transformed colonies selected by colony PCR. Cells stemmed from theses colonies were cultured in liquid EMM medium until exponential growth and then subjected to phase contrast fluorescence microscopy. One sample of a false positive colony was also prepared as the negative control. A set of representative pictures was shown here (Figure 5.16). We found that all the colonies selected by the colony PCR exhibited positive fluorescence signal. Hereby we obtained 8 colonies carrying a *GFP*-tagged MCM2-7 subunit gene. We started our next experiment by using a colony carrying *mcm6:GFP:nat* (2016), and we refer to it as *nmt41.cdt2 mcm6:GFP* strain for simplicity.

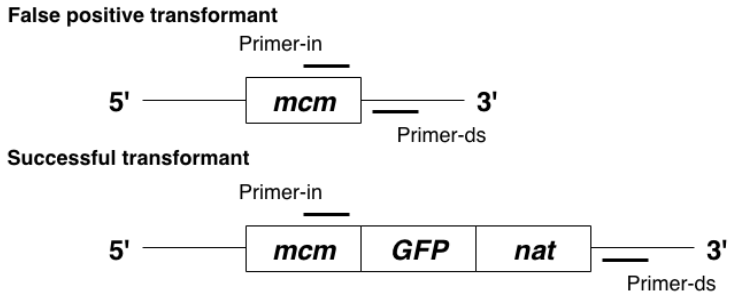

Figure 5.14. Schematic depicting the principle of colony PCR. Due to the regions on the chromosome which the primers anneal to, colony PCR on false positive transformants without the insertion of transforming DNA at the right locus on the chromosome will yield short fragments, while for successful transformants with the insertion of transforming DNA at the right locus on the chromosome will yield long fragments. Primer-in indicates the 5'primer annealing to the sequence inside *mcm*, primer-ds indicates the 3'primer annealing to the sequence downstream *nat*.

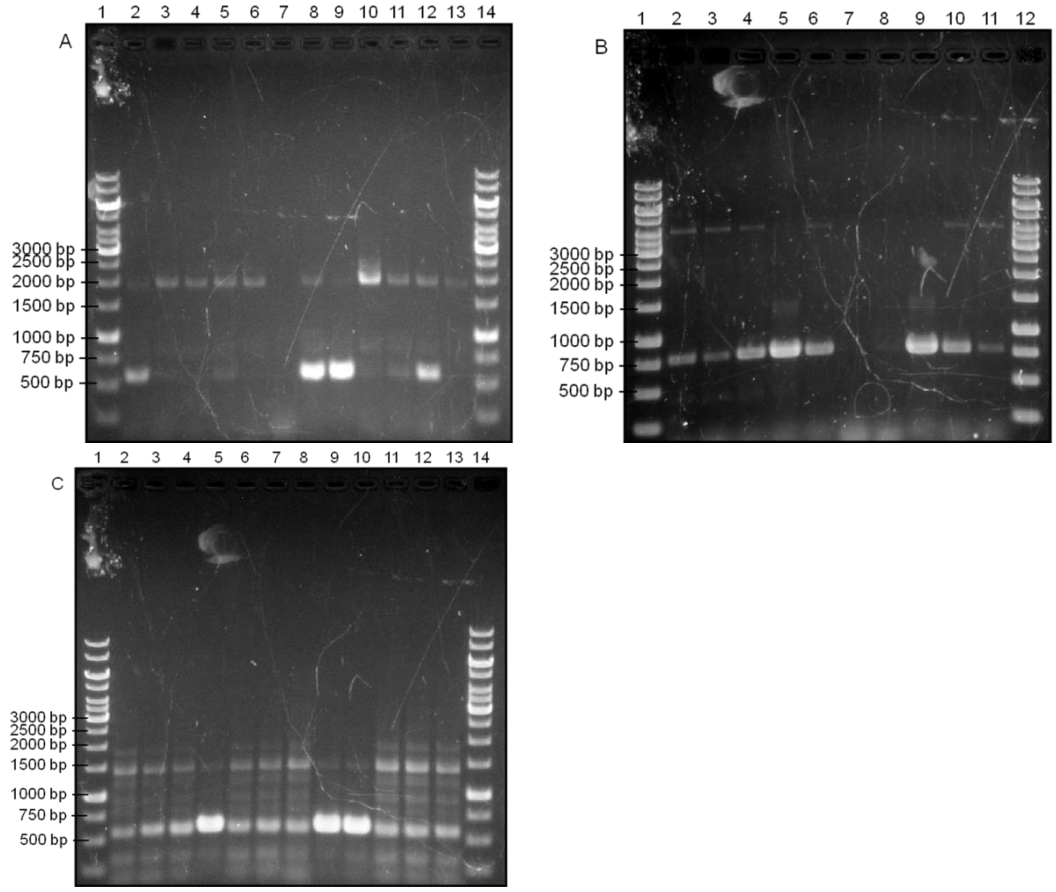

Figure 5.15. Screening for successful transformants by agarose gel electrophoresis after colony PCR. Note that the colony PCR cannot amplify long fragments efficiently, therefore the long fragments (around 3000 bp) amplified from the successful transformants could not be visualized after gel electrophoresis. (A) Screening for colonies transformed with *mcm2:GFP:nat.* Marker was loaded in lane 1 and 14, and colony PCR products was loaded in lane 2-13. Size of fragments amplified from false positive colonies is 571 bp, and size of fragments amplified from successful transformants is 2961 bp. 6 colonies (lane 3, 4, 6, 7, 10, 13) were successfully transformed. (B) Screening for colonies transformed with *mcm6:GFP:nat*. Marker was loaded in lane 1 and 12, and colony PCR products was loaded in lane 2-11. Size of fragments amplified from false positive colonies is 776 bp, and size of fragments amplified from successful transformants is 3126 bp. 2 colonies (lane 7 and 8) were successfully transformed. (C) Screening for colonies transformed with *mcm7:GFP:nat.* Screening for

colonies transformed into mcm2:GFP:nat. Marker was loaded in lane 1 and 14, and colony PCR products was loaded in lane 2-13. Size of fragments amplified from false positive colonies is 589 bp, and size of fragments amplified from successful transformants is 2939 bp. All colonies were false positive.

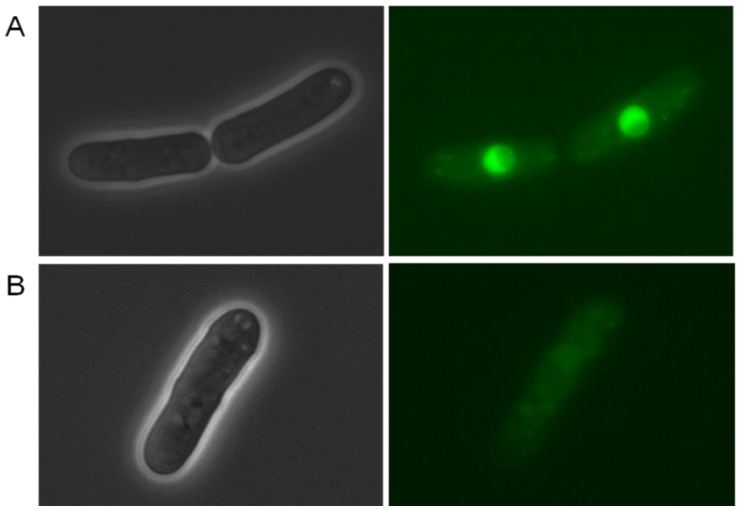

Figure 5.16. Checking GFP signal by phase contrast fluorescence microscopy. (A) Upper panel displays two cells were successfully transformed with *mcm6:GFP:nat* . From the left: a phase contrast microscopy picture of these cells, a fluorescence microscopy picture showing GFP signals from these cells. (B) Lower panel displays a cell from a false positive colony serving as a negative control. From the left: a phase contrast microscopy picture of the cell, a fluorescence microscopy picture showing no positive signal is given by this cell.

5.4 The protein level of Cdt1 in *nmt41.cdt2 mcm6:GFP* cells released from the *cdc10*-block

The next step was to test the Cdt1 level in *nmt41.cdt2 mcm6:GFP* cells released from the *cdc10*-block before using the this strain to study whether higher Cdt1 level could lead to more pre-RC formation after UVC irradiation. The *nmt41.cdt2 mcm6:GFP* cells were first cultivated in liquid EMM medium, thiamine of 5 μg/mL was added to the culture meanwhile the *cdc10*-block was started. Flow cytometry samples and proteins samples were taken from both UV irradiated cells and non-irradiated cells following the same time course. In this study we counted the time of thiamine treatment as the period from the addition of thiamine until the first sample was taken, and we did not wash out thiamine from the medium once it was added. Therefore in this experiment cells were treated with thiamine for 4 h.

5.4.1 Cell synchronization and DNA content

Flow cytometry data showed that the thiamine-treated *nmt41.cdt2 mcm6:GFP* cells were properly synchronized (Figure 5.17), and we also needed to make sure that these cells contained normal DNA content.

Our previous data (Figure 5.10) had shown that in the log-phase *nmt41.cdt2* cells which were treated with thiamine for two hours, Cdt1 had already been accumulated to a comparable level as that in *wt* cells, implying the down-regulation of *cdt2* by blocking the *nmt41* promoter was very fast. And one study has shown that the overexpression of Cdc18 which is another pre-RC component, could lead to over re-replication regardless of the levels of other required factors (Nishitani et al., 2000). Therefore we were concerned that during the 4 h *cdc10*-block when Cdt1 was accumulated due to the lack of Cdt2-dependent degradation, increased Cdt1 level might also induce re-replication of DNA. This possibility would be troublesome in the future work, thus it had to be excluded at the beginning.

Here a flow cytometry experiment was designed to introduce a control 1C peak in the same histogram by using a strain (489) only carrying *cdc10-M17.* One flow cytometry sample of 489 cells was taken immediately after release from the *cdc10*-block, therefore most of the cells contained 1C DNA content. Cell density of this 489 sample and the *nmt41.cdt2 mcm6:GFP* cell sample were measure by a spectrophotometer (data not shown). We next took out the same number of cells from each sample and mix them into one sample, then subjected it to flow cytometry for checking the DNA content. The histogram of this mixed sample (Figure 5.18A) was compared with that of the sample containing only 489 cells (Figure 5.18B), and two histograms looked similar indicating that the majority of cells in both 489 and *nmt41.cdt2 mcm6:GFP* sample contained 1C DNA content. Therefore there was no significant re-replication in the *nmt41.cdt2 mcm6:GFP* cells treated with thiamine. This result is also consistent with previous work from Hideo Nishitani, who showed that co-overexpression of Cdt1 and Cdc18 or overexpression of Cdc18 alone, but not overexpression of Cdt1 alone can lead to over re-replication measurable by the flow cytometry (Grallert, B., personal communication).

We thereby concluded that the *nmt41.cdt2 mcm6:GFP* cells treated with thiamine for 4 hours were properly synchronized after release from the *cdc10*-block, and the synchronized cells contained 1C DNA content; therefore this *nmt41.cdt2 mcm6:GFP* strain can be used for future study.

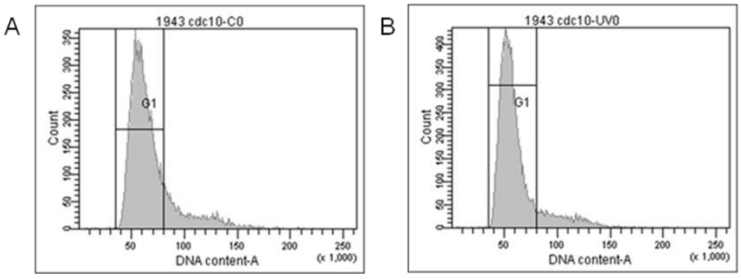

Figure 5.17. Monitoring cell cycle progression of early G1-synchronized *nmt41.cdt2 mcm6:GFP* cells treated with thiamine for 4 h by flow cytometry. Thiamine was added when the *cdc10*-block

was started. Histograms of samples +/- UVC taken right after release from *cdc10*-block are shown here. (A) Histogram of non-irradiated sample. (B) Histogram of UVC-irradiated sample. Number of cells is shown on vertical axis and stained-DNA signal intensity is shown on horizontal axis. The peak in the G1 gate represents early G1-synchronized cells.

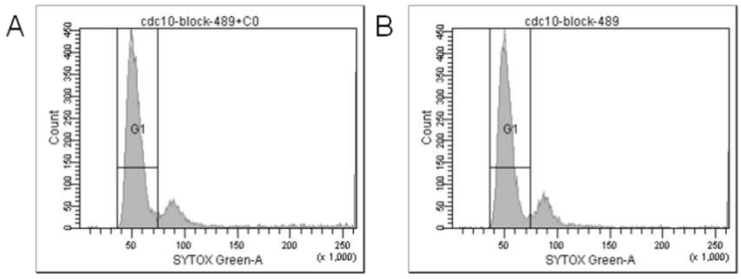

Figure 5.18. Checking the DNA content of early G1-synchronized *nmt41.cdt2 mcm6:GFP* cells treated with thiamine for 4 h by flow cytometry. Thiamine was added to the *nmt41.cdt2 mcm6:GFP* cells at the beginning of the 4 h *cdc10*-block. (A) Histogram of the mixed sample with the same number of early G1-synchronized 489 cells and early G1-synchronized *nmt41.cdt2 mcm6:GFP* cells treated with thiamine for 4 h. (B) Histogram of early G1-synchronized 489 cells the majority of which contained 1C DNA content. Number of cells is shown on vertical axis and stained-DNA signal intensity is shown on horizontal axis. The peak in the G1 gate represents early G1-synchronized cells which contained 1C DNA content.

5.4.2 Analysis of the protein level of Cdt1

Before detecting the Cdt1 level in the samples taken together with the samples for the previous flow cytometry experiment, we investigated whether there was any Cdt1 accumulated in these *nmt41.cdt2 mcm6:GFP* cells during the 4 h of thiamine treatment. Therefore we compared the Cdt1 level in the early G1-synchronized *wt* cell sample and in the early G1-synchronized *nmt41.cdt2 mcm6:GFP* cells which were treated with thiamine for 4 h, a *wt* sample taken 30 min after release from the *cdc10*-block was loaded as positive control (Figure 5.19). This Western blot showed that there was no Cdt1 accumulated during the *cdc10*-block in the *nmt41.cdt2 mcm6:GFP* cells which were treated with thiamine for 4 h.

Next, we examined the Cdt1 level in the *nmt41.cdt2 mcm6:GFP* samples taken together with the samples for the previous flow cytometry experiment by Western blot (Figure 5.20). The result showed that in non-irradiated cells Cdt1 appeared 30 min after release from *cdc10*-block, and the Cdt1 level was increasing throughout the whole time course tremendously; while in UVC-irradiated cells Cdt1 also appeared 30 min after release from *cdc10*-block, however, the level was still much lower than that in non-irradiated cells, and the Cdt1 level was also increasing throughout the whole time course to a large extent. Until 60 min after release from the *cdc10*-block, a clear difference could be observed between the Cdt1 level in cells with and without UVC irradiation, however, at 90 min, the Cdt1 level in cells with and without UVC irradiation became very similar and they continued increasing at a similar rate until 120 min.

We have observed from previous experiments from this study that Cdt1 level was lower in *wt* cells after UVC irradiation in early G1, and we hypothesized that Cdt1 level might be limiting for the pre-RC formation in *wt* cells after UVC irradiation. Here we investigated whether Cdt1 in UVC-irradiated *nmt41.cdt2 mcm6:GFP* cells could reach a level as high as that in non-irradiated *wt* cells. Therefore we analyzed Cdt1 levels in UVC-irradiated *nmt41.cdt2 mcm6:GFP* cells treated with thiamine for 4 h and non-irradiated *wt* cells by Western blot (Figure 5.21). The result showed that 30 min after release from *cdc10*-block, Cdt1 level was slightly higher in *wt* cells; while at 50 min, Cdt1 level was comparable in *nmt41.cdt2 mcm6:GFP* cells and in *wt* cells indicating Cdt1 was being accumulated at a higher rate in *nmt41.cdt2 mcm6:GFP* cells; from 60 min to 90 min, Cdt1 was still being accumulated in *nmt41.cdt2 mcm6:GFP* cells, while being degraded in *wt* cells (the degradation of Cdt1 corresponds with the result from previous experiment in this study, see Figure 5.4). This blot confirmed that after 4h of thiamine treatment, Cdt1 level was still lower in UVC-irradiated *nmt41.cdt2 mcm6:GFP* cells than that in non-irradiated *wt* cells, however, it could reach a level higher than that in non-irradiated *wt* cells from 50 min after release from the *cdc10*-block.

The data we obtained so far showed that in the thiamine treated *nmt41.cdt2 mcm6:GFP* cells, the expression of Cdt1 could be manipulated to a high level after UVC irradiation, a good synchronization could still be achieved by *cdc10*-block, and their DNA content was not affected by thiamine treatment during the *cdc10*-block. Therefore we concluded that these cells could be used in our next step.

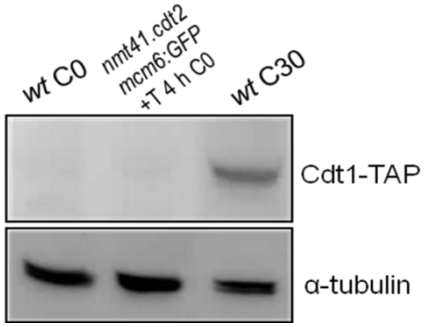

Figure 5.19. Western blot for detection of Cdt1 in thiamine treated *nmt41.cdt2 mcm6:GFP* sample taken right after release from the *cdc10*-block. Cdt1 was detected by an antibody against TAP-tag which gave a band at 70 kDa. The *wt* sample taken right after release from the *cdc10*-block did not have Cdt1 (as proved in Figure 5.3) and served as a negative control, while the *wt* sample taken 30 min after release from the *cdc10*-block had Cdt1 expressed (as proved in Figure 5.4) and served as a positive control. The *nmt41.cdt2 mcm6:GFP* sample taken right after release from the *cdc10*-block was shown in the middle. The blot was re-probed with anti-α-tubulin antibody which gave a band at 50 kDa serving as loading control.

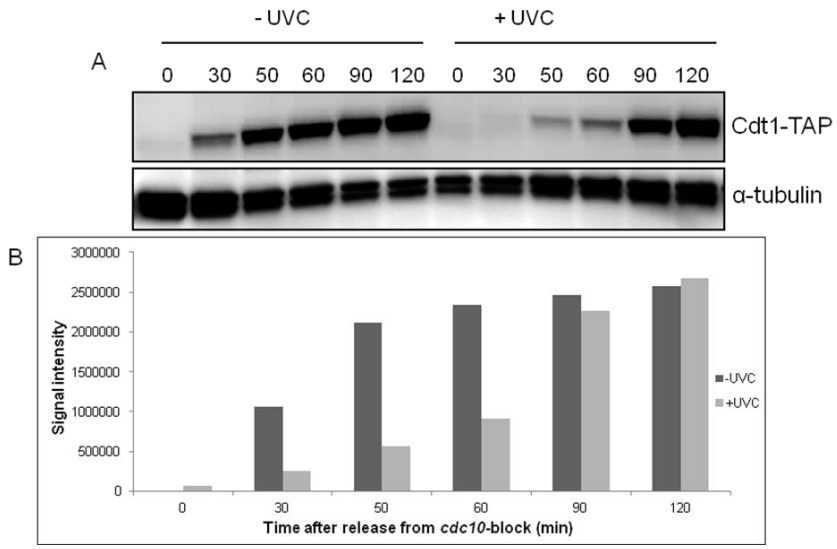

Figure 5.20. Western blot for detection of Cdt1 in *nmt41.cdt2 mcm6:GFP* cells treated with thiamine for 4 h. (A) Cdt1 was detected by an antibody against TAP-tag which gave a band at 70 kDa. Samples +/- UVC were taken at 0 min, 30 min, 50 min, 60 min, 90min, and 120 min after release from *cdc10*-block. UVC irradiation was added immediately after release from the *cdc10*-block. The blot was re-probed with anti-α-tubulin antibody which gave a band at 50 kDa serving as loading control.(B) Column chart showing quantified Cdt1 level by normalizing it to α-tubulin level.

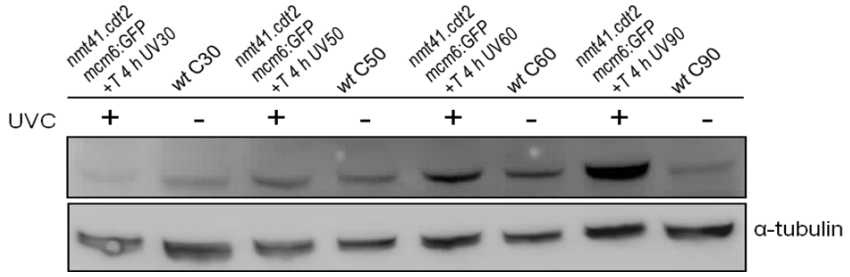

Figure 5.21. Comparing Cdt1 levels in UVC-irradiated *nmt41.cdt2 mcm6:GFP* cells treated with thiamine for 4 h and non-irradiated *wt* cells by Western blot. Cdt1 was detected by an antibody against TAP-tag which gave a band at 70 kDa. Samples +/- UVC were taken at 30 min, 50 min, 60 min, and 90min after release from *cdc10*-block. UVC irradiation was added immediately after release from the *cdc10*-block. The blot was re-probed with anti-α-tubulin antibody which gave a band at 50 kDa serving as loading control. We did not include samples taken right after UVC irradiation (sample UV0 and C0) because we have already shown that at in these samples Cdt1 is not yet expressed (see Figure 5.3 & 5.19).

5.5 Effect on pre-RC formation of overexpressed Cdt1

We next investigated whether up-regulated Cdt1 level could affect pre-RC formation in UVC-irradiated cells. The MCM-chromatin binding assay was performed to quantify pre-RC-formed cells.

5.5.1 Pre-RC formation in *cdt2*+ cells

We first looked at MCM-chromatin binding assay results of two *cdt2*+ strains (983 and 1830, carrying *cdc10-M17* and a *GFP*-tagged MCM2-7 subunit gene) (Figure 5.22). Note that these two assays were not carried out by the author; and in our experience the background signal and thereby the absolute numbers of GFP positive cells varies from experiment to experiment and from person to person performing the experiment. However, the kinetics of pre-RC formation is always the same, regardless of how the background is set. Therefore we could tell from these data that in non-irradiated *cdt2*+ cells, percentage of pre-RC-formed cells increased after release from the *cdc10*-block and peaked at 60 min; and when 120 min after release from the *cdc10*-block, the percentage of pre-RC-formed cells went down to almost as low as that at 0 min. This phenomenon corresponds with the flow cytometry data which demonstrated that cells were undergoing DNA synthesis at 60 min, and at 120 min cells had doubled their DNA content (Figure S3); while in the UVC-irradiated *cdt2*+ cells, percentage of pre-RC-formed cells increased gradually and was lower at all time points than that in their non-irradiated counterparts, and it peaked at least 30 min later than in non-irradiated cells, this phenomenon also corresponds with the flow cytometry data (Figure S3) which demonstrated that the DNA content of UVC-irradiated cells remained almost unchanged until 90 min.

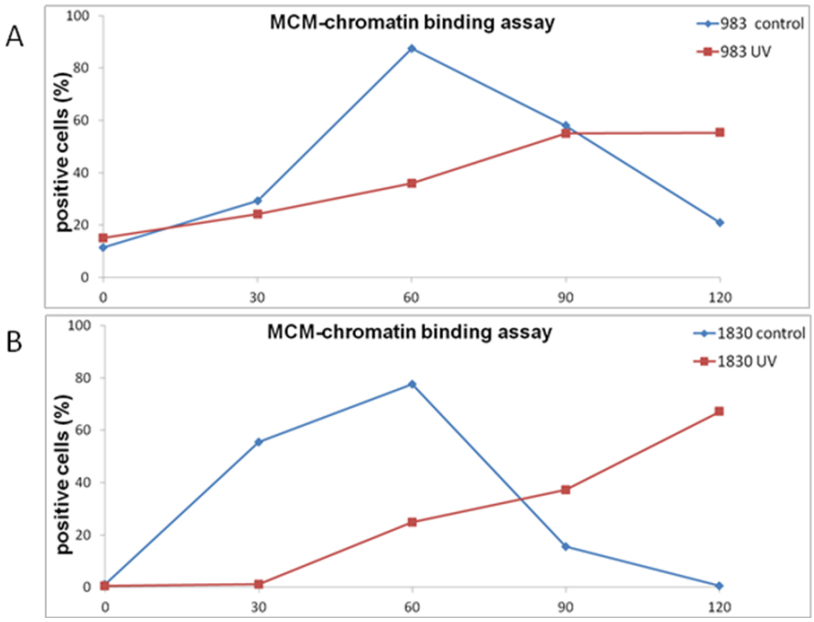

Figure 5.22. MCM-chromatin binding assay of *cdt2*+ cells. Samples were taken at 0 min, 30 min, 60 min, 90 min, and 120 min after release from the *cdc10*-block. At least 200 cells were counted from each sample. Percentage of pre-RC-formed cells is shown on vertical axis and time is shown on horizontal axis. (A) Strain 983 carrying *GFP*-tagged *mcm4*. (B) Strain 1830 carrying *GFP*-tagged *mcm7*.

5.5.2 Pre-RC formation in *nmt41.cdt2 mcm6:GFP* cells treated with thiamine for 4 h

A previous Western blot performed on *nmt41.cdt2 mcm6:GFP* cells treated with thiamine for 4 h (Figure 5.20) had demonstrated that Cdt1 was overexpressed tremendously in both UVC-irradiated and non-irradiated cells. Therefore we next assayed pre-RC formation in *nmt41.cdt2 mcm6:GFP* cells treated with thiamine for 4 h (Figure 5.23). The result showed that in non-irradiated cells, percentage of pre-RC-formed cells increased after release from the *cdc10*-block and peaked after around 60 min, but it went down so gradually that at 120 min the MCM-loaded state was still remained. Cell cycle progression monitored by flow cytometry (Figure 5.24) showed that in non-irradiated cells, DNA content increased from 60 min after release from the *cdc10*-block indicating DNA synthesis had started by then, however, at 120 min, unlike what was observed from *cdt2*+ cells (Figure S3, histogram of sample C120), the DNA content was not doubled indicating S phase was prolonged. It is known that in *cdt2*+ cells in which Cdt1 expression is under normal regulation, MCM2-7 complex stays with the replication fork until the end of DNA replication, while Cdt1 is released and degraded after aiding the loading of MCM2-7 complex before DNA replication takes place (G1/S transition). However, these non-irradiated *nmt41.cdt2 mcm6:GFP* cells overexpressing Cdt1 had prolonged DNA replication, implicating that the abnormal level of Cdt1 might have hampered the advancing of replication fork somehow.

In UVC-irradiated cells (Figure 5.23), the percentage of pre-RC-formed cells increased gradually after release from the *cdc10*-block then peaked as high as the peak of non-irradiated cells after around 90 min, and the MCM-loaded state remained until 120 min, which presumably was due to the overepression of Cdt1. Flow cytometry data (Figure 5.24) demonstrated that DNA content in these UVC-irradiated cells remained unchanged throughout the time course indicating DNA synthesis was still somehow hampered. In contrast with the non-irradiated cells, even though these UVC-irradiated cells had high pre-RC formation at 90 min, DNA synthesis was not observed by flow cytometry, most likely because the intra-S checkpoint was activated by damaged DNA.

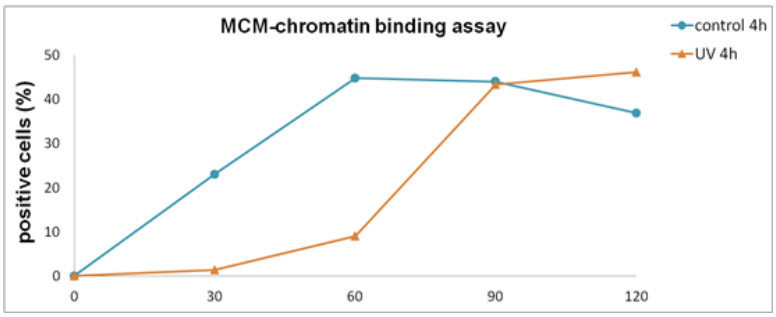

Figure 5.23. MCM-chromatin binding assay of *mt41.cdt2 mcm6:GFP* cells treated with thiamine for 4 h. Samples were taken at 0 min, 30 min, 60 min, 90 min, 120 min after release from the *cdc10*-block. At least 200 cells were counted from each sample. Percentage of pre-RC-formed cells is shown on vertical axis and time is shown on horizontal axis.

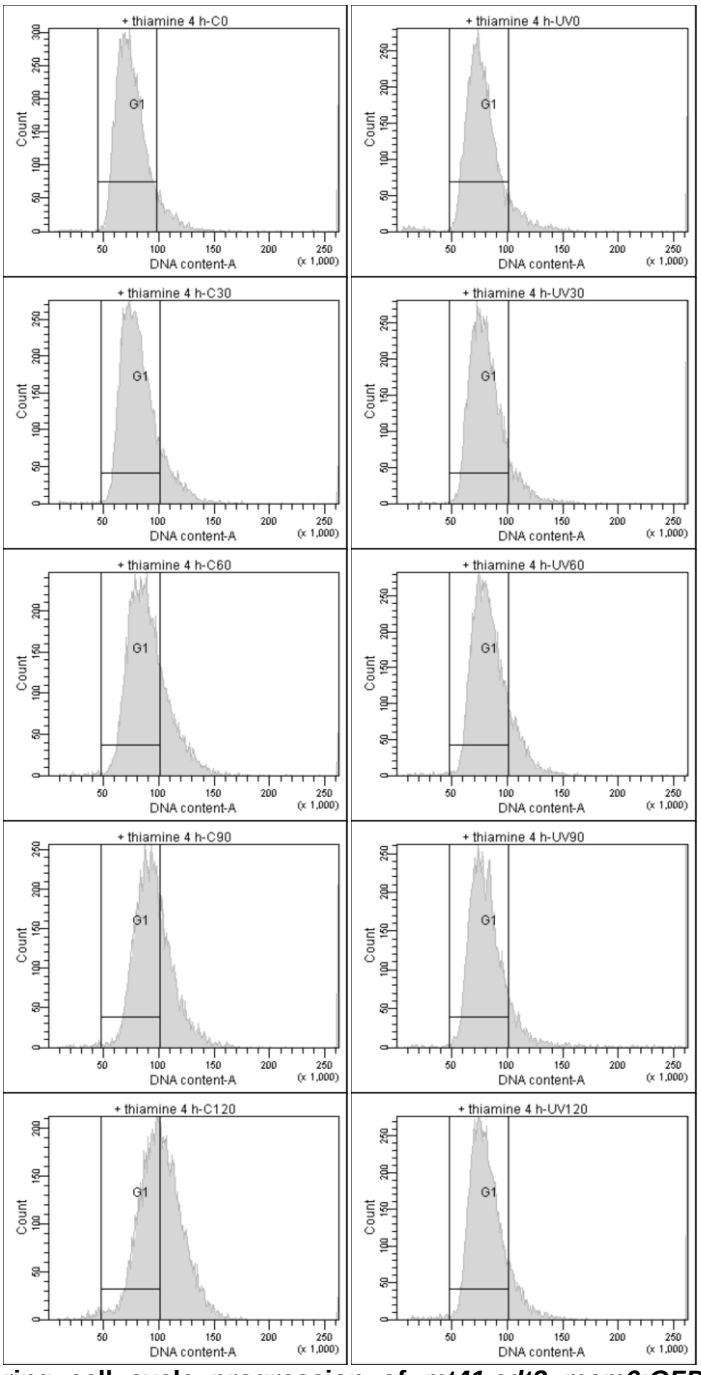

Figure 5.24. Monitoring cell cycle progression of *mt41.cdt2 mcm6:GFP* cells treated with thiamine for 4 h by flow cytometry. On the left are histograms of non-irradiated samples taken at 0 min, 30 min, 60 min, 90 min, and 120 min after release from *cdc10*-block. On the right are histograms of UVC-irradiated samples taken at the same time points. Number of cells is shown on vertical axis and stained-DNA signal intensity is shown on horizontal axis. The peak in the G1 gate represents cells containing 1C DNA content.

5.5.3 Pre-RC formation in *nmt41.cdt2 mcm6:GFP* cells treated with thiamine for 6 h

MCM-chromatin binding assay on *nmt41.cdt2 mcm6:GFP* cells treated with thiamine for 4 h had already shed light on the hypothesis that Cdt1 level is limiting for pre-RC

formation after UVC irradiation in early G1 phase, since in UVC-irradiated cells overexpressing Cdt1, the percentage of pre-RC-formed cells could peak as high as the peak of non-irradiated cells (Figure 5.23). To further prove our hypothesis, we decided to manipulate the overexpression of Cdt1 in UVC-irradiated cells to an even higher level, and then examine whether the formation of pre-RC would also become higher together with Cdt1 level. To further elevate Cdt1 level, this time we treated *nmt41.cdt2 mcm6:GFP* cells with thiamine for 6 h (2 h at 25°C before shift-up and 4 h during the *cdc10*-block at 36°C). Since we know that non-irradiated cells have enough Cdt1 for pre-RC formation, we only compared Cdt1 level in UVC-irradiated cells treated with thiamine for 4 h and 6 h by Western blot (Figure 5.25). The result showed that after UVC irradiation, Cdt1 level in cells treated with thiamine for 6 h was higher than that in cells treated with thiamine for 4 h at all time points.

After confirming that the level of Cdt1 was indeed further elevated after 6 h of thiamine-treatment, cells were subjected to MCM-chromatin binding assay. The result (Figure 5.26) showed after UVC irradiation, percentage of pre-RC positive cells went up to a rather high level already at 60 min after release from the block, and peaked at 90 min. Comparing MCM-chromatin binding assay results of *nmt41.cdt2 mcm6:GFP* cells treated with thiamine for 4 h and 6 h (Figure 5.27), we found that in the non-irradiated cells the pre-RC formation was almost the same regardless of that the cells treated with thiamine for 6 had higher Cdt1 level; however in the UVC-irradiated cells a clear difference was observed at 60 min after release from the block, that the pre-RC formation was significantly higher in UVC-irradiated cells treated with thiamine for 6 h. This difference is in correspondence with the Western blot result (Figure 5.25, UV60), that after UVC irradiation, cells (treated with thiamine for 6 h) with more Cdt1 had a higher percentage of the pre-RC formation.

In addition, flow cytometry data for monitoring the cell cycle progression of *nmt41.cdt2 mcm6:GFP* cells treated with thiamine for 6 h (Figure 5.28) were similar to that of *nmt41.cdt2 mcm6:GFP* cells treated with thiamine for 4 h (Figure 5.24), showing that the DNA replication was also prolonged in non-irradiated *nmt41.cdt2 mcm6:GFP* cells treated with thiamine for 6 h; and DNA content in the UVC-irradiated cells remained unchanged throughout the time course indicating DNA synthesis was still somehow hampered.

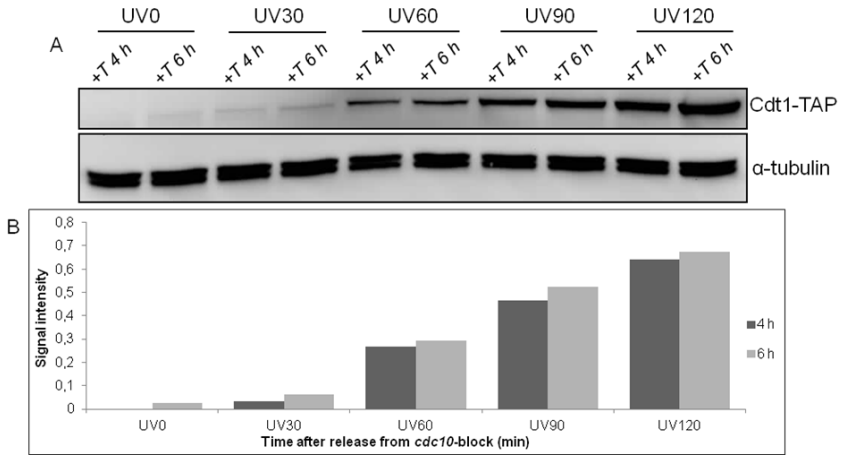

Figure 5.25 . Comparing the protein level of Cdt1 in UVC-irradiated *nmt41.cdt2 mcm6:GFP* cells treated with thiamine for 4 h and 6 h by Western blot. (A) Cdt1 was detected by an antibody against TAP-tag which gave a band at 70 kDa. Samples +UVC were taken at 0 min, 30 min, 60 min, 90 min, and 120 min after release from *cdc10*-block. UVC irradiation was added immediately after release from the *cdc10*-block. The blot was re-probed with anti-α-tubulin antibody which gave a band at 50 kDa serving as loading control. (B) Column chart showing quantified Cdt1 level by normalizing it to α-tubulin level.

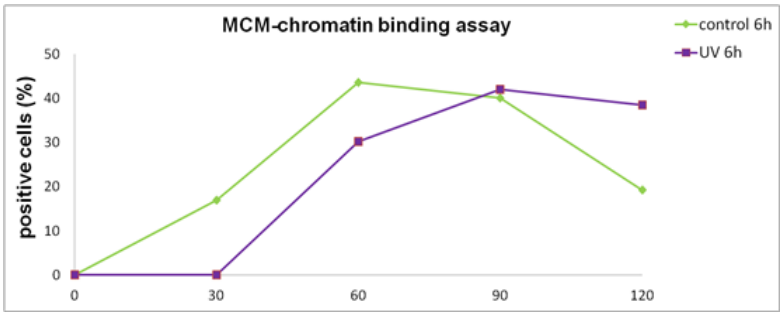

Figure 5.26. MCM-chromatin binding assay of *mt41.cdt2 mcm6:GFP* cells treated with thiamine for 6 h. Samples were taken at 0 min, 30 min, 60 min, 90 min, 120 min after release from the *cdc10*-block. At least 200 cells were counted from each sample. Percentage of pre-RC-formed cells is shown on vertical axis and time is shown on horizontal axis.

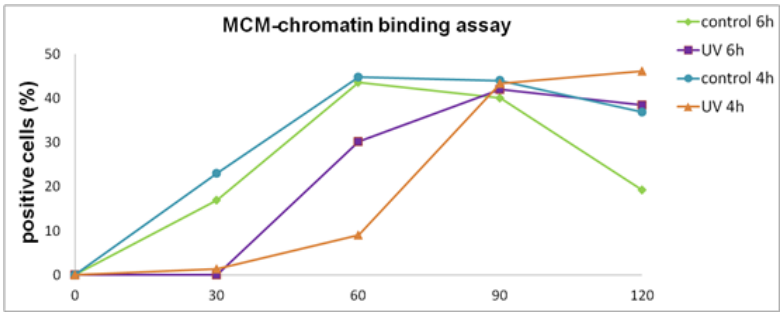

Figure 5.27. Comparing MCM-chromatin binding assay results of *nmt41.cdt2 mcm6:GFP* cells treated with thiamine for 4 h and 6 h. Samples were taken at 0 min, 30 min, 60 min, 90 min, 120 min after release from the *cdc10*-block. At least 200 cells were counted from each sample. Percentage of pre-RC-formed cells is shown on vertical axis and time is shown on horizontal axis.

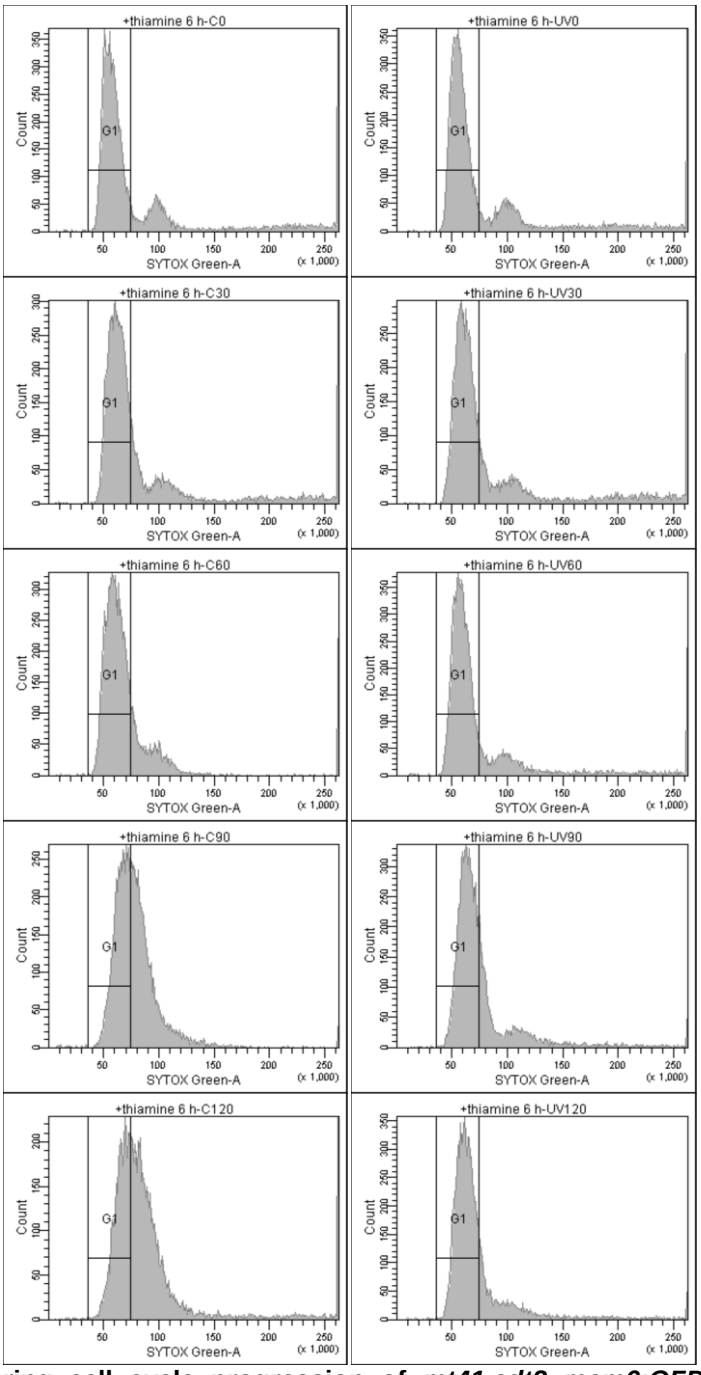

Figure 5.28. Monitoring cell cycle progression of *mt41.cdt2 mcm6:GFP* cells treated with thiamine for 6 h by flow cytometry. On the left are histograms of non-irradiated samples taken at 0 min, 30 min, 60 min, 90 min, and 120 min after release from *cdc10*-block. On the right are histograms of UVC-irradiated samples taken at the same time points. Number of cells is shown on vertical axis and stained-DNA signal intensity is shown on horizontal axis. The peak in the G1 gate represents cells containing 1C DNA content.

The preliminary MCM-chromatin binding assay data we obtained so far support our hypothesis that Cdt1 is limiting for pre-RC formation after UVC irradiation in early G1 of fission yeast. We also find that in UVC-irradiated cells, although overexpression of Cdt1 can increase pre-RC formation, DNA synthesis is still delayed. This indicates

that the progression of some downstream events after pre-RC formation might be hampered. Moreover, in non-irradiated cells, DNA synthesis seems to be prolonged when Cdt1 is overexpressed, implying that too much Cdt1 in the cell might somehow interfere with the advancing of replication fork during S phase, and consequently, lead to a sluggish DNA replication.

6 DISCUSSION

Our group has discovered a novel G1/S checkpoint in fission yeast that arrests the cell cycle through delaying pre-RC formation, the very first step of the preparation process for entering into S phase, and this checkpoint is dependent on Gcn2 kinase. Previous work on the Gcn2-dependent checkpoint has demonstrated that when it is activated in wild-type cells by UVC irradiation, the percentage of pre-RC-loaded cells is lower than that in non-irradiated cells, leading to a delayed entry into S phase; while in UVC-irradiated *gcn2Δ* cells which have a defective G1/S checkpoint, the percentage of pre-RC-loaded cells remains the same as in the non-irradiated ones (Tvegard et al., 2007). However, the downstream events of this checkpoint that affect the pre-RC formation are not yet well studied, and the molecular mechanisms underlying these events also require elucidation.

Here, we have investigated the relationship between the replication initiation factor Cdt1 and pre-RC formation. We present evidence showing that the pre-RC formation exhibits a corresponding increase with the increase of Cdt1 after the G1/S checkpoint is activated by UVC irradiation. In this chapter I will discuss my results in light of other studies. I will also bring out the future work which could be done to extend what we have found in this study. In the end I will give considerations on what could be optimized in some experiments performed in this study.

General discussion and future work

6.1 The protein level of Cdt1 is reduced after UVC irradiation in early G1 phase

We have shown that in the wild-type cells released from the *cdc10*-block, the protein level of Cdt1 is lower in UVC-irradiated cells than in the non-irradiated ones at all time points. It has been reported that in mammalian cells Cdt1 is proteolysed through ubiquitination in response to DNA damage induced by UVC irradiation (Kondo et al., 2004; Sakaguchi et al., 2012; Stathopoulou et al., 2012); and an essential molecular platform, the chromatin-bound PCNA, is required in this process (Arias and Walter, 2006). In fission yeast it has been shown that the chromatin-bound PCNA is also required for DNA damage-induced proteolysis of Cdt1; and the work on this discovery was carried out on cells synchronized in mitosis using an *nda3* mutant that can be arrested in metaphase (Guarino et al., 2011; Ralph et al., 2006).

In the current study, UVC irradiation was performed in cells synchronized in early G1 by inactivating the Cdc10 transcription factor, and hence when cell were released from the block 1) they did not have Cdt1, 2) they also did not have chromatin-bound PCNA. Furthermore, Cdt2, which is essential for the UVC-induced degradation of Cdt1 in fission yeast, also depends on Cdc10 for transcription. Thus the lower protein level of Cdt1 was determined by the contradicting effects of Cdc10-dependent transcription and Cdt2-dependent degradation, where the Cdc10-driven accumulation of Cdt2 competes with the Cdc10-driven accumulation of Cdt1. It seems that in our study, the reduced Cdt1 level is a consequence of different regulations. Here a simplified schematic diagram depicting gene expression regulation at different levels is shown (Figure 6.1). I will discuss the regulation of Cdt1 level in fission yeast after UVC irradiation in early G1 phase in light of these considerations.

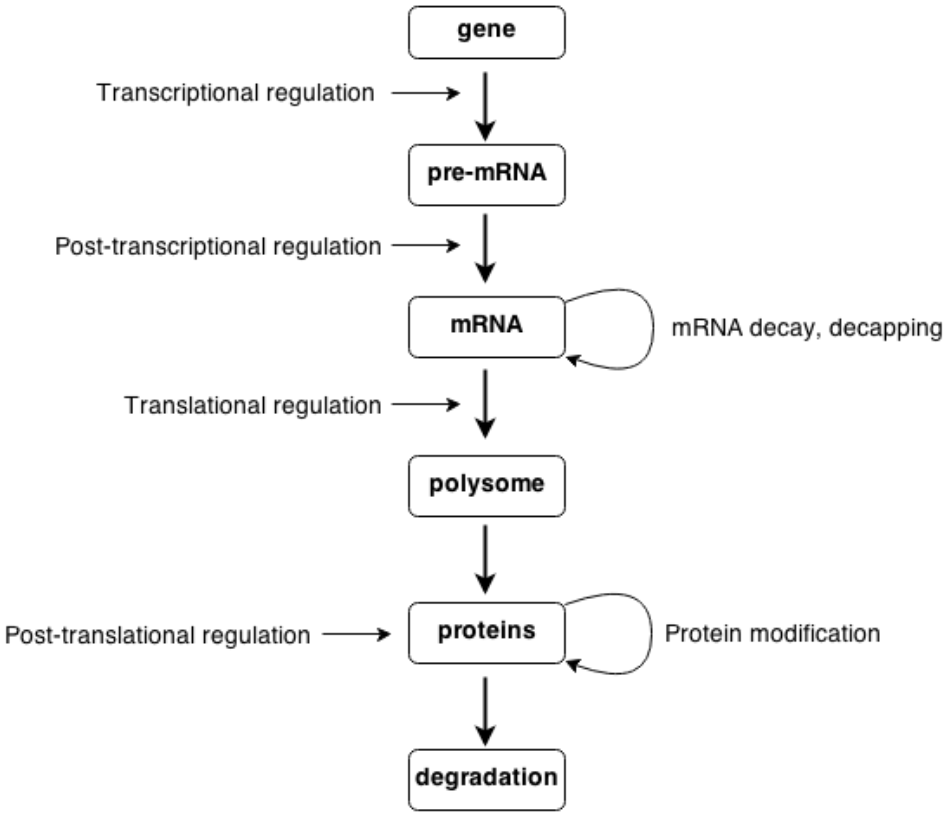

Figure 6.1. Schematic of the regulation of gene expression at different levels.

1) Regulation of Cdt1 is not likely to occur at transcriptional level

Cdt1 is the product of *cdt1*, a gene under the control of the transcription factor Cdc10. After release from the *cdc10*-block, the Cdc10 transcription factor functions normally again eliciting the transcription of its target genes such as *cdt1, cdc18, cdt2* and *cig2*. Previous work from our group has shown by Northern blot that total RNA amount of *cig2* is not affected after UVC irradiation in early G1 (Nilssen et al., 2004).

In the current study we have checked the levels of Cig2 by Western blot, and the blot showed that Cig2 levels were not significantly affected by UVC irradiation in early G1 (Figure S4), which correlates with the Northern blot result. Putting such evidence together, it is demonstrated that the expression of *cig2* in the cells released from the *cdc10*-block is not affected by UVC irradiation neither at transcriptional level nor at translational level. This result also indicates that the expression of the transcription factor Cdc10 is not affected; and hence the Cdc10-dependent transcription of *cdt1* is not likely to be affected either. Still, a Northern blot to verify the total RNA amount of *cdt1* is needed for providing convincing evidence. Furthermore, there is another study supporting the notion that the transcription of *cdt1* was not affected by UVC irradiation in early G1. By exploiting microarray analysis, this study shows that the global transcriptional response is little after the G1/S checkpoint is activated by UVC irradiation of fission yeast, this study also indicates that genes of which the transcription is induced or repressed after UVC irradiation are unlikely to be involved in the G1/S checkpoint mechanism, suggesting this UVC-induced G1/S checkpoint functions independently of transcriptional regulation (Skjolberg et al., 2009). In addition, this study also implies that the activation of the G1/S checkpoint does not lead to transcriptional response in fission yeast.

2) Regulation of cdt1 mRNA at post-transcriptional level is unknown

Control at post-transcriptional regulation level by processing mRNA precursors (pre-mRNA) and regulating mature mRNA stability serves as a significant means to regulate gene expression and links the development of organisms and human diseases (reviewed in (Chen and Manley, 2009)). Since the processing of pre-mRNA is rapid and occurs co-transcriptionally, it is not likely that Cdt1 is regulated at pre-mRNA level when the transcription of *cdt1* is not affected.

RNA granule-mediated post-transcriptional control pathways including processing granules, stress granules, and germ cell granules are key modulators of gene expression at post-transcriptional level (reviewed in (Anderson and Kedersha, 2009)). Cytoplasmic processing bodies (PBs) have been found in fission yeast contributing to mRNA turnover through several devices such as mRNA decay and mRNA decapping (Wang et al., 2013); it has also been demonstrated that stress granules (SGs) containing poly(A)-binding protein (PABP) which acts as a central modulator of mRNA stability are induced in fission yeast in order to survive from cellular stress (Nilsson and Sunnerhagen, 2011). In light of these discoveries, it is possible that fission yeast cells respond to UVC irradiation through post-transcriptionally regulating the stability of the mRNA of certain target genes. By using an inhibitor of transcription, a study has shown that the change of gene expression is due to the change of mRNA stability with conditions such as hormonal stimulation or

cellular stress (Marin-Navarro et al., 2011). The evidence provided in these studies makes us suggest whether the stability of the mRNA of *cdt1* is affected in response to UVC-induced cellular stress. However, we do not yet have data that can be used for analyzing the regulation of *cdt1* mRNA stability from the current study.

It would be interesting to carry out further experiments to isolate *cdt1* mRNA by using pre-mRNA by poly(A) tail-binding column and quantify the amount of both species of RNA respectively in both UVC-irradiated and non-irradiated cells by semi-quantitative RT-PCR, then compare the results of corresponding samples; the analysis of the data might tell us whether *cdt1* is a target of post-transcriptional regulation when the G1/S checkpoint is activated by UVC irradiation of fission yeast.

3) Regulation of Cdt1 at translational level

Regulation of the abundances of protein is in principle focused on the translational initiation stage because it provides a reversible and more rapid means to control gene expression (reviewed in (Jackson et al., 2010)). A study has shown that in response to environmental stress, fission yeast exhibits strong correlation in regulating gene expression at mRNA level and translational level. Intriguingly this study further shows that regulation patterns of a subgroup of genes are discordant only under oxidative and heat stress; whereas in the situation that DNA damage is induced by alkylating agent MMS (methyl methane sulfonate), majority of genes are still regulated concordantly at both mRNA level and translational level (Lackner et al., 2012). As discussed in 1) and 2), it is unlikely that gene expression of *cdt1* after UVC irradiation is affected at transcriptional level, while the regulation at mRNA level remains unknown. People in our lab have performed polysome profiling to examine the abundances of ribosome-associated mRNA in cells released from the *cdc10*-block with and without UVC irradiation. The data showed that in the UVC-irradiated cell sample taken 30 min after release from the *cdc10*-block, the amount of ribosome-associated *cdt1* mRNA was only 20% of that in the non-irradiated cells; in addition, a global downregulation at translational level in the UVC-irradiated cells has also been found, indicating that Cdt1 is downregulated at translational level after UVC irradiation (Knutsen JH., unpublished data). However, we do not know whether the downregulation of Cdt1 at translational level after UVC irradiation is due to the decreased *cdt1* mRNA stability or selective translation of mRNA.

An alternative explanation for the polysome profiling data is that at 30 min after release from the *cdc10*-block the abundance of *cdt1* mRNA is very low, making it difficult and inaccurate to analyze its level in the polysome fraction. However, data in this work showed that Cdt1 protein is detectable at this time point (Figure 5.4),

arguing against this explanation and thus suggesting that Cdt1 translation is indeed downregulated at a time when transcription is induced.

Therefore the evidence obtained from polysome profiling not only shows that downregulation of the protein abundance of Cdt1 at translational level after UVC irradiation is very likely, it also emphasizes the importance of specifically examining the *cdt1* mRNA level in order to know whether the reduced ribosome-associated *cdt1* mRNA level after UVC irradiation in early G1 is due to decreased *cdt1* mRNA stability, or due to selective translation of mRNA.

4) Regulation of Cdt1 through protein degradation

It has been demonstrated in exponentially growing mammalian cells that irradiation-induced DNA damage triggers rapid degradation of Cdt1 in a manner independent of the classic G1/S checkpoint, since players such as ATM and Chk2 are not found to be involved in this process, and this mechanism is thought to be evolutionarily conserved (Higa et al., 2003). We have also examined the DNA damage-triggered degradation of Cdt1 in log-phase fission yeast cells exposed to UVC irradiation (Figure 5.11B). Consistent with the work from Ralph et al., which shows Cdt1 degradation is triggered by DNA damage, we found that the degradation of Cdt1 triggered by UVC irradiation was rapid and sensitive, since the Cdt1 decreased dramatically right after UVC irradiation. However, in this experiment log-phase cells were used; and given the fact that the majority of log-phase fission yeast cells are in G2 phase (Figure 1.4), the result still could not tell us whether the activation of G1/S checkpoint by UVC irradiation in fission yeast triggers Cdt1 degradation.

We know that the pathway for DNA damage-induced Cdt1 proteolysis in fission yeast is dependent on a ubiquitin E3 ligase component Cdt2 (Ralph et al., 2006), therefore cells lacking Cdt2 are not competent to degrade Cdt1 (Figure 5.11A). In this study we used a thiamine-repressible promoter *nmt41* to regulate the abundance of Cdt2 independently of Cdc10. As shown by our data (Figure 5.20), 60 min after release from the *cdc10*-block, the level of Cdt1 was still much lower in UVC-irradiated Cdt2-lacking *nmt41.cdt2* cells than in their non-irradiated counterparts, while at 90 min the Cdt1 level in both cells with and without UVC reached the same height. These results imply that although the Cdt2-dependent Cdt1 proteolysis is functioning, it does not seem to be, at least during the 60 min at the beginning, the main mechanism responsible for the reduced Cdt1 level after UVC irradiation in early G1. However, we are unsure about whether the interpretation from these data is a consequence due to the synchronization method by using the *cdc10*-block; since cells released from the *cdc10*-block need some time for synthesizing Cdt2, and they probably do not have sufficient Cdt2 to undergo the degradation of Cdt1 during the 60 min at the

beginning. We speculate what the case will be if the UVC irradiation is added to early G1-synchronized cells which already have a normal amount of Cdt2. To explore this, one approach is through treating the *nmt41.cdt2* cells with thiamine for shorter time or of a lower concentration, in order to allow Cdt2 to be accumulated to a certain level in the cells when they are released from the *cdc10*-block; and then analyze the Cdt1 level in these cells by Western blot, to see whether Cdt1 amount after UVC irradiation is unchanged or reduced to an even lower level.

To sum up, our data suggest that the regulation of the Cdt1 level after UVC irradiation in early G1 should be focused on several levels, among which the regulation at the protein degradation level is already supported by direct evidence from this study, and it would be interesting to explore the regulation of Cdt1 at other levels as well.

6.2 Cell cycle progression is delayed after UVC irradiation of *wt* cells

Our flow cytometry data showed that cell cycle progression of *wt* cells released from the *cdc10*-block became delayed after they were exposed to UVC irradiation (Figure S1), and MCM-chromatin binding assay results showed that in UVC-irradiated *cdt2*+ cells released from the *cdc10*-block, the percentage of pre-RC-formed cells was lower at all time points than that in the non-irradiated cells (Figure 5.22). Putting these data together, a main reason for the delayed cell cycle progression could be the low level of Cdt1 leading to delayed formation of pre-RC after UVC irradiation. However, the significance for the low level of Cdt1 after UVC irradiation should not to be emphasized on delaying the pre-RC formation only.

Given the fact that PCNA, which takes part in the degradation of Cdt1 in a chromatin-bound form in fission yeast, is pivotal for orchestrating multiple aspects of DNA metabolism through playing as a versatile protein scaffold for multiple proteins (Moldovan et al., 2007), a recent study has demonstrated that UV-induced DNA damage activates the degradation of PIP (PCNA-interacting protein) degron-containing proteins in order to prevent them from interfering the focus formation of Y-family DNA polymerase η and κ, since DNA polymerase η and κ also bind to chromatin in a PIP box-dependent manner (Tsanov et al., 2014). DNA polymerase κ is known to be recruited to UV-damaged site for nucleotide excision repair (NER) in the G1 phase (Ogi and Lehmann, 2006), and Cdt1 in fission yeast has been shown to contain dual PIP degrons (Guarino et al., 2011). Therefore it is also highly

probable that after UVC irradiation in early G1, cells downregulate Cdt1 level in order to promote the occupancy of DNA polymerase κ on chromatin to undergo NER. Since the NER in G1 phase occurs at least by out-competing Cdt1, it also contributes to slowing down the pace of pre-RC formation which consequently delays the cell cycle progression.

6.3 Overexpression of Cdt1 in G1 does not lead to DNA re-replication but a delayed cell cycle progression

It has been shown that in fission yeast, overexpression of Cdc18 alone leads to DNA re-replication, and co-overexpression of Cdt1 together with Cdc18 also leads to re-replication presumably due to the stabilization of MCM2-7 complexes by Cdt1 at the replication origins (Gopalakrishnan et al., 2001; Nishitani et al., 2000; Nishitani and Nurse, 1995; Yanow et al., 2001). Cdc18 and Cdt1 are both licensing factors playing essential roles in the formation of pre-RC, the expression and degradation of them are tightly regulated in a cell-cycle phase-specific manner. Thus when the expression of either of them is uncontrolled, it is more likely that DNA re-replication will be induced. However in this study, we found that in the *nmt41.cdt2* cells overexpression of Cdt1 alone did not lead to DNA re-replication (Figure 5.18), on the contrary a delayed cell cycle progression with a prolonged DNA synthesis was observed (Figure 5.24 & 5.28).

There are studies in different model systems showing that in cancer cell lines Cdt1 overexpression induces DNA re-replication (Nishitani et al., 2004; Saxena and Dutta, 2005; Vaziri et al., 2003), while in non-transformed cells overexpression of Cdt1 leads to damage of chromatin rather than re-replication, and also activates ATM-Chk2 pathways in the absence of detectable re-replication (Tatsumi et al., 2006). In fact, in mammalian cells there exist several redundant pathways regulating Cdt1 scrupulously, implying that there might be more unidentified crucial roles of Cdt1 (reviewed in (Fujita, 2006)). These discoveries lead to the following speculations: 1) what can be affected by overexpressing Cdt1 in early G1 in fission yeast to delay the cell cycle progression, and the possible molecular mechanisms behind such effect; 2) whether Rad3/Tel1 is also activated in this case.

1) What can be affected by overexpressing Cdt1 in early G1 of fission yeast cells to delay cell cycle progression?

Tsanov et al. reported that high level of Cdt1 impairs DNA polymerase η and κ focus formation through hampering the accessibility of these polymerases to PCNA. This

study has shown that the PIP degron domain in Cdt1 sequence plays the key role in interfering the binding of other factors to PCNA. Fission yeast Cdt1 contains dual PIP degrons which interact with PCNA, mediating the degradation of Cdt1 in response to DNA damage in a Cdt2 and Ddb1-dependent manner (Guarino et al., 2011; Ralph et al., 2006). It is a possibility that in the absence of DNA damage, overexpressed Cdt1 associates with PCNA via PIP degrons, thereby blocks PCNA from interacting with other factors that are essential for DNA replication, and consequently hinders the sliding of replication fork. This hypothesis could be tested by mutating dual PIP degron domains of Cdt1 in the *nmt41.cdt2* strain so that the PCNA-binding affinity of Cdt1 is defective while its replication licensing function is preserved; then through monitoring the cell cycle progression by flow cytometry, we can see under the overexpression of Cdt1, whether cell cycle progression in these PIP-mutants will become faster than that in *nmt41.cdt2* cells without PIP-mutation.

2) Is Rad3/Tel1 activated?

ATM pathways can be triggered by different signals. When DNA re-replication forks are stalled and collapse or when they collide with other (re-)replication forks, DSBs may be accumulated and then activate the ATM pathway (Davidson et al., 2006; Liu et al., 2007). One study has suggested that in mammalian cells ATM can be activated by structural alteration of chromatin in the absence of DSBs (Bakkenist and Kastan, 2003). In fission yeast, Human ATR ortholog Rad3 and ATM homolog Tel1 have been shown to sense DSBs; however, it is unclear whether Rad3 and Tel1 can also be activated by other signals such as structural alteration of chromatin.

So far, several proteins physically interacting with Cdt1 have been identified (Figure 6.2) in fission yeast, and some of them are chromatin-binding (Cdc18, Mcm6 and Pcn1). It is plausible that overexpressed Cdt1 alters chromatin architecture by interplaying with other chromatin-binding protein(s), and then activates human Rad3/Tel1 in fission yeast. One can check whether Rad3/Tel1 is activated via deleting *rad3/tel1* in the *nmt41.cdt2* strain to see if cell cycle progression varies when overexpressing Cdt1 in the absence of Rad3/Tel1; or via detecting the phosphorylation state of the signal transducer Cds1/Chk1 of Rad3/Tel1 in the presence of overexpressed Cdt1 in the *nmt41.cdt2* strain.

It is noteworthy that, the delayed cell cycle progression observed in our study was the consequence of overexpressing Cdt1 from G1 phase where the Cdt1 level peaks in normal cycling fission yeast cells; while quite a number of studies on differential model organisms have found out that overexpression of Cdt1 in S phase can induce

re-replication (Iwahori et al., 2014; Li and Blow, 2005; Maiorano et al., 2005; Sugimoto et al., 2009; Thomer et al., 2004). It seems that overexpressed Cdt1 has dual directional deleterious effects on DNA replication depending on at which stage within a cell cycle it occurs, and also depending on in which model organism it occurs. However, one may speculate that in our case Cdt1 was still overexpressed when cells entered S phase, while DNA re-replication was not detected by flow cytometry. One explanation to this speculation could be that when Cdt1 was overexpressed in G1, the pathways for delaying the cell cycle progression were already triggered leading to the changes of a series of downstream events, and hence DNA re-replication did not occur.

It is also interesting to speculate why overexpressing another licensing factor, Cdc18, alone or together with Cdt1 is sufficient to induce such tremendous DNA re-replication in fission yeast, while overexpressing Cdt1 alone does not induce detectable re-replication. One intriguing study on *Xenopus* egg extracts has shown that Cdc6 and Cdt1 must follow a strict order to assemble a functional pre-RC, that Cdc6 has to bind to chromatin before Cdt1 (Tsuyama et al., 2005). And in budding yeast it has also been revealed that during the formation of pre-RC, Cdc6 binds to the chromatin first recruiting Cdt1-MCM complex, and Cdt1 stabilizes the MCM2-7 onto the chromatin (Fernandez-Cid et al., 2013). These studies suggest a plausible explanation to the speculation mentioned at the beginning of this paragraph, that co-overexpression of Cdc18 and Cdt1 can load many more MCM2-7 complexes onto the chromatin, hence lead to DNA re-replication; while when Cdc18 is overexpressed alone, and given the fact that Cdt1 is recycled in the cell during pre-RC formation, MCM2-7 could still be overloaded and result in DNA re-replication. However, when only Cdt1 is overexpressed, due to the limited amount of Cdc18, the amount of Cdt1-MCM complex which can be loaded to the chromatin is also limited, and hence re-replication will not occur.

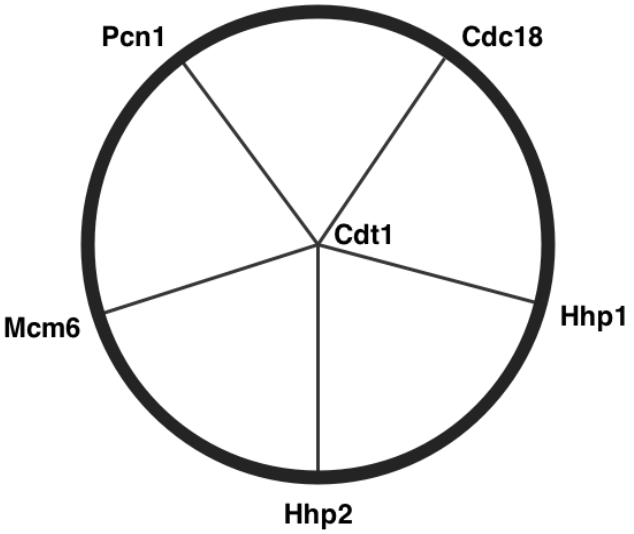

Figure 6.2. Proteins physically interacting with Cdt1. Figure adapted from http://thebiogrid.org/viewer.php?geneID=277364

6.4 The increase in pre-RC formation correlates with the increase in Cdt1 level in UVC-irradiated cells released from the *cdc10*-block

Both previous studies in our group and this study have shown that after UVC irradiation in early G1, percentage of pre-RC-formed cells was lower at all time points than that in non-irradiated cells (Boe et al., 2012; Tvegard et al., 2007) (Figure 5.22). In this study we speculated if the low pre-RC formation after UVC irradiation was due to the low level of Cdt1. By elevating Cdt1 level to different extent in UV-irradiated cells, our preliminary data demonstrated that the increase in pre-RC formation correlated with the increase in Cdt1 level (Figure 5.25 & 5.27, UV60), supporting our hypothesis that Cdt1 is limiting for pre-RC formation after UVC irradiation in early G1. This result provides one molecular explanation for the delayed cell cycle progression of cells exposed to UVC irradiation in early G1.

Even though we managed to increase the pre-RC formation in UVC-irradiated cells via elevating the Cdt1 level, the flow cytometry data of these cell showed that their DNA synthesis was still delayed regardless of the fact that the percentage of pre-RC-formed cells was already as high as that of the non-irradiated cells which were undergoing DNA synthesis (Figure 5.23 & 5.24, 5.26 & 5.28, time point 90 min and 120 min), indicating that some downstream events of pre-RC formation might also be affected in response to UVC irradiation.

It has been shown in both fission and budding yeast that Sld3 and Cdc45, components of pre-IC which is an intermediate downstream pre-RC, are also regulated to determine the timing of origin-firing (Takara and Bell, 2011; Yabuuchi et al., 2006). In budding yeast the phosphorylation of Sld3 by the Rad3 homolog, MEC1, in response to DNA damage blocks DNA replication initiation of late-firing origins (Lopez-Mosqueda et al., 2004; Zegerman and Diffley, 2010). Such factors might also be candidates responsible for delaying DNA synthesis in fission yeast after UVC irradiation in early G1. To elucidate events downstream of pre-RC formation that hinder the cell cycle progression after exposure to UVC irradiation in fission yeast, screening multiple strains carrying different mutations such as *sid3*- and *cdc45*- is required to identify responsible factor(s).

In addition, in order to generate convincing data, at least two more replicates for verifying the preliminary MCM-chromatin binding assay results (Figure 5.23 & 5.26) discussed in this section are required in the future work.

EXPERIMENTAL CONSIDERATIONS

6.5 Working with fission yeast strains

Fission yeast is a popular model organism for cell cycle study due to its unique cell-cycle phase distribution and easy handling. I will give discussion based on the strains used in this study.

6.5.1 Strains carrying *cdt1-TAP*

Strains carrying *cdt1-TAP* were used in this study for investigating Cdt1 levels by Western blot. Given the fact that the anti-TAP antibody has been conjugated with the enzyme already, a secondary antibody is not needed for detecting Cdt1-TAP. Such a Western blot without using the secondary antibody yields quite high background, therefore we loaded positive and negative control samples to the same gel when performing the first Western blot for detection of Cdt1-TAP, so that we could be aware of the correct position of Cdt1-TAP bands on the membrane (Figure 5.3).

As described in 5.1.1, cells carrying *cdc10-M17* and *cdt1-TAP* exhibited a delayed cytokinesis resulted from the *cdc10*-block, which presumably was due to the interference between *cdc10-M17* and *cdt1-TAP*. However, from strains carrying *cdc10-M17* and *cdt1-TAP* in addition to other mutations (such as strains also carrying *gcn2Δ* or *nmt41.cdt2*), a delayed cytokinesis was not observed after release from the *cdc10*-block, which probably was due to that other gene mutation in these strains

made compensation. To avoid such a trouble when using the *cdc10*-block to synchronize cells in early G1, one can attempt to tag Cdt1 with other tags such as HA-tag or PK-tag.

6.5.2 Strains carrying *nmt41.cdt2*

Cdt2 is a component of an E3 ubiquitin ligase Cul4-Ddb1^{Cdt2} that plays an essential role in the degradation of Cdt1 in fission yeast. By crossing two strains from our lab collection (1920 and 1237), we made a strain which carries the thiamine-repressible *nmt41.cdt2* in this study to manipulate the protein level of Cdt1 in fission yeast cells, and the Cdt1 level was indeed elevated to a much higher level after the transcription of *cdt2* was repressed by thiamine treatment (Figure 5.10, 5.20 & 5.21). However, to increase Cdt1 level through regulating Cdt2 level is not an optimal choice for several reasons.

First, Cdt1 is not the only target of Cul4-Ddb1^{Cdt2}. There are studies reporting that Cul4-Ddb1^{Cdt2} is also required for partitioning of chromosomes into euchromatic and heterochromatic domains through aiding the formation of heterochromatin in fission yeast (Braun et al., 2011); in Hela cells, the PCNA-coupled Cul4-Ddb1^{Cdt2} is involved in the degradation of CDK inhibitor p21 after UV irradiation via a similar pathway as that of the degradation of Cdt1 in fission yeast (Nishitani et al., 2008), implying Cul4-Ddb1^{Cdt2} might also have such a similar function in fission yeast. Second, Cdt2 is also playing a role in other E3 ubiquitin ligases. For instance, it has been shown that Cdt2 is acting as a regulatory subunit of the Pcu4-Ddb1^{CSN} complex in fission yeast, and the deletion of *cdt2* stabilizes the expression of the ribonucleotide reductase (RNR) regulator Spd1 which is a target of this ubiquitin ligase (Liu et al., 2005). Third, the Cdt2 level increases in S phase and also increases in response to DNA damage in G2 in fission yeast (Liu et al., 2005). Putting the known and putative roles of Cdt2 together, it is possible that a varied expression profile of Cdt2 might bring some side-effects to the regulation of other proteins in the cell.

To achieve a manipulatable expression of Cdt1 while minimizing the disturbance brought by the genetic modifications to the homeostasis of the cell, one workable approach could be making a strain which carries *nmt41.cdt1,* so that the expression of Cdt1 can be controlled directly by the addition of thiamine. One can further attempt to fuse an aid-tag to the Cdt1, so that the degradation of Cdt1 could be induced when required by adding auxin.

6.6 MCM-chromatin binding assay

MCM-chromatin binding assay was used to quantify the percentage of pre-RC-loaded cells in this study. In order to gain robustness of the results, at least 200 cells should be counted from each sample, and a control of the corresponding sample should always be checked before cell counting. In our lab we count cells manually, therefore to perform a single MCM-chromatin binding assay on one strain, the cell-counting step alone normally takes at least several hours. Another caution about this experiment is that within one study, it is favored to have the same person performing this assay every time, for the reason there is a subjective element in identifying positive signals, and different amount of background signals might be accepted. Even though such difference in counting does not affect the result of samples within one assay performed by one person, it might make trouble when one needs to compare the results from several assays performed by different people. Therefore in order to include the same background signals for all assays, it is important to always have the same person carrying out the counting. Due to limited time, I did not manage to perform the MCM-chromatin binding assays on *cdt2*+ strains by myself, or to perform replicates on the *nmt41.cdt2 mcm6:GFP* strain.

Since the signals from positive cells are generated by the fluorescent protein GFP, it is theoretically workable to employ flow cytometry for quantifying positive cells. Applying flow cytometry to this assay will not only make it possible to quantify a large population of cells within very short time, but can also guarantee that the same background signals are included among different experiments.

In this study two strains carrying a GFP-tagged MCM2-7 subunit (*nmt41.cdt2 mcm2:GFP* and *nmt41.cdt2 mcm6:GFP*) were made, but we only used the *nmt41.cdt2 mcm6:GFP* strain in the MCM-chromatin binding assay. It is also necessary to assay MCM-chromatin binding in the *nmt41.cdt2 mcm2:GFP* cells; and if possible, strains carrying other GFP-tagged MCM2-7 subunits should also be made and subjected to the assay. The reason for doing so is that MCM2-7 is loaded as a ring and all its subunits are loaded at the same time, thus assays on strains carrying different GFP-tagged MCM2-7 subunits are expected to generate the same result; however, adding the tag to different subunits might affects the function and regulation of MCM2-7 in different ways, leading to different timing for MCM2-7 loading and hence different results of the assay. Therefore in order to obtain convincing data, it is necessary to perform the MCM-chromatin binding assay on several strains carrying different tagged subunits, so that the impact on the assay result brought by the tag can be minimized.

7 CONCLUSION

The formation of pre-RC is a key event during DNA replication initiation, and delayed pre-RC loading has been shown to be responsible for delayed G1/S transition after the activation of G1/S checkpoint by UVC irradiation in fission yeast. In this work we show that Cdt1, a pre-RC component, is downregulated and limiting for pre-RC formation after UVC irradiation in early G1 phase.

We have shown that the level of Cdt1 is reduced after UVC irradiation in early G1 phase, indicating that Cdt1 is a target of the G1/S checkpoint. We have generated a strategy to elevate Cdt1 level in cells after UVC irradiation by inhibiting the Cdt2-dependent degradation of Cdt1. Using the cells overexpressing Cdt1, we show that as a consequence of increasing the Cdt1 level after UVC irradiation, the pre-RC formation occurs earlier and can reach a level as high as that in the non-irradiated cells.

Our preliminary data suggest that the increase in pre-RC formation correlates with the increase in Cdt1 level in UVC-irradiated cells. Additionally, we find that in the absence of UVC irradiation, overexpression of Cdt1 leads to prolonged DNA synthesis, suggesting that Cdt1 might have more unidentified roles other than taking part in pre-RC formation.

REFERENCES

Anderson, P., and Kedersha, N. (2009). RNA granules: post-transcriptional and epigenetic modulators of gene expression. Nat Rev Mol Cell Biol *10*, 430-436.

Andrews, B.J., and Herskowitz, I. (1989). The yeast SWI4 protein contains a motif present in developmental regulators and is part of a complex involved in cell-cycle-dependent transcription. Nature *342*, 830-833.

Aparicio, O.M., Weinstein, D.M., and Bell, S.P. (1997). Components and dynamics of DNA replication complexes in S. cerevisiae: redistribution of MCM proteins and Cdc45p during S phase. Cell *91*, 59-69.

Arias, E.E., and Walter, J.C. (2006). PCNA functions as a molecular platform to trigger Cdt1 destruction and prevent re-replication. Nature cell biology *8*, 84-90.

Aves, S.J. (2009). DNA replication initiation. Methods in molecular biology (Clifton, NJ *521*, 3-17.

Bahler, J., Wu, J.Q., Longtine, M.S., Shah, N.G., McKenzie, A., 3rd, Steever, A.B., Wach, A., Philippsen, P., and Pringle, J.R. (1998). Heterologous modules for efficient and versatile PCR-based gene targeting in Schizosaccharomyces pombe. Yeast (Chichester, England) *14*, 943-951.

Bakkenist, C.J., and Kastan, M.B. (2003). DNA damage activates ATM through intermolecular autophosphorylation and dimer dissociation. Nature *421*, 499-506.

Basi, G., Schmid, E., and Maundrell, K. (1993). TATA box mutations in the Schizosaccharomyces pombe nmt1 promoter affect transcription efficiency but not the transcription start point or thiamine repressibility. Gene *123*, 131-136.

Bell, S.P., and Dutta, A. (2002). DNA replication in eukaryotic cells. Annual review of biochemistry *71*, 333-374.

Benito, J., Martin-Castellanos, C., and Moreno, S. (1998). Regulation of the G1 phase of the cell cycle by periodic stabilization and degradation of the p25rum1 CDK inhibitor. The EMBO journal *17*, 482-497.

Boe, C.A., Krohn, M., Rodland, G.E., Capiaghi, C., Maillard, O., Thoma, F., Boye, E., and Grallert, B. (2012). Induction of a G1-S checkpoint in fission yeast. Proceedings of the National Academy of Sciences of the United States of America *109*, 9911-9916.

Booher, R., and Beach, D. (1987). Interaction between cdc13+ and cdc2+ in the control of mitosis in fission yeast; dissociation of the G1 and G2 roles of the cdc2+ protein kinase. The EMBO journal *6*, 3441-3447.

Boye, E., and Grallert, B. (2009). In DNA replication, the early bird catches the worm. Cell *136*, 812-814.

Braun, S., Garcia, J.F., Rowley, M., Rougemaille, M., Shankar, S., and Madhani, H.D. (2011). The Cul4-Ddb1(Cdt)(2) ubiquitin ligase inhibits invasion of a boundary-associated antisilencing factor into heterochromatin. Cell *144*, 41-54.

Breeden, L., and Nasmyth, K. (1987). Similarity between cell-cycle genes of budding yeast and fission yeast and the Notch gene of Drosophila. Nature *329*, 651-654.

Breeden, L.L. (2003). Periodic transcription: a cycle within a cycle. Curr Biol *13*, R31-38.

Bueno, A., Richardson, H., Reed, S.I., and Russell, P. (1991). A fission yeast B-type cyclin functioning early in the cell cycle. Cell *66*, 149-159.

Chen, M., and Manley, J.L. (2009). Mechanisms of alternative splicing regulation: insights from molecular and genomics approaches. Nat Rev Mol Cell Biol *10*, 741-754.

Cook, J.G., Chasse, D.A., and Nevins, J.R. (2004). The regulated association of Cdt1 with minichromosome maintenance proteins and Cdc6 in mammalian cells. The Journal of biological chemistry *279*, 9625-9633.

Correa-Bordes, J., and Nurse, P. (1995). p25rum1 orders S phase and mitosis by acting as an inhibitor of the p34cdc2 mitotic kinase. Cell *83*, 1001-1009.

Costanzo, V., Shechter, D., Lupardus, P.J., Cimprich, K.A., Gottesman, M., and Gautier, J. (2003). An ATR- and Cdc7-dependent DNA damage checkpoint that inhibits initiation of DNA replication. Molecular cell *11*, 203-213.

Davidson, I.F., Li, A., and Blow, J.J. (2006). Deregulated replication licensing causes DNA fragmentation consistent with head-to-tail fork collision. Molecular cell *24*, 433-443.

Diffley, J.F. (1996). Once and only once upon a time: specifying and regulating origins of DNA replication in eukaryotic cells. Genes & development *10*, 2819-2830.

Diffley, J.F., Cocker, J.H., Dowell, S.J., and Rowley, A. (1994). Two steps in the assembly of complexes at yeast replication origins in vivo. Cell *78*, 303-316.

Dutta, A., and Bell, S.P. (1997). Initiation of DNA replication in eukaryotic cells. Annual review of cell and developmental biology *13*, 293-332.

Fernandez-Cid, A., Riera, A., Tognetti, S., Herrera, M.C., Samel, S., Evrin, C., Winkler, C., Gardenal, E., Uhle, S., and Speck, C. (2013). An ORC/Cdc6/MCM2-7 complex is formed in a multistep reaction to serve as a platform for MCM double-hexamer assembly. Molecular cell *50*, 577-588.

Frigola, J., Remus, D., Mehanna, A., and Diffley, J.F. (2013). ATPase-dependent quality control of DNA replication origin licensing. Nature *495*, 339-343.

Fujita, M. (2006). Cdt1 revisited: complex and tight regulation during the cell cycle and consequences of deregulation in mammalian cells. Cell division *1*, 22.

Gilbert, D.M. (2001). Making sense of eukaryotic DNA replication origins. Science (New York, NY *294*, 96-100.

Gopalakrishnan, V., Simancek, P., Houchens, C., Snaith, H.A., Frattini, M.G., Sazer, S., and Kelly, T.J. (2001). Redundant control of rereplication in fission yeast.

Proceedings of the National Academy of Sciences of the United States of America *98*, 13114-13119.

Grallert, B., and Nurse, P. (1996). The ORC1 homolog orp1 in fission yeast plays a key role in regulating onset of S phase. Genes & development *10*, 2644-2654.

Guarino, E., Shepherd, M.E., Salguero, I., Hua, H., Deegan, R.S., and Kearsey, S.E. (2011). Cdt1 proteolysis is promoted by dual PIP degrons and is modulated by PCNA ubiquitylation. Nucleic acids research *39*, 5978-5990.

Hall, J.R., Lee, H.O., Bunker, B.D., Dorn, E.S., Rogers, G.C., Duronio, R.J., and Cook, J.G. (2008). Cdt1 and Cdc6 are destabilized by rereplication-induced DNA damage. The Journal of biological chemistry *283*, 25356-25363.

Hartwell, L.H., and Weinert, T.A. (1989). Checkpoints: controls that ensure the order of cell cycle events. Science (New York, NY *246*, 629-634.

Hayles, J., Fisher, D., Woollard, A., and Nurse, P. (1994). Temporal order of S phase and mitosis in fission yeast is determined by the state of the p34cdc2-mitotic B cyclin complex. Cell *78*, 813-822.

Hedges, S.B. (2002). The origin and evolution of model organisms. Nature reviews *3*, 838-849.

Higa, L.A., Mihaylov, I.S., Banks, D.P., Zheng, J., and Zhang, H. (2003). Radiation-mediated proteolysis of CDT1 by CUL4-ROC1 and CSN complexes constitutes a new checkpoint. Nature cell biology *5*, 1008-1015.

Hinnebusch, A.G. (1993). Gene-specific translational control of the yeast GCN4 gene by phosphorylation of eukaryotic initiation factor 2. Molecular microbiology *10*, 215-223.

Hofmann, J.F., and Beach, D. (1994). cdt1 is an essential target of the Cdc10/Sct1 transcription factor: requirement for DNA replication and inhibition of mitosis. The EMBO journal *13*, 425-434.

Hu, J., McCall, C.M., Ohta, T., and Xiong, Y. (2004). Targeted ubiquitination of CDT1 by the DDB1-CUL4A-ROC1 ligase in response to DNA damage. Nature cell biology *6*, 1003-1009.

Hu, J., and Xiong, Y. (2006). An evolutionarily conserved function of proliferating cell nuclear antigen for Cdt1 degradation by the Cul4-Ddb1 ubiquitin ligase in response to DNA damage. The Journal of biological chemistry *281*, 3753-3756.

Ilves, I., Petojevic, T., Pesavento, J.J., and Botchan, M.R. (2010). Activation of the MCM2-7 helicase by association with Cdc45 and GINS proteins. Molecular cell *37*, 247-258.

Ishimi, Y. (1997). A DNA helicase activity is associated with an MCM4, -6, and -7 protein complex. The Journal of biological chemistry *272*, 24508-24513.

Iwahori, S., Kohmon, D., Kobayashi, J., Tani, Y., Yugawa, T., Komatsu, K., Kiyono, T., Sugimoto, N., and Fujita, M. (2014). ATM regulates Cdt1 stability during the

unperturbed S phase to prevent re-replication. Cell cycle (Georgetown, Tex *13*, 471-481.

Jackson, R.J., Hellen, C.U., and Pestova, T.V. (2010). The mechanism of eukaryotic translation initiation and principles of its regulation. Nat Rev Mol Cell Biol *11*, 113-127.

Johnston, L.H., and Lowndes, N.F. (1992). Cell cycle control of DNA synthesis in budding yeast. Nucleic acids research *20*, 2403-2410.

Kearsey, S.E., and Cotterill, S. (2003). Enigmatic variations: divergent modes of regulating eukaryotic DNA replication. Molecular cell *12*, 1067-1075.

Kelly, T.J., and Brown, G.W. (2000). Regulation of chromosome replication. Annual review of biochemistry *69*, 829-880.

Kniola, B., O'Toole, E., McIntosh, J.R., Mellone, B., Allshire, R., Mengarelli, S., Hultenby, K., and Ekwall, K. (2001). The domain structure of centromeres is conserved from fission yeast to humans. Molecular biology of the cell *12*, 2767-2775.

Knutsen, J.H., Rein, I.D., Rothe, C., Stokke, T., Grallert, B., and Boye, E. (2011). Cell-cycle analysis of fission yeast cells by flow cytometry. PloS one *6*, e17175.

Kondo, T., Kobayashi, M., Tanaka, J., Yokoyama, A., Suzuki, S., Kato, N., Onozawa, M., Chiba, K., Hashino, S., Imamura, M.*, et al.* (2004). Rapid degradation of Cdt1 upon UV-induced DNA damage is mediated by SCFSkp2 complex. The Journal of biological chemistry *279*, 27315-27319.

Krohn, M., Skjolberg, H.C., Soltani, H., Grallert, B., and Boye, E. (2008). The G1-S checkpoint in fission yeast is not a general DNA damage checkpoint. Journal of cell science *121*, 4047-4054.

Lackner, D.H., Schmidt, M.W., Wu, S., Wolf, D.A., and Bahler, J. (2012). Regulation of transcriptome, translation, and proteome in response to environmental stress in fission yeast. Genome biology *13*, R25.

Lee, M.G., and Nurse, P. (1987). Complementation used to clone a human homologue of the fission yeast cell cycle control gene cdc2. Nature *327*, 31-35.

Li, A., and Blow, J.J. (2005). Cdt1 downregulation by proteolysis and geminin inhibition prevents DNA re-replication in Xenopus. The EMBO journal *24*, 395-404.

Li, C.J., and DePamphilis, M.L. (2002). Mammalian Orc1 protein is selectively released from chromatin and ubiquitinated during the S-to-M transition in the cell division cycle. Molecular and cellular biology *22*, 105-116.

Li, X., Zhao, Q., Liao, R., Sun, P., and Wu, X. (2003). The SCF(Skp2) ubiquitin ligase complex interacts with the human replication licensing factor Cdt1 and regulates Cdt1 degradation. The Journal of biological chemistry *278*, 30854-30858.

Liu, C., Poitelea, M., Watson, A., Yoshida, S.H., Shimoda, C., Holmberg, C., Nielsen, O., and Carr, A.M. (2005). Transactivation of Schizosaccharomyces pombe cdt2+ stimulates a Pcu4-Ddb1-CSN ubiquitin ligase. The EMBO journal *24*, 3940-3951.

Liu, E., Lee, A.Y., Chiba, T., Olson, E., Sun, P., and Wu, X. (2007). The ATR-mediated S phase checkpoint prevents rereplication in mammalian cells when licensing control is disrupted. The Journal of cell biology *179*, 643-657.

Lopez-Mosqueda, J., Maas, N.L., Jonsson, Z.O., Defazio-Eli, L.G., Wohlschlegel, J., and Toczyski, D.P. (2004). Damage-induced phosphorylation of Sld3 is important to block late origin firing. Nature *467*, 479-483.

Lundgren, K., Walworth, N., Booher, R., Dembski, M., Kirschner, M., and Beach, D. (1991). mik1 and wee1 cooperate in the inhibitory tyrosine phosphorylation of cdc2. Cell *64*, 1111-1122.

Lygerou, Z., and Nurse, P. (1999). The fission yeast origin recognition complex is constitutively associated with chromatin and is differentially modified through the cell cycle. Journal of cell science *112 (Pt 21)*, 3703-3712.

MacNeill, S.A., and Fantes, P.A. (1997). Genetic and physiological analysis of DNA replication in fission yeast. Methods in enzymology *283*, 440-459.

Maiorano, D., Krasinska, L., Lutzmann, M., and Mechali, M. (2005). Recombinant Cdt1 induces rereplication of G2 nuclei in Xenopus egg extracts. Curr Biol *15*, 146-153.

Marin-Navarro, J., Jauhiainen, A., Moreno, J., Alepuz, P., Perez-Ortin, J.E., and Sunnerhagen, P. (2011). Global estimation of mRNA stability in yeast. Methods in molecular biology (Clifton, NJ *734*, 3-23.

Martienssen, R.A., Zaratiegui, M., and Goto, D.B. (2005). RNA interference and heterochromatin in the fission yeast Schizosaccharomyces pombe. Trends Genet *21*, 450-456.

Martin-Castellanos, C., Blanco, M.A., de Prada, J.M., and Moreno, S. (2000). The puc1 cyclin regulates the G1 phase of the fission yeast cell cycle in response to cell size. Molecular biology of the cell *11*, 543-554.

Martin-Castellanos, C., Labib, K., and Moreno, S. (1996). B-type cyclins regulate G1 progression in fission yeast in opposition to the p25rum1 cdk inhibitor. The EMBO journal *15*, 839-849.

Maundrell, K. (1990). nmt1 of fission yeast. A highly transcribed gene completely repressed by thiamine. The Journal of biological chemistry *265*, 10857-10864.

McCulloch, S.D., and Kunkel, T.A. (2008). The fidelity of DNA synthesis by eukaryotic replicative and translesion synthesis polymerases. Cell research *18*, 148-161.

McGarry, T.J., and Kirschner, M.W. (1998). Geminin, an inhibitor of DNA replication, is degraded during mitosis. Cell *93*, 1043-1053.

Moldovan, G.L., Pfander, B., and Jentsch, S. (2007). PCNA, the maestro of the replication fork. Cell *129*, 665-679.

Mondesert, O., McGowan, C.H., and Russell, P. (1996). Cig2, a B-type cyclin, promotes the onset of S in Schizosaccharomyces pombe. Molecular and cellular biology *16*, 1527-1533.

Morgan, D.O. (1995). Principles of CDK regulation. Nature *374*, 131-134.

Moser, B.A., and Russell, P. (2000). Cell cycle regulation in Schizosaccharomyces pombe. Current opinion in microbiology *3*, 631-636.

Nasmyth, K., and Dirick, L. (1991). The role of SWI4 and SWI6 in the activity of G1 cyclins in yeast. Cell *66*, 995-1013.

Nasmyth, K., and Nurse, P. (1981). Cell division cycle mutants altered in DNA replication and mitosis in the fission yeast Schizosaccharomyces pombe. Mol Gen Genet *182*, 119-124.

Nguyen, V.Q., Co, C., and Li, J.J. (2001). Cyclin-dependent kinases prevent DNA re-replication through multiple mechanisms. Nature *411*, 1068-1073.

Niida, H., and Nakanishi, M. (2006). DNA damage checkpoints in mammals. Mutagenesis *21*, 3-9.

Nilssen, E.A., Synnes, M., Kleckner, N., Grallert, B., and Boye, E. (2003). Intra-G1 arrest in response to UV irradiation in fission yeast. Proceedings of the National Academy of Sciences of the United States of America *100*, 10758-10763.

Nilssen, E.A., Synnes, M., Tvegard, T., Vebo, H., Boye, E., and Grallert, B. (2004). Germinating fission yeast spores delay in G1 in response to UV irradiation. BMC cell biology *5*, 40.

Nilsson, D., and Sunnerhagen, P. (2011). Cellular stress induces cytoplasmic RNA granules in fission yeast. RNA (New York, NY *17*, 120-133.

Nishitani, H., Lygerou, Z., and Nishimoto, T. (2004). Proteolysis of DNA replication licensing factor Cdt1 in S-phase is performed independently of geminin through its N-terminal region. The Journal of biological chemistry *279*, 30807-30816.

Nishitani, H., Lygerou, Z., Nishimoto, T., and Nurse, P. (2000). The Cdt1 protein is required to license DNA for replication in fission yeast. Nature *404*, 625-628.

Nishitani, H., and Nurse, P. (1995). p65cdc18 plays a major role controlling the initiation of DNA replication in fission yeast. Cell *83*, 397-405.

Nishitani, H., Shiomi, Y., Iida, H., Michishita, M., Takami, T., and Tsurimoto, T. (2008). CDK inhibitor p21 is degraded by a proliferating cell nuclear antigen-coupled Cul4-DDB1Cdt2 pathway during S phase and after UV irradiation. The Journal of biological chemistry *283*, 29045-29052.

Nishitani, H., Sugimoto, N., Roukos, V., Nakanishi, Y., Saijo, M., Obuse, C., Tsurimoto, T., Nakayama, K.I., Nakayama, K., Fujita, M.*, et al.* (2006). Two E3 ubiquitin ligases, SCF-Skp2 and DDB1-Cul4, target human Cdt1 for proteolysis. The EMBO journal *25*, 1126-1136.

Nurse, P. (1975). Genetic control of cell size at cell division in yeast. Nature *256*, 547-551.

Nurse, P. (1997). The Josef Steiner Lecture: CDKs and cell-cycle control in fission yeast: relevance to other eukaryotes and cancer. International journal of cancer *71*, 707-708.

Ogi, T., and Lehmann, A.R. (2006). The Y-family DNA polymerase kappa (pol kappa) functions in mammalian nucleotide-excision repair. Nature cell biology *8*, 640-642.

Pardee, A.B. (1974). A restriction point for control of normal animal cell proliferation. Proceedings of the National Academy of Sciences of the United States of America *71*, 1286-1290.

Ralph, E., Boye, E., and Kearsey, S.E. (2006). DNA damage induces Cdt1 proteolysis in fission yeast through a pathway dependent on Cdt2 and Ddb1. EMBO reports *7*, 1134-1139.

Ramirez, M., Wek, R.C., and Hinnebusch, A.G. (1991). Ribosome association of GCN2 protein kinase, a translational activator of the GCN4 gene of Saccharomyces cerevisiae. Molecular and cellular biology *11*, 3027-3036.

Ravanat, J.L., Douki, T., and Cadet, J. (2001). Direct and indirect effects of UV radiation on DNA and its components. Journal of photochemistry and photobiology *63*, 88-102.

Remus, D., Blanchette, M., Rio, D.C., and Botchan, M.R. (2005). CDK phosphorylation inhibits the DNA-binding and ATP-hydrolysis activities of the Drosophila origin recognition complex. The Journal of biological chemistry *280*, 39740-39751.

Remus, D., and Diffley, J.F. (2009). Eukaryotic DNA replication control: lock and load, then fire. Current opinion in cell biology *21*, 771-777.

Romanowski, P., Madine, M.A., Rowles, A., Blow, J.J., and Laskey, R.A. (1996). The Xenopus origin recognition complex is essential for DNA replication and MCM binding to chromatin. Curr Biol *6*, 1416-1425.

Russell, P., and Nurse, P. (1987). Negative regulation of mitosis by wee1+, a gene encoding a protein kinase homolog. Cell *49*, 559-567.

Rustici, G., Mata, J., Kivinen, K., Lio, P., Penkett, C.J., Burns, G., Hayles, J., Brazma, A., Nurse, P., and Bahler, J. (2004). Periodic gene expression program of the fission yeast cell cycle. Nature genetics *36*, 809-817.

Sakaguchi, H., Takami, T., Yasutani, Y., Maeda, T., Morino, M., Ishii, T., Shiomi, Y., and Nishitani, H. (2012). Checkpoint kinase ATR phosphorylates Cdt2, a substrate receptor of CRL4 ubiquitin ligase, and promotes the degradation of Cdt1 following UV irradiation. PloS one *7*, e46480.

Saxena, S., and Dutta, A. (2005). Geminin-Cdt1 balance is critical for genetic stability. Mutation research *569*, 111-121.

Senga, T., Sivaprasad, U., Zhu, W., Park, J.H., Arias, E.E., Walter, J.C., and Dutta, A. (2006). PCNA is a cofactor for Cdt1 degradation by CUL4/DDB1-mediated N-terminal ubiquitination. The Journal of biological chemistry *281*, 6246-6252.

Sivaraman, T., Kumar, T.K., Jayaraman, G., and Yu, C. (1997). The mechanism of 2,2,2-trichloroacetic acid-induced protein precipitation. Journal of protein chemistry *16*, 291-297.

Skjolberg, H.C., Fensgard, O., Nilsen, H., Grallert, B., and Boye, E. (2009). Global transcriptional response after exposure of fission yeast cells to ultraviolet light. BMC cell biology *10*, 87.

Smith, P.K., Krohn, R.I., Hermanson, G.T., Mallia, A.K., Gartner, F.H., Provenzano, M.D., Fujimoto, E.K., Goeke, N.M., Olson, B.J., and Klenk, D.C. (1985). Measurement of protein using bicinchoninic acid. Analytical biochemistry *150*, 76-85.

Stathopoulou, A., Roukos, V., Petropoulou, C., Kotsantis, P., Karantzelis, N., Nishitani, H., Lygerou, Z., and Taraviras, S. (2012). Cdt1 is differentially targeted for degradation by anticancer chemotherapeutic drugs. PloS one *7*, e34621.

Sugimoto, N., Yoshida, K., Tatsumi, Y., Yugawa, T., Narisawa-Saito, M., Waga, S., Kiyono, T., and Fujita, M. (2009). Redundant and differential regulation of multiple licensing factors ensures prevention of re-replication in normal human cells. Journal of cell science *122*, 1184-1191.

Sun, W.H., Coleman, T.R., and DePamphilis, M.L. (2002). Cell cycle-dependent regulation of the association between origin recognition proteins and somatic cell chromatin. The EMBO journal *21*, 1437-1446.

Tabancay, A.P., Jr., and Forsburg, S.L. (2006). Eukaryotic DNA replication in a chromatin context. Current topics in developmental biology *76*, 129-184.

Tada, S. (2007). Cdt1 and geminin: role during cell cycle progression and DNA damage in higher eukaryotes. Front Biosci *12*, 1629-1641.

Tada, S., and Blow, J.J. (1998). The replication licensing system. Biological chemistry *379*, 941-949.

Takara, T.J., and Bell, S.P. (2011). Multiple Cdt1 molecules act at each origin to load replication-competent Mcm2-7 helicases. The EMBO journal *30*, 4885-4896.

Takeda, D.Y., Shibata, Y., Parvin, J.D., and Dutta, A. (2005). Recruitment of ORC or CDC6 to DNA is sufficient to create an artificial origin of replication in mammalian cells. Genes & development *19*, 2827-2836.

Tatsumi, Y., Sugimoto, N., Yugawa, T., Narisawa-Saito, M., Kiyono, T., and Fujita, M. (2006). Deregulation of Cdt1 induces chromosomal damage without rereplication and leads to chromosomal instability. Journal of cell science *119*, 3128-3140.

Thomer, M., May, N.R., Aggarwal, B.D., Kwok, G., and Calvi, B.R. (2004). Drosophila double-parked is sufficient to induce re-replication during development and is regulated by cyclin E/CDK2. Development (Cambridge, England) *131*, 4807-4818.

Tsanov, N., Kermi, C., Coulombe, P., Van der Laan, S., Hodroj, D., and Maiorano, D. (2014). PIP degron proteins, substrates of CRL4Cdt2, and not PIP boxes, interfere with DNA polymerase eta and kappa focus formation on UV damage. Nucleic acids research *42*, 3692-3706.

Tsuyama, T., Tada, S., Watanabe, S., Seki, M., and Enomoto, T. (2005). Licensing for DNA replication requires a strict sequential assembly of Cdc6 and Cdt1 onto chromatin in Xenopus egg extracts. Nucleic acids research *33*, 765-775.

Tvegard, T., Soltani, H., Skjolberg, H.C., Krohn, M., Nilssen, E.A., Kearsey, S.E., Grallert, B., and Boye, E. (2007). A novel checkpoint mechanism regulating the G1/S transition. Genes & development *21*, 649-654.

Vaziri, C., Saxena, S., Jeon, Y., Lee, C., Murata, K., Machida, Y., Wagle, N., Hwang, D.S., and Dutta, A. (2003). A p53-dependent checkpoint pathway prevents rereplication. Molecular cell *11*, 997-1008.

Wang, C.Y., Chen, W.L., and Wang, S.W. (2013). Pdc1 functions in the assembly of P bodies in Schizosaccharomyces pombe. Molecular and cellular biology *33*, 1244-1253.

Wohlschlegel, J.A., Dwyer, B.T., Dhar, S.K., Cvetic, C., Walter, J.C., and Dutta, A. (2000). Inhibition of eukaryotic DNA replication by geminin binding to Cdt1. Science (New York, NY *290*, 2309-2312.

Wood, V., Gwilliam, R., Rajandream, M.A., Lyne, M., Lyne, R., Stewart, A., Sgouros, J., Peat, N., Hayles, J., Baker, S.*, et al.* (2002). The genome sequence of Schizosaccharomyces pombe. Nature *415*, 871-880.

Wu, P.Y., and Nurse, P. (2009). Establishing the program of origin firing during S phase in fission Yeast. Cell *136*, 852-864.

Yabuuchi, H., Yamada, Y., Uchida, T., Sunathvanichkul, T., Nakagawa, T., and Masukata, H. (2006). Ordered assembly of Sld3, GINS and Cdc45 is distinctly regulated by DDK and CDK for activation of replication origins. The EMBO journal *25*, 4663-4674.

Yanagi, K., Mizuno, T., You, Z., and Hanaoka, F. (2002). Mouse geminin inhibits not only Cdt1-MCM6 interactions but also a novel intrinsic Cdt1 DNA binding activity. The Journal of biological chemistry *277*, 40871-40880.

Yanow, S.K., Lygerou, Z., and Nurse, P. (2001). Expression of Cdc18/Cdc6 and Cdt1 during G2 phase induces initiation of DNA replication. The EMBO journal *20*, 4648-4656.

Zegerman, P., and Diffley, J.F. (2010). Checkpoint-dependent inhibition of DNA replication initiation by Sld3 and Dbf4 phosphorylation. Nature *467*, 474-478.

APPENDIX

Appendix 1: Internet references

Appendix 2: Molecular weight standards

Appendix 3: Supplemental information

Appendix 1: Internet references

http://thebiogrid.org/

http://www.pombase.org

http://www-bcf.usc.edu/~forsburg

http://utbiorad.casaccia.enea.it/facs-flow-cytometry.html

http://www.uwplatt.edu/~sundin/351/351h-pro.htm

http://www.bio-rad.com/ja-jp/applications-technologies/protein-electrophoresis-methods

http://eishinoguchi.com/checkpoint.htm

Appendix 2: Molecular weight standards

Precision Plus Protein Dual Color Standards, Bio-Rad

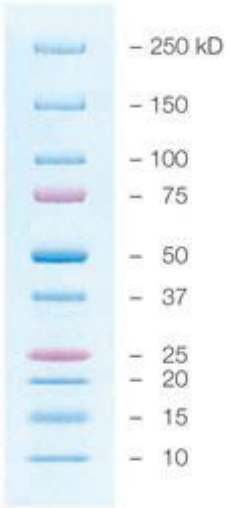

GeneRuler 1 kb DNA Ladder, Thermo Scientific

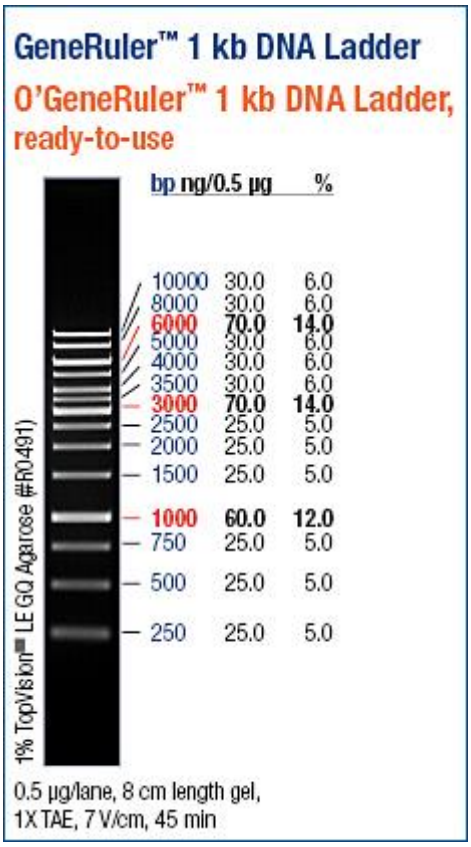

Appendix 3: Supplemental information

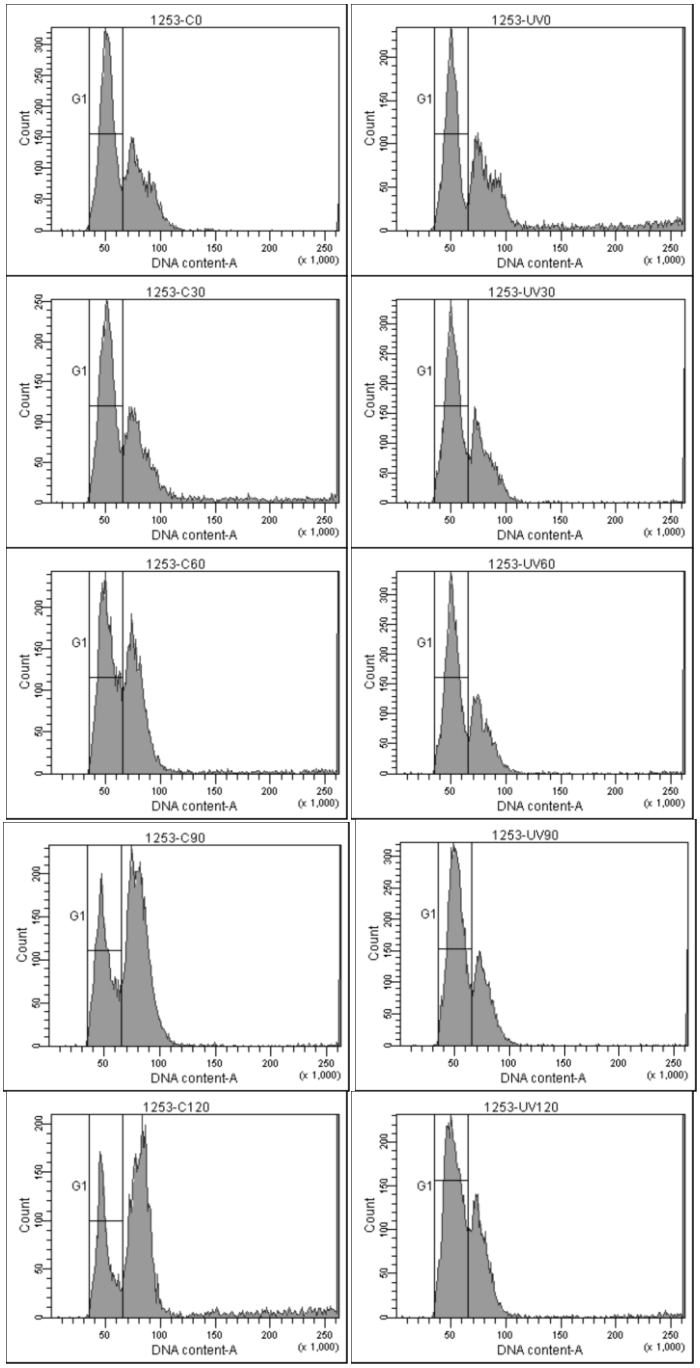

Figure S1. Monitoring cell cycle progression of *wt* cells (1253) released from the *cdc10*-block by flow cytometry. Related to Figure 5.1

On the left are histograms of non-irradiated samples taken at 0 min, 30 min, 60 min, 90 min, and 120 min after release from *cdc10*-block. On the right are histograms of UVC-irradiated samples taken at the same time points. Number of cells is shown on vertical axis and stained-DNA signal intensity is shown on horizontal axis. The peak in the G1 gate represents cells containing 1C DNA content.

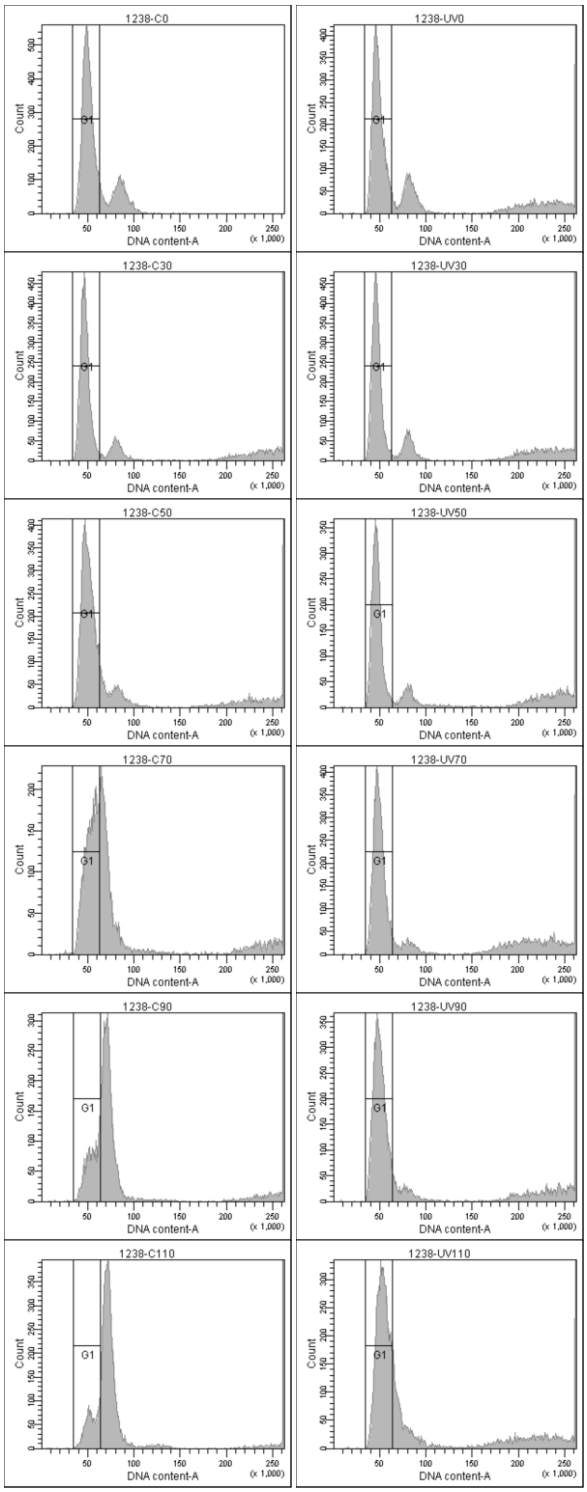

Figure S2. Monitoring cell cycle progression of *gcn2Δ* cells released from the *cdc10*-block by flow cytometry. Related to Figure 5.5

On the left are histograms of non-irradiated samples taken at 0 min, 30 min, 50 min, 70 min, 90 min, and 110 min after release from *cdc10*-block. On the right are histograms of UVC-irradiated samples taken at the same time points. Number of cells is shown on vertical axis and stained-DNA signal intensity is shown on horizontal axis. The peak in the G1 gate represents cells containing 1C DNA content.

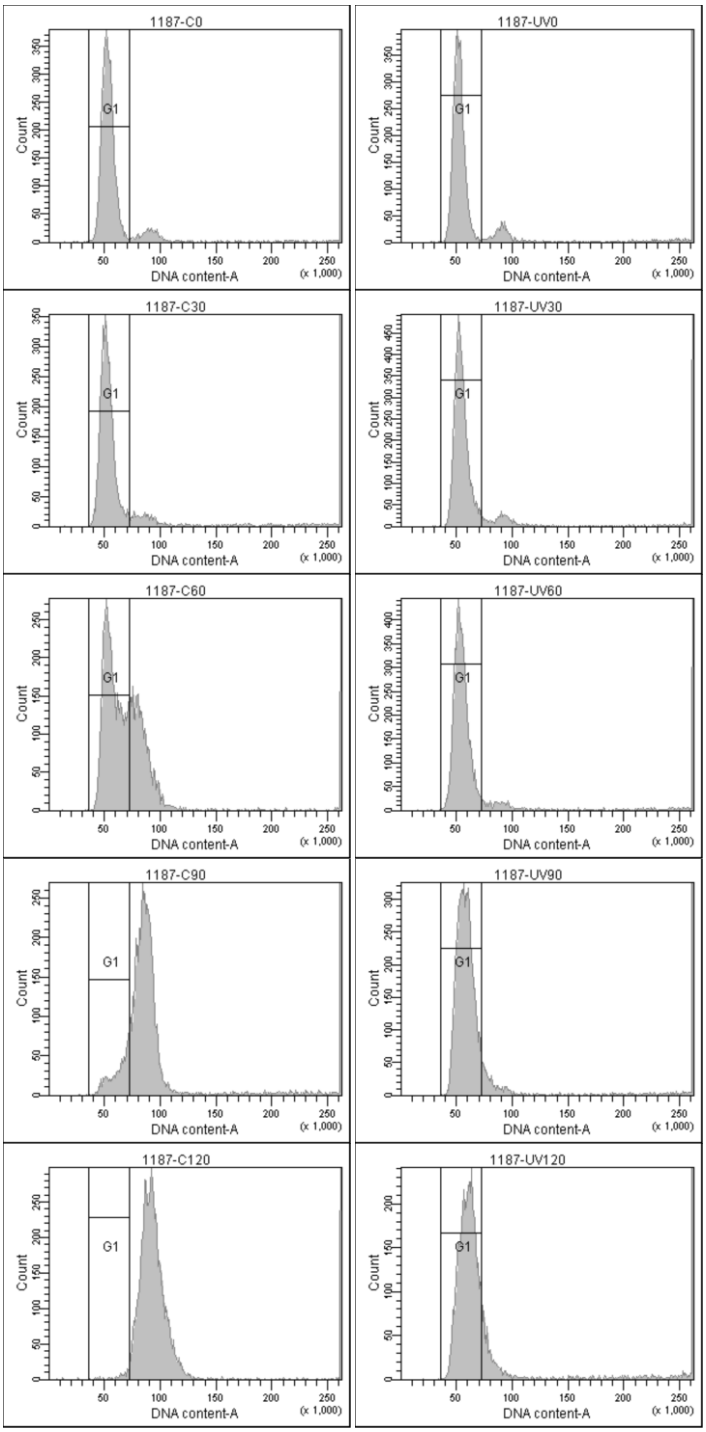

Figure S3. Representative flow cytometry data showing typical cell cycle progression of cells released from the *cdc10*-block.

On the left are histograms of non-irradiated samples taken at 0 min, 30 min, 60 min, 90 min, and 120 min after release from the *cdc10*-block. On the right are histograms of UVC-irradiated samples taken at the same time points. Number of cells is shown on vertical axis and stained-DNA signal intensity is shown on horizontal axis. The peak in the G1 gate represents cells containing 1C DNA content.

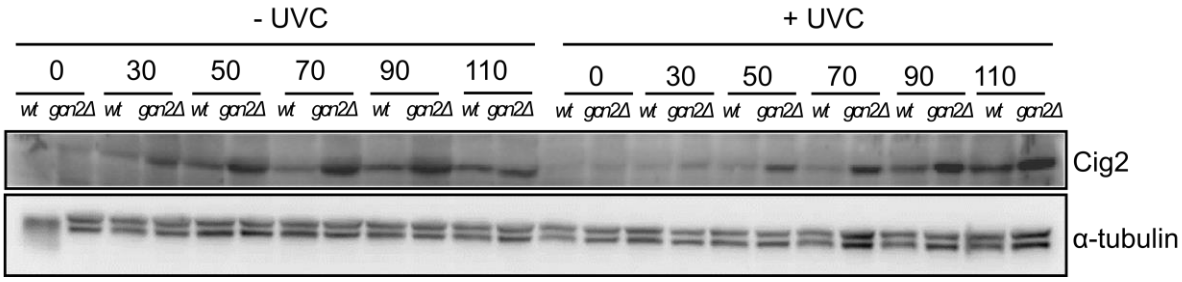

Figure S4. Western blot for detection of Cig2 in *wt* cells and *gcn2Δ* cells released from the *cdc10*-block.

Anti-Cig2 antibody was used for the detection which gave bands at 47 kDa. Samples +/- UVC were taken at 0 min, 30 min, 50 min, 70 min, 90 min, and 110 min after release from *cdc10*-block. UVC irradiation was added immediately after release from the *cdc10*-block. The blot was re-probed with anti-α-tubulin antibody which gave a band at 50 kDa serving as loading control.

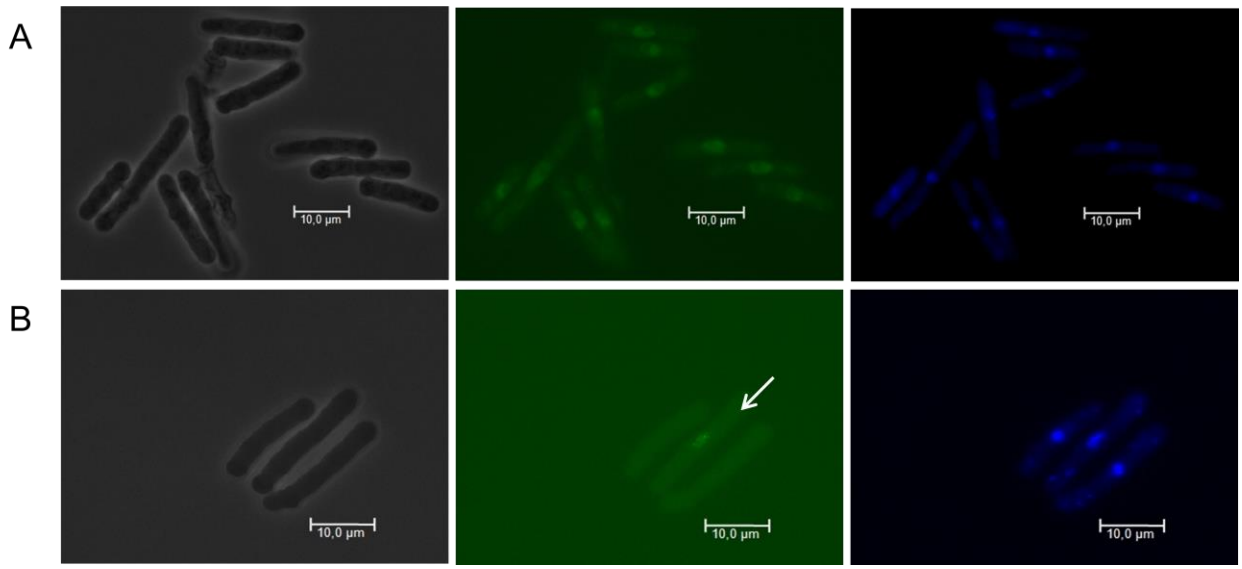

Figure S5. Representative phase contrast fluorescence microscopy pictures of the control sample and the extracted sample of cells carrying *mcm6:GFP*.

(A) The upper panel displays pictures of the control sample taken right after cell synchronization (without 10% Triton X-100). From the left: a phase contrast microscopy picture of cells, a fluorescence microscopy picture showing GFP signals from these cells (because all cells have intact membrane, they all give out GFP signals), a fluorescence microscopy picture showing DAPI stained nuclei of these cells.

(B) The lower panel displays pictures of the extracted sample taken right after cell synchronization (with 10% Triton X-100). From the left: a phase contrast microscopy picture of cells, a fluorescence microscopy picture showing GFP signals from these cells (because these cells have permeabilized cytoplasmic and nuclear membrane, MCM2-7 complexes that have not bound to the chromatin are washed out from the cells, resulting in some cells without GFP signals; in this picture a cell with GFP signal is indicted by the arrow), a fluorescence microscopy picture showing DAPI stained nuclei of these cells.

Scale bar indicated 10.0 µm.